6-2016

Flexographic Printing of Conductive Silver Inks onto PDMS: Surface Treatment and Novel Processes for Creating Printed Electronic Devices

Michael James Joyce
Western Michigan University

FLEXOGRAPHIC PRINTING OF CONDUCTIVE SILVER INKS ONTO PDMS: SURFACE TREATMENT AND NOVEL PROCESSES FOR CREATING PRINTED ELECTRONIC DEVICES

by

Michael James Joyce

A dissertation submitted to the Graduate College
in partial fulfillment of the requirements
for the degree of Doctor of Philosophy
Chemical and Paper Engineering
Western Michigan University
June 2016

Dissertation Committee:

Paul D. Fleming III, Ph.D., Chair
Alexandra Pekarovicova, Ph.D.
Xiaoying Rong, Ph.D.
Massood Atashbar, Ph.D.

FLEXOGRAPHIC PRINTING OF CONDUCTIVE SILVER INKS ONTO PDMS: SURFACE TREATMENT AND NOVEL PROCESSES FOR CREATING PRINTED ELECTRONIC DEVICES

Michael James Joyce, Ph.D.

Western Michigan University, 2016

For the continued advancement of the field of printed electronic (PE), there is a need for a better understanding of the interactions between functional inks and substrates, which is required to optimize printability, mechanical, and functional properties for the creation of more robust and efficient printed devices. This body of work aims to advance the knowledge of the material properties of poly-di-methyl-siloxane, PDMS, films, their interactions with flexo inks, and their flexographic printability. As the printing of metals (i.e., Ag & Au) is a known area of interest pertaining to PE, this work focused on the characterization and optimization of the properties known to promote the adhesion between materials, and their effects on the functional performance of printed conductive ink films. PDMS is an especially important substrate for use in the creation of biocompatible sensors and devices, which is an area predicted to experience much growth in the coming years. But, PDMS has known complications pertaining to its printing and adhesion of materials to its surface. To accomplish this goal, four studies were completed: 1- The Characterization of Surface Treated Silica-Filled and Non-Filled Polydimethylsiloxane Films, 2- Use of Atmospheric-Plasma Treatment to alter the Surface Energy of PDMS Films, and 3- Feasibility for the Development of a Repulpable Silicone Release Paper. From these studies, a need for a high throughput processing and production method for rol-to-roll production and printing of thin (<100 micron) PDMS films was realized and a fourth work performed 4- A Novel Method for the High Throughput Processing and Production of Thin (<100 micron) PDMS Films in which novel method for the roll-to-roll printing of PDMS films was created. The results of these studies provide information on the influences of surface treatments and material interactions on the printability of PDMS films.

ACKNOWLEDGEMENTS

I would like to thank my advisor Dr. Dan Fleming for all his contributions to this work, and my education. Who, without his dedicated assistance and guidance this work would have not been possible. I also thank Dr. Alexandra Pekarovicova, Dr. Massood Atashbar and Dr. Xiaoying Rong for all their valuable contributions and insight into this research, and the knowledge they helped me gain throughout my works.

I sincerely appreciate all the assistance provided by Mr. Matthew Stoops for his assistance in helping me to understand and use the testing equipment necessary for completion of this work. I also appreciate all the assistance from the Electrical and Computer Engineering Graduate Students (Ali Eshkeiti, Binu Baby Narakathu, Sai Guruva R Avuthu, and Sepehr Emamian) for all their contributions to my knowledge of electrical performance characterization and analysis. I would like to thank my family, friends, and love ones for all their encouragement and support, without which, this work would have not been possible.

With a special thanks to my mother Dr. Margaret Joyce, and father Dr. Thomas Joyce, for all they have done for me both for my education and personal life; without which, none of this would be possible.

Michael Joyce

TABLE OF CONTENTS

Table of Contents- continued

LIST OF TABLES

LIST OF FIGURES

CHAPTER 1

INTRODUCTION

In recent years the use of Roll to Roll (R2R) printing techniques, such as flexography, have been utilized for the creation of printed electronics (PE) in applications where low-cost and flexibility have been the main desire. The use of PDMS, poly(dimethylsiloxane), Figure 1, in medical devices and applications also continues to grow, and there have been many studies done on the creation of medical devices using PDMS. However, due to limitations of metallic ink adhesion to PDMS, the printing of PDMS films for flexible PE applications has not been widely studied. Wiring is one of the essential technologies, not only for PE, but also for all kinds of electronic products, including sensors. Since electrical conductivity is the most important property for wiring materials to have, metallic materials are the materials of choice. Therefore, the goal of this work was to characterize the influence of surface treated PDMS film properties and ink properties on the print quality of metallic conductive inks. This chapter provides a brief introduction to the field of printed electronics and discusses some common nomenclature. Motivations and objectives are also discussed.

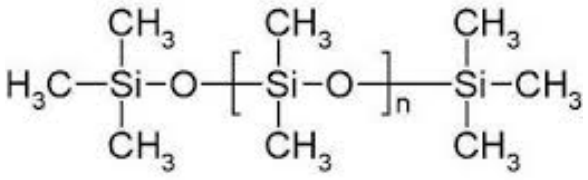

Figure 1. Poly(dimethylsiloxane) (PDMS) molecular structure.

1.1 Printing Electronics (PE)

Using a very broad definition of printing, a wide variety of materials may be processed for the creation of PE devices. By combining this broad definition of printing with a wide array of materials, all types of electrical components and devices may be processed and

created using printing techniques. The idea of printing electronics using conventional (additive) printing technologies has been around since the early 1950s [1], though, due to technological limitations, it had not become widely implemented until more recently.

Photolithography is a subtractive process that has been, and continues to be, widely used for the fabrication of integrated circuits. It requires physical and chemical depositions to be performed on a semiconductor (e.g. silicon) substrate. With the growing desire to use additive-printing methods to reduce wastes, costs, and process complexity, graphic printing technologies (gravure, screen, inkjet, flexography) are able to employ solution processable functional materials. This greater availability of materials, coupled with the combination of much research in their use in PE applications, has led to many innovations and achievements in PE. However, it is still unlikely that the fully additive-printing technologies will ever surpass the sophistication of the outputs of photolithography, such as microprocessors. As such, the goal of printing electronics is not to replace nano devices, but rather to supplement and complement their use and allow for the creation of new flexible form factors.

Subtractive processing methods are most often utilized in conventional or traditional electronics manufacture. Conventional PE (Patterned Electronics) systems refer to the traditional fabrication of components and devices (most often) using subtractive processing methods, such as: photolithography [2], soft lithography [3], reactive ion etching (RIE) [4], chemical etching [5], and electroless etching [6]. Due to the extremely fine resolution of the images produced by these methods (which are actually nano-devices such as switches or transistors), which can fail in the presence of small errant particles, these processes require high-level clean room facilities and highly controlled environmental conditions. This greatly adds to capital investment and operational costs. Thus, in cases where high levels of sophistication are not needed, PEs can fill a product need at a lower cost.

Photolithography is a process used in both the fabrication of integrated circuits and by the printing industries for the imaging of plates used to create an image carrier. So, it is a process technology not foreign to printers. In its use for the creation of integrated circuits,

a layer of photoresist (a polymer that is altered by UV exposure by becoming more basic, acidic, or neutral) is deposited evenly onto a substrate, covered with a mask bearing the desired pattern to be created. The photoresist layer is then exposed to a dosage of UV light that is specific to its particular formulation and layer thickness. Depending on the type of photoresist used, the type of chemical bath to wash away the unreacted areas is chosen, allowing reacted areas to remain [4]. The use of environmentally unfriendly chemicals is inherent in these processes, which produce large amounts of waste. In addition to generating much waste, photolithography being a subtractive process, requires multiple costly and time consuming processing steps. The complexity of the subtractive process in comparison to the additive printing process is shown in Figures 2 and 3.

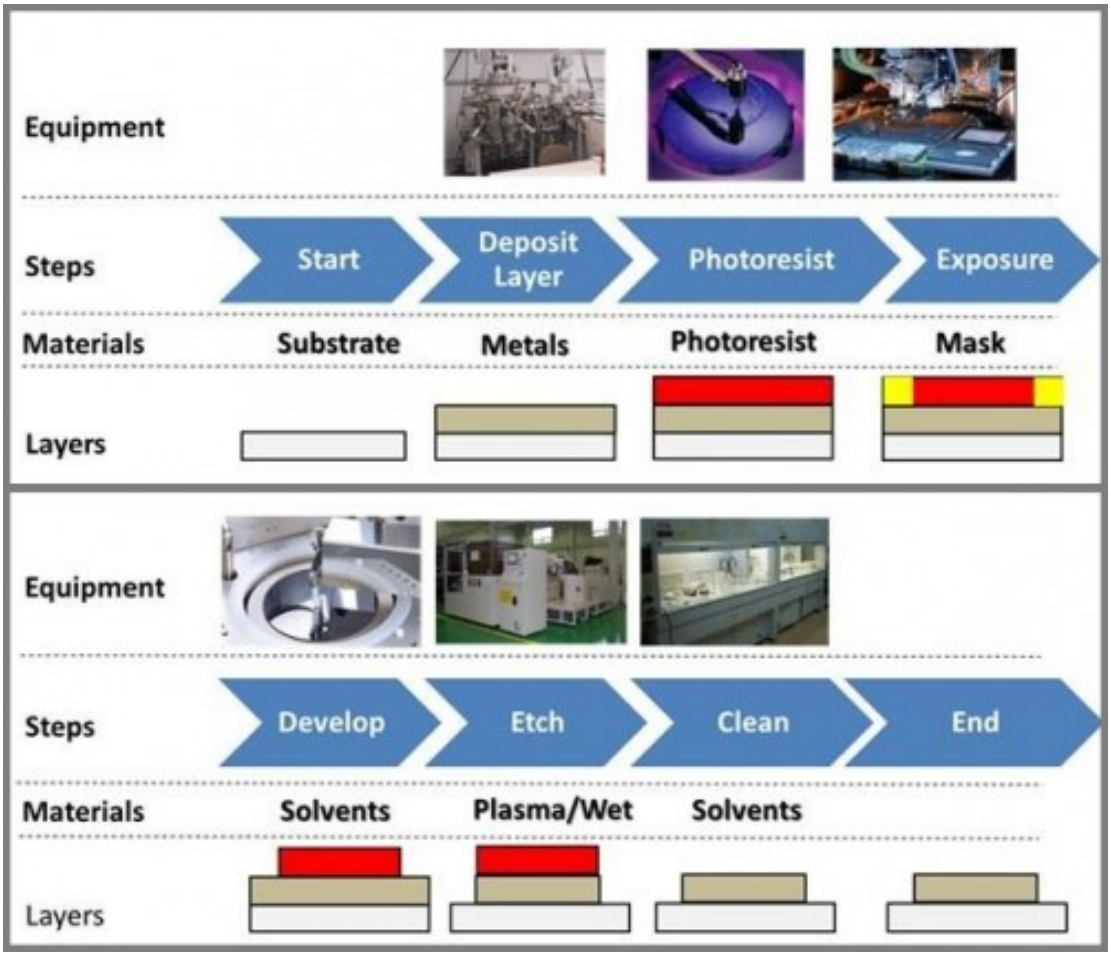

Figure 2. Subtractive Photolithography.

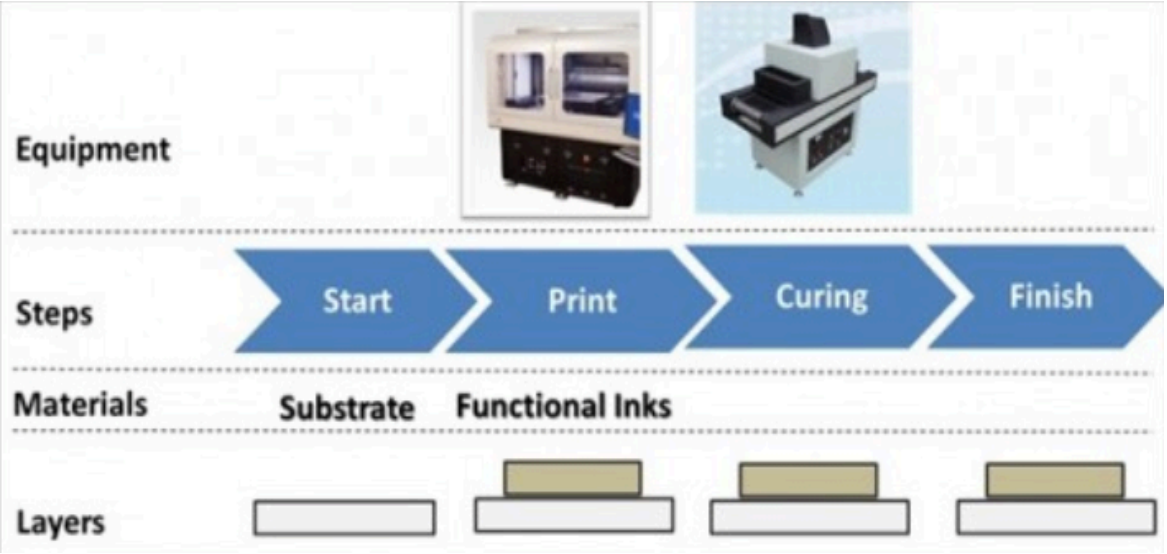

Figure 3. Additive Photolithography (Conventional Graphic Printing Method).

Shown in Figure 3 is a conventional graphic printing method. Being an additive process, it requires fewer processing steps, and since material is deposited only where needed, less waste is generated and disposal costs are reduced. Additive PE does not require expensive vacuum processing, etching, stripping, cleaning, high temperature baking and polishing processing steps. For these reasons, it is an attractive fabrication technique for the manufacture of electronic devices where the main desire is a low cost per unit, and the lower performance drawbacks are acceptable.

Recent advancements in flexo plate materials and platemaking technology have brought flexography to the forefront of printing technologies. Flexography is a direct rotary relief printing process, which utilizes a relief image produced on a resilient photopolymer plate. The plate is fixed to a plate-cylinder that can vary in diameter, to achieve the desired size of the image. The plate is then inked by an engraved, cell-structured, ink-metering roll, called an anilox roll. A schematic of the flexo printing process and 3D image of the cells of an anilox roll can be seen in Figure 4.

Unlike the gravure and screen-printing processes, the amount of ink delivered to the substrate in the flexo process is not mainly dependent on the image carrier. This is because in the flexo process, the anilox roll (which contains ink carrying cells) is surface

metered with a doctor blade, and is used to deliver a specified amount of ink to the flexible plate, which then transfers the inked image to the substrate. To obtain ink films of different thicknesses for the same nominal resolution plate, anilox rolls of different cell volumes can be used. Hence, in comparison to the screen and rotogravure printing processes, ink films of varying thicknesses can be more readily achieved through this process.

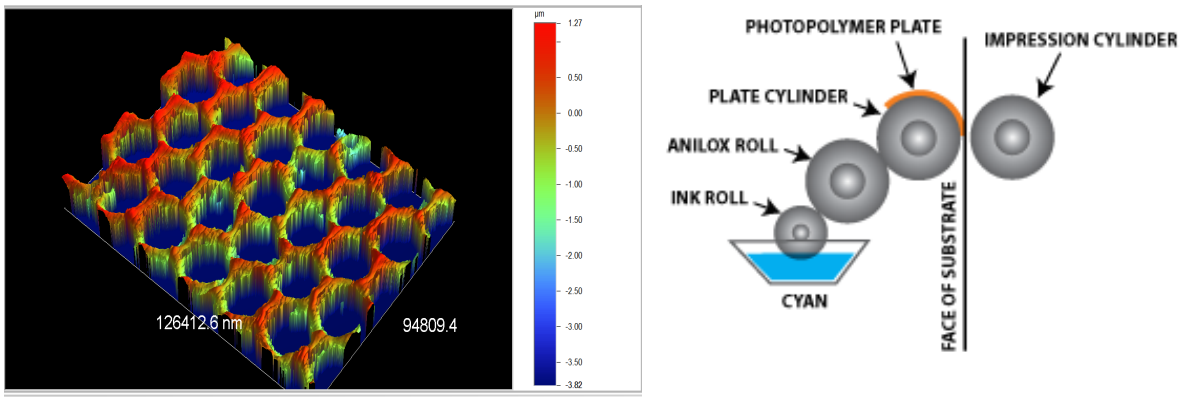

Figure 4. 3D image of the cells of an anilox roll (Left), and schematic of the flexo printing process (Right) [7].

Recent advancements in flexo plate materials and platemaking technology have greatly increased the resolutions at which plates can be imaged. Newer, thinner photopolymer plates are available that require less processing time, because less image depth has to be etched, cured, or uncured and washed away. The shorter processing time results in less loss of detail. As a result, the new plates can hold finer image detail and can be imaged at much higher resolutions. Digital plates can now be imaged at resolutions up to 10,000 dpi [8], which enables ultra fine features to be printed. At this resolution, lines that are one pixel wide on the plate could ideally print (if no spreading) a line under 1 micron wide (at 10,0000 dpi, one pixel = 0.3937 microns). However, due to the failure of one dot (pixel) to transfer from plate to substrate, this would result in a disconnected circuit. For this reason it is less risky to print lines with a minimal width of at least two pixels. Even working within this minimal recommended design rule, the ability to print sub 10-micron lines puts flexo in the forefront of printing ultra fine line electrodes for printed electronics applications. Another advantage of flexo printing over screen and rotogravure printing is

that the amount of ink delivered to the substrate is not mainly dependent on the image carrier (open area of the screen or size of the gravure cells), but rather can be altered based on the anilox roll selected. As shown in Figure 5, the resolution of the plates must be matched to the resolution of the anilox roll in order to avoid the dot on the plate being smaller than the opening of the cell - a condition termed dot dipping. If this occurs, the dot will enter the anilox cell, picking up excess ink resulting in poor printed line quality (ragged lines, ink smearing, etc.). Thus, the relationship between the resolution of the printing plate and the line screen of the anilox roll directly affects print quality and functional performance of the printed lines. When using a high-resolution printing plate, that is a plate with a high lines per inch (lpi) count, an anilox of a higher line screen (cells per inch, cpi) should be used. Typically for high definition flexo graphic printing a ratio of 6 to 10 anilox cells are required for each plate halftone dot. For example, for a plate screen of 150 lpi, at a minimum of 6-anilox cells/halftone dot, an anilox of 900 cpi should be used.

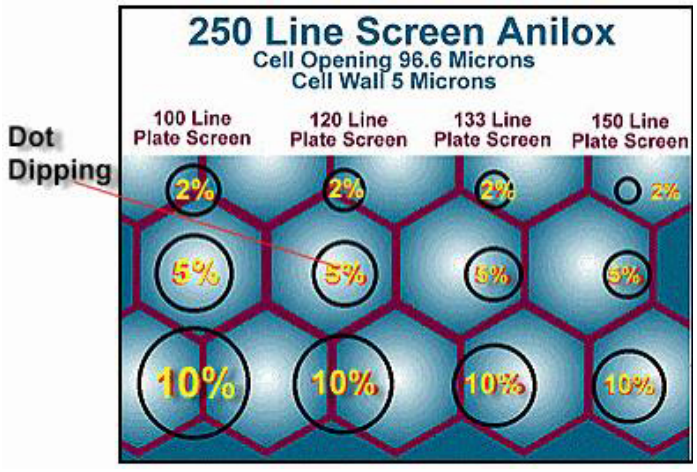

Figure 5. Dot Dipping [9].

Though the line screen will dictate the opening of each cell, the depth of the cell can be varied. However, there are limitations in how deep a cell can be engraved without adversely impacting ink release. The width and depth of the cells, the so-called aspect ratio, determines the cell volume and hence the volume of ink available to ink the plate. A depth to opening ratio of 28 to 33% has been established for graphic printing, but ratios for functional inks have yet to be established; most likely a different ratio will be needed

for each functional ink type since performance is related to ink film thickness (something graphic printers do not have to contend with).

Thus, in comparison to screen and rotogravure printing, flexo printing enables more control of the ink film delivered to the substrate, and deposits a much thinner ink film. In comparison to inkjet printing, flexo enables higher solids and a broader range of inks (viscosity and surface tension) to be printed, if the solvents in the inks do not swell the flexo plates. In comparison to rotogravure printing that uses metallic cylinders, the flexo image carrier is less expensive and can be produced more quickly. In comparison to screen and gravure printing, the ability to manipulate more process variables to control ink film thickness could be a major advantage for the printing of fine lines. Nanoparticle flexo inks are also commercially available, whereas nano screen inks are just now being investigated. Previous work has shown the difficulty in printing functional fine lines by the microgravure process due to the difficulty in engraving cells deep enough [10] to carry enough ink for the fine lines to be functional. However, if regular electromechanical or laser engraving is used, gravure offers a huge variety of cell shapes and volumes enabling the deposition of a variety of ink film thicknesses. Gravure, because of its copper engraved chromium coated surface, allows for strong solvents in inks, which is not the case for flexography. An advantage of flexo in comparison to the screen and inkjet printing processes is that it is a higher throughput process. For these reasons, flexography has been selected for this study.

For all printing processes, the properties of the ink are important to maintaining good print quality and functional performance. The flow and leveling properties, size of the ink particles, surface tension of the ink, and drying rate of the solvent carriers in the ink must all be matched to the process in order for the ink to print well on press. In addition to matching an ink to a process, the ink must also be matched to the substrate to which it is to be printed. For good print quality and functional performance, the ink must wet and adhere well to the substrate. If the ink spreads too much, then not only is too much line gain of concern, but thinning of the ink film could result in a loss in functional performance. Incomplete wetting will result in discontinuities, which will also compromise, if not destroy, functional performance.

Wiring is one of the essential technologies not only for PE but also for all kinds of electronic products, including sensors. The ability to print conductive lines is important to the manufacture of low-cost printed sensors. Due to its flexibility and biocompatibility the use of PDMS as a substrate for printed sensors is of high interest. However, the low surface energy of PDMS film makes it difficult to print on it. The problem of ink wetting can be overcome by manipulating the surface energy and increasing the spreading angle of the ink on the PDMS film by altering the properties of the ink to better wet the PDMS film and by making the PDMS film more porous. After improving ink wetting, the process parameters can be manipulated to improve print quality and increase the functional performance of the printed ink.

1.2 Motivations for Study

The use of PE devices in athletic fitness/wellness and healthcare applications require lightweight, thin, and conformal wearable/implantable devices that can be worn or implanted without discomfort. The devices should work as standalone devices, either passively or actively, and should preferably be able to communicate wirelessly with other systems or networks. An example of such a wearable device is a health-care patch developed by MC10. This sensor (Figure 6) has the ability to sense temperature, blood pressure, and glucose [11].

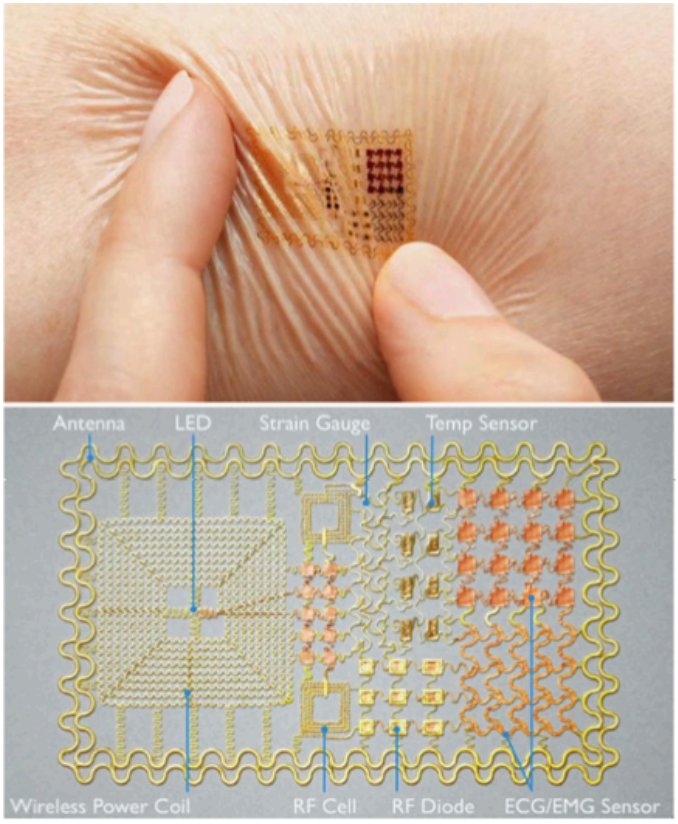

Figure 6. Wearable health-care patch developed by MC10 (Cambridge, MA).

Wearable, healthcare monitoring sensors, which enable physiological events to be tracked, are also of considerable interest to healthcare, wellness, and defense workers. Clothing-integrated electrochemical sensors are promising, however, some key challenges such as sample delivery to the electrode surface, sensor calibration, and robust interconnections still require advancement. Thus, before a variety of wearable or implantable PE products can incur a widespread commercial acceptance, it must first be demonstrated that these devices will provide the value, comfort, and functionality demanded by manufacturers and consumers alike. For optimal comfort, these devices should be thin, lightweight, form fitting, and biocompatible. PDMS can provide these properties, but due to its low surface energy, ink wetting and adhesion are poor. As a result, its print quality and functional performance is poor. Studies are needed to examine how the surface characteristics of these films can be altered to improve these properties, which was the aim of this work.

1.3 Objectives of Research

To create more robust, biocompatible devices, there exists a need for a better understanding of the interactions between functional inks and PDMS films in order to improve their printability, mechanical and functional properties. The objective of this research was to advance the knowledge of the impact of surface treatment technologies on the interaction of PDMS films with aqueous silver flexo conductive ink, and flexographic printability. Another objective was to discover a method to enable thin PDMS films to be printed on a roll-to-roll flexographic press for higher throughput to extend its use as a biocompatible material for the fabrication of PE devices. To accomplish these objectives, this dissertation research was organized and advanced in three projects.

In the first project, the surface energy and roughness of filled and unfilled prepared PDMS films were characterized before and after UV ozone, and chemical treatment with piranha solution.

In the second project, PDMS films were surface treated with O_2 and N_2 plasma gas using a Surfx atmospheric plasma unit. The influence of plasma gas treatment on the surface energy and surface interaction of the films with water and an aqueous conductive silver nano ink was examined.

In the third project, a novel method to enable the high throughput manufacture and printing of poly(dimethylsiloxane) (PDMS) films was created by first pre-coating a paper substrate with a water soluble polymer, then applying and drying a thin coating (< 100 microns) of PDMS to the pre-coated layer. The water soluble polymer, sodium alginate, enabled the PDMS polymer to be supported by the paper web during printing, then separated from the paper by moistening the backside of the paper with water to dissolve the sodium alginate.

In the fourth project, the repulpability of PDMS coated paper samples was studied. Here two sacrificial coatings were utilized, sodium alginate, and polyvinyl alcohol (PVA) to enhance the recyclability of the PDMS coated paper samples.

In the final project a novel method for producing self supported electronic devices was created by printing electronic materials to create an electronic device onto a sacrificial coating layer that could be removed from its base carrier layer by dissolution in an appropriate solvent.

CHAPTER 2

LITERATURE REVIEW

2.1 Introduction

The purpose of this chapter is to provide readers with basic information pertaining to PE. What PE are, as well as the basic motivations for use of printing technology for creation of functional devices. Ink and substrate materials used in PE are discussed, with a focus on the benefits of improving performance of printed metallic inks onto a PDMS substrate. Current applications of PEs, as well as some current limiting factors pertaining to the implementation of printing for the creation of functional devices are reviewed. Lastly, current research on the use of PDMS for the creation of biosensors is discussed.

2.2 Applications of PEs

The applications of additive PE have been very diverse with the creation of many devices such as RFIDs [12], solar cells (photovoltaics) [13], flexible displays [14], sensors [15], flexible batteries [16], and memory and logic components [17, 18] to name a few. Many of these devices have been developed using multiple contemporary printing techniques, further solidifying their use and applicability in the electronics market. The end-use solutions processed have shown the value in the use of functional printing as an industrial application; however, these developments are more simplistic compared to the sophistication and obtainable image-density of conventional PE manufacturing techniques. The advantage in using contemporary PE is not just the ability to use flexible substrates (allowing roll-to-roll processing) but in the ability to create systems through simplified solutions, enabling products to have thinner profiles, and new form factors. The ability to use R2R processing techniques enables lower production costs, and higher throughput; however, the need for functional inks to undergo high temperature processing has limited its adoption within industry [19]. The ability to create new form factors, such as those for use in medical applications, also have their own key challenges, such as requirements of materials to be biocompatible. Materials such as PDMS are biocompatible, but have known problems pertaining to the adhesion to metals [20]. The ability to create devices with functionality unobtainable by conventional silicon-based

electronics [21] has generated focused research [4] to discover solutions to such issues. The discovery of new answers to improve the durability of created devices will enable the development of new market applications.

2.3 Printing Electronics

The creation of PE devices and components most often do not, and perhaps will never be able to provide the level of sophistication and functionality of conventional silicon-based electronics, but they can help to replace and advance certain features or components related to these devices and components as a whole. Printed electronics also enables the creation of devices providing new form factors for designs not achievable by contemporary systems, such as those desired for use with wearable or implantable devices for medical applications [22].

Printing electronics is a more environmentally friendly [23] (theoretically speaking, as there is more opportunity for the reclamation of materials) alternative to conventional methods for the creation of PE devices and components. Printing electronics may be accomplished with the use of (additive) printing methods, which include: screen printing [24], inkjet [25], gravure [26], flexography [27], and offset lithography [28] printing processes. The processes involved in the use of conventional graphic printing, are one in the same as the processes used to print electronics, the only difference is that of the materials used for the creation of functional inks. This is why printing electronics is often referred to as functional printing. For example, screen-printing uses thick films of polymer pastes (inks) that may either contain metallic particles or flakes for functional printing, or pigments and dyes for graphic printing. The screen-printing process is very simple, but yields high material costs due to the inherent thick ink-film produced and subsequent larger ink volumes used. As mentioned above, an advantage of PE is its environmental friendliness, which results from the ability to reclaim a large portion of the high value materials used. The ability to reclaim a high portion of these materials is economically favorable by helping to lower waste. Another economic benefit is that some inks can be reclaimed. For example, precious metals used for conductive inks, such as silver or gold can be reclaimed and re-used. As the world demand of electronics

continues to grow, and resources continue to dwindle, the use of PE will likely be progressively used for this increasingly important benefit.

Many different printing methods have been used for the creation of PE devices. Screen printing, inkjet printing, gravure printing, flexo printing, and offset lithographic printing have all been tried. Depending on the nature of the PE products and process or processes used to create the device, one must make a suitable choice regarding the ink, substrate, device design structure, manufacturing speed, desired yield, quality, and production cost. The important printing parameters are as follows:

- Printing accuracy and resolution
- Multilayer printing accuracy
- Uniformity of the printed ink film and substrate surface
- Ink compatibility with press materials and substrate
- Ink drying time and temperature requirements
- Wetting control and interface formation
- Throughput and cost considerations

Roll-to-roll (R2R) printing is one of the active research areas in PE technology because it enables large-scale production by high-speed web handling. Nevertheless, the R2R printing of PE devices is not mature enough to be applied to many areas where PE technology is used since adjustments among materials, printing methods, and inspection methods with definitions of defect criteria have not yet been established. Sheet-fed production is still a major printing method for most PE products. To shift from sheet-fed printing to R2R printing will require time to develop the printing technologies with suitable parameters including materials development. The development and advancement of these materials (especially inks) is a costly and time consuming process, requiring the creation of tailored characteristics dependent upon print process requirements. As can be seen in Table 1 there may be drastic variations in the required properties of inks, and achievable print attributes dependent upon the desired printing process.

Table 1. Comparison of (functional) ink properties and print attributes of various print methods (Modified from [29])

Printing Method	Ink Viscosity (cP)	Line Width (μm)	Line thickness (μm)	Print Speed (m/min)
Inkjet	5-20	30-50	Approx. 1	Slow
Offset	400-1,000	Approx. 10	< 10	Middle-fast Approx. 1,000
Gravure	5-20	10-50	Approx. 1	Fast Approx. 1,000
Flexo	50-200	45-100	< 1	Fast Approx. 500
Screen	1,000-10,000	30-50	5-100	Middle

As can be further seen in Table 1, each print method not only has limitations with regards to the required materials, but also with the achievable speed of printing. The ability to print at higher speeds enables lower cost of manufacture; hence, the ability to print at high speeds is essential for the advancement of PE technologies. However, as print speeds increase, the achievable image resolution is often degraded. Figure 7 compares the throughput to pitch resolution of a few of the conventional graphic printing methods.

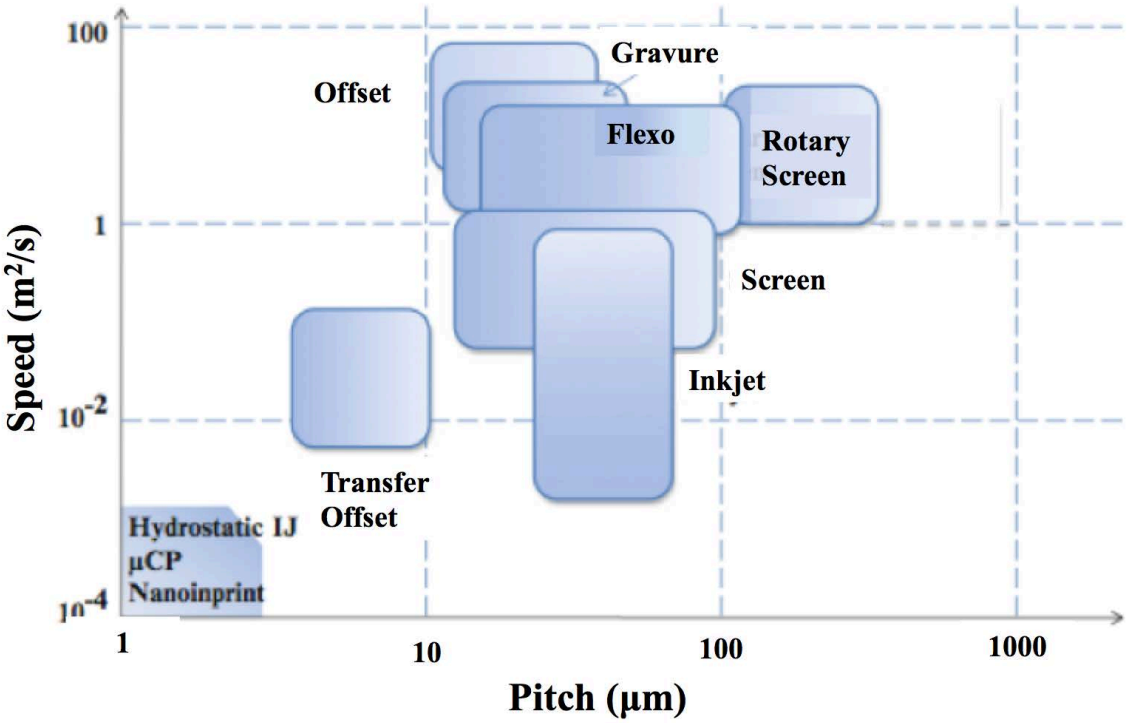

Figure 7. Comparison of throughput to pitch resolution [29].

As can be seen in Figure 7, the flexo process allows for some of the highest speeds of production of any of the conventional printing methods, however, in comparison to the gravure and offset processes, the achievable pitch is more negatively affected as print speeds increase. This is most likely due to the compressible nature of the flexographic plates and the increase in distortion of plate and image with increased print pressures and speeds.

2.4 Current Limitations of PE

The choice of printing methods is sometimes a major issue before launching research projects. There is no single selection for one application. There are certain suitable pairings between inks and print methods. A substrate may play a role in this choice. Not only must the viscosity/surface tension of the ink be considered, but also the device structures and whether the device line/layer is thin or narrow must be considered, as these parameters will inevitably affect the decision of what process should be used.

The cross-section profile of a printed circuit or a device can be of a distinctive shape that is related to the printing process used. Figure 8 shows typical wiring cross-sectional shapes formed by high and low viscosity inks. For printed electrodes, the rectangular cross section (seen in Figure 8) is most desirable for optimizing conductivity. Unfortunately, this shape is only achievable when using high-viscosity inks, such as those used with screen-printing. For inkjet printing, the coffee ring shape is often obtained due to the low-viscosity of the ink. This shape is not appropriate in most cases because many defects are likely to form in the concave central area; at the very least, the semi cylindrical arc shape is desired.

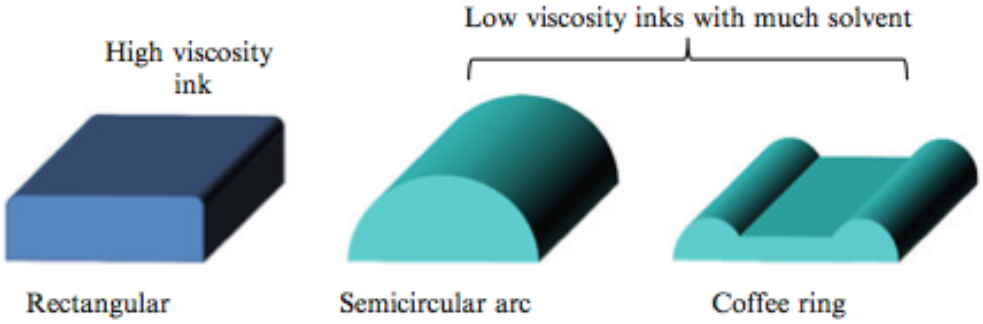

Figure 8. Typical wiring cross-sectional shapes formed by high and low viscosity inks [29].

The shape of the printed ink film is not only dependent upon the printing processes and ink viscosity. Substrate properties also play a key role in the shape formation of the printed ink films, particularly with regards to the way in which these properties affect the wetting and spreading of the printed ink film.

2.5 Wetting and Spreading

The wetting ability of a liquid on a solid substrate may be measured by a simple sessile drop method (Figure 9). The wetting angle is a good parameter for understanding the wettability and adhesion of a liquid onto a surface. Where the wetting angle θ is larger than 90°, it is called non-wetting, while an angle less than 90° is known as wetting. The

wetting phenomenon is governed by the surface energies of the liquid and substrate and the interface energy as expressed by the Young's equation [30].

$$\gamma_{LV} \cos\theta = \gamma_{SV} - \gamma_{SL} \quad (1)$$

Where, γ_{LV} is the liquid-vapor interfacial tension or surface energy, γ_{SV} is the solid-vapor interfacial tension, and γ_{SL} is the solid-liquid interfacial tension, and θ is the contact angle.

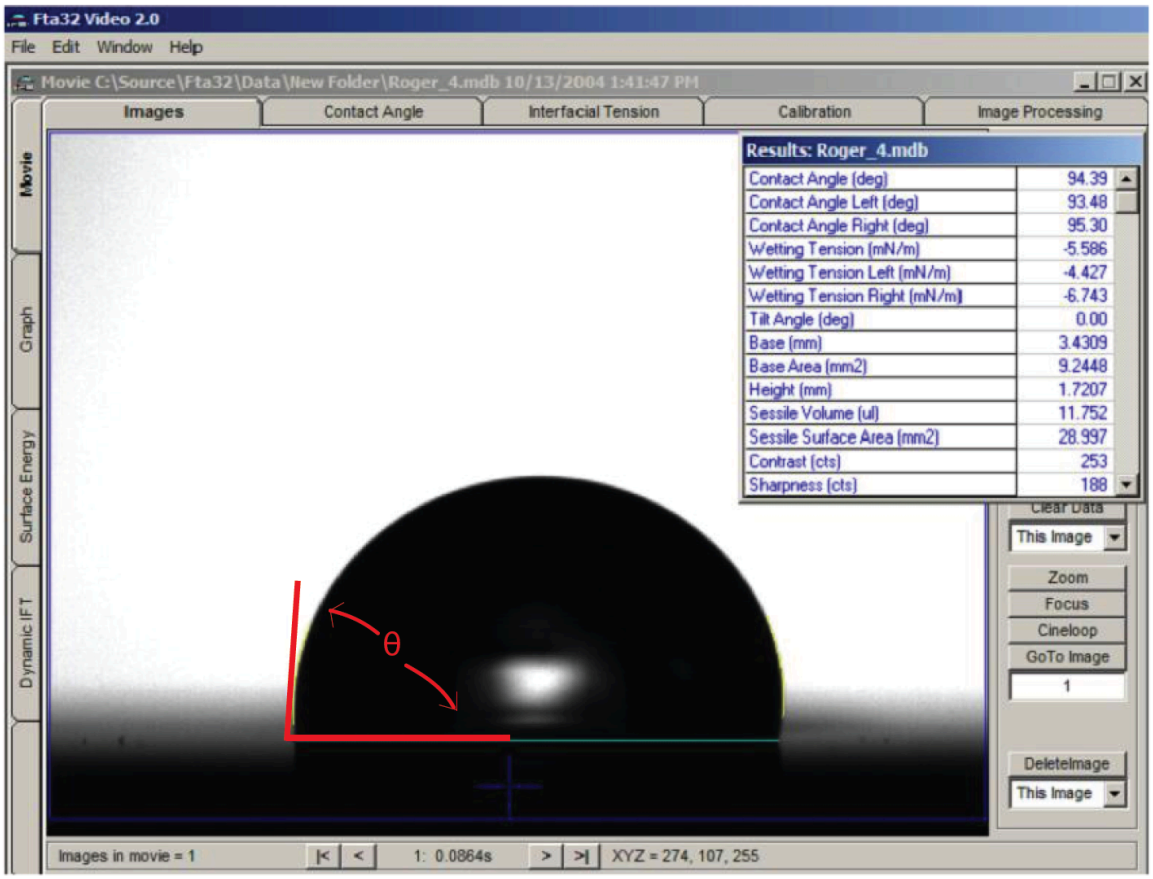

Figure 9. Depiction of sessile drop method.

To obtain the desired shapes for printed wires and devices, wetting control is required on the substrate surface. Many methods to control wetting exist, and are utilized to either promote or prevent the spread of printed inks. Historically, in graphic printing, two main methods have been utilized for the control of ink wetting: chemical treatment and physical treatment.

Making a low-/high-energy state of the surface is the basic idea behind chemical treatments. Table 2 provides a few surface energies for some typical polymer substrates. Plasma cleaning of substrate surfaces usually creates a high-energy state on most surfaces, resulting in the promotion of wetting and spreading. CF_4 plasma treatment, in contrast, creates a fluorinated layer on the surface in a very low-energy state. A CF_4 plasma treatment of 1 to 2 minutes will very rapidly decrease the contact angle, making it very useful in R2R production. A selective hydrophobic treatment such as fluoridation can create a fine pitch pattern at widths of less than 1 μm.

Table 2. Surface energies for some typical polymer substrates (Taken from [29]).

Surface Energy (mN/m)	Typical plastic	Properties
10-20	Silicone Fluorocarbon polymers	Water Repellant
20-35	Polyethylene Polypropylene	Hydrophobic
35-50	Polyester Nylon Epoxy Acrylic Resin PET	Polar
50-60	Polyvinyl alcohol Cellulose Polyvinylpyrrolidone	Hydrophilic

The ability to achieve high ink wetting of a substrate is essential for promoting adhesion. Adhesion is defined by surface energy and interfacial tension. The term adhesion refers to the attraction of molecules within one material to the molecules of a different material. One of the most common methods of adhesion used in the graphic printing industry is that which is produced through hydrogen bonding. As many of the substrates used in graphic printing are cellulose and/or pulp based, they provide an abundance of hydrogen bonding sites enabling high levels of adhesion. Cellulose-based substrates are often highly porous, at least in comparison to the polymer substrates dominant in functional

printing, allowing for high levels of ink absorption further increasing adhesive properties. Though, the graphic industry also uses polymer substrates such as PET, the ability to use resin systems with appropriate chemistry enabling lower surface tension of ink than the surface energy of the substrate, enable proper adhesion of graphic inks to these substrates. In functional printing, the use of high levels of resin and/or other additives results in detrimental negative effects to conductive functional properties and thus renders their implementation implausible as a means of optimizing adhesion, thus ink needs to be modified more with solvents, given that proper resin chemistry and resin properties were chosen. Also, while the adhesion of graphic inks to cellulose-based and PET (polyethyleneterepthalate) substrates have been well studied, similar studies with functional inks have not yet been conducted to any great extent. Since the chemical composition of functional inks varies greatly in comparison to graphic inks, due to limitations in the amount of resin and additives that can be used without interfering with the functional properties of the ink, such studies are warranted if their adhesion properties are to be improved.

2.6 Inks for Printed Electronics

Functional inks for PE applications are not new. Screen printable conductive paste inks have been commercially available for almost 25 years for use in membrane switches, discrete touch device activated products and touch array display screens. These formulations have high solids loadings with most the solids being contributed by the metallic constituents that make them conductive. Silver, carbon and copper paste inks are some of the more common inks available, with silver being the most predominant ink used in current PE market applications [2]. By using existing ink formulation knowledge, new lower viscosity inks that overcome the challenges of ink stability, compatibility, wetting properties, functional requirements and costs are being studied and developed for use with higher throughput gravure [31] and flexo [32] printing processes. Functional inks in use today include metallic flake, nanoparticle, and metal-organic-decomposition (MOD) conductive inks, dielectric inks, conductive polymeric inks, semi-conductive inks, resistive inks, and even those containing biological materials such as DNA [29]. Functional inks for PE are often

categorized by either their electrical functionality (as mentioned above), solvent system (non-polar, polar aprotic, and polar protic), or lastly by the morphological makeup of the functional components (i.e., flake/nano-particles, metal-organic-decomposition, and polymeric). Depending on the end-use of the ink, printers need to first choose the functional characteristics of the ink, then depending on the printing process and substrate to be used, will most likely choose the solvent system, and will subsequently (likely) choose the constitutive makeup. There may be some interchangeability between or even the possibility of multiple process-ink combinations that will work for a particular application, though, as in any other industry, there is always a best choice based on economic benefits. The critical attributes for a conductive ink to have for use in PE applications are shown in Table 3.

Table 3. Critical attributes for a conductive ink to have for use in PE applications.

	Attributes
Conductor	• Metal or conductive organic polymer base • Transparency (For certain applications) • Bulk conductivity > 10^4 S/m • Low processing temperature (< 200 °C)

Previous knowledge from graphic ink formulations can be applied for functional inks; however, the effect of traditional ink ingredients on final electrical performance must be well appreciated due to the potential negative influence on final performance. Inks for conductive layers are typically based on dispersions of metal or graphite particles or intrinsically conductive polymers in an appropriate solvent/binder system. Metal particles can be of various shapes and sizes. Very often, silver flakes are used in conductive ink formulations for passive components. Such inks typically contain a high loading of silver flakes leading to complex rheology and reduced stability in storage [33]. Nanosized metal particle inks are also popular due to lower sintering temperatures [34]. The high surface area of nanoparticles leads to increased agglomeration and thus such inks are usually formulated with organic stabilizers, which keep the nanoparticles apart and stable [35]. Considering conductive and semiconductive polymers, their limited solubility and processability make it more difficult to formulate inks. The concentration of conductive polymers is typically very small (approximately 1% for inkjet and up to 5 to 6% for

gravure or flexographic printing depending on materials solubility). Low concentration inks require longer drying times, due to the increased amount of solvent and additives present, and hence, are often created with thinner ink films to allow for adequate drying times.

The major component of any conductive ink is its conductive filler, or conducting polymer. Metallic inks can be composed of metallic flakes or metallic nanoparticles. While there is no universally accepted definition of a nanoparticle, the United Kingdom's Publicly Available Specification 71 (PAS71) does state that a nanoparticle is, "A particle having one or more dimensions of the order of 100 nm or less". The PAS71 also notes these particles' characteristics, stating: "Novel properties that differentiate nanoparticles from the bulk material typically develop at a critical length scale of under 100 nm" [35]. Nanoparticles may come in many different shapes, including spheres, flakes, rods, tubes, fibers, wires, and random assortments of such. The size and shapes of these particles play an important role in determining their printability, functionality, and cost. It is commonly believed that for the screen printing process it is required to have a particle size to (pixel) screen-open-area ratio of 1:3, to allow particles to readily pass through the screen in order to retard plugging. It has also been thought that the aspect ratio (length to width ratio) of these particles is correlative to percolation threshold, as generally it appears conductive percolation paths (often) are more easily set up between long and thin nanoparticles. Typical methods of dispersing these particles in inks are either physical or chemical. Physical dispersion, separation of nanoparticle agglomerates (which are held together by van der Waals forces), is accomplished mainly by three processes: (a) ultrasonic agitation, (b) shear mixing, and (c) ball milling. In the most popular dispersion method, ultrasonic agitation, particles first are manually stirred in a solvent before subsequently being exposed to the ultrasonic waves/irradiation breaking the agglomerates apart. In shear mixing, the particles are forced apart by high-speed shear. Lastly, ball milling consists of a rotary cylinder and metallic or composite balls, which break aggregates apart. In chemical dispersion methods, there are covalent and non-covalent bonding methods. The exact techniques used in performing these methods will vary based on the [precise atomic make-up of particles, as-well-as their desired functional/performance characteristics.

Printed electrodes are one of the essential components of any PE or conventional electronic product. There are several types of electric conducting materials available for use in PE applications. They include metallic materials such as Ag, Cu, and Au, organic molecules such as PEDOT/PSS Poly(3,4-ethylenedioxythiophene)poly (styrenesulfonate), and ceramics, such as oxides and carbon nanomaterials. As for their use in printing wires or electrode materials, electrical conductivity is the most important property; hence, metallic materials are usually the first material of choice. Table 2.4 compares the electrical conductivity of these materials. The electrical conductivity of carbon materials such as carbon nanotubes (CNTs) and graphene cannot be directly compared with that of other materials because no bulk material property information is available for these nanomaterials. As shown in Table 4, metallic materials, especially Ag and Cu, possess the best values among all the different types of conductive materials, and it should also be noted that these values represent the bulk properties of these materials; hence, there is the possibility of even greater (higher) values when they are formed into nanoparticles.

Table 4. Comparison of electrical conductivity of materials used in printing conductive tracks (Modified from [29]).

Materials		Electrical conductivity (Siemens/cm)
Metals	Ag	6.2×10^5
	Cu	5.9×10^5
	Au	4.4×10^5
	Pt	1.0×10^5
	Ni	1.4×10^5
Organic	PEDOT/PSS	$1\text{-}10^3$ (Will vary based on doping/composition, oxygen, defects, and crystallinity)
Inorganic	ITO	$10^3\text{-}10^4$
	CNT	1×10^5 cm^2/V s
	Graphene	2×10^5 cm^2/V s

For most types of metallic inks, water-based and solvent-based inks exist. Nanoparticles can be fabricated at different temperatures, e.g., room temperature up to 200 °C, for a few minutes using solution-based processes. Metallic nanoparticles are usually formulated after stabilization using a thin organic layer (or oxide layer) on them. Organic layers can be monomers or polymers suitable to each core metal. An appropriate surfactant or additive (Table 5) is added to preserve nanoparticles at the nanometer scale by preventing their agglomeration.

Table 5. Common additives used with respective metallic particles (Taken from [29]).

Nanoparticles	Additive
Au	Dodecanethiol, octadecanethiol Triphenylphosphine Phthalocyanine Polyvinylpyrrolidone (PVP) Polyethylene glycol (PEG)
Ag	Dodecanamine Phthalocynine Polyvinylpyrrolidone (PVP) Polyethylene glycol (PEG)
Cu	Polyvinylpyrrolidone (PVP) Polyethylene glycol (PEG)

Polymeric surfactants or additives usually work with most inorganic nanomaterials since they themselves cover nano objects well by forming networks. Since their networks are so strong, they are usually not easily removed during application and processing.

Rod/wire or sheet like nano-scale particles can be achieved by modifying the reaction composition by adding small amounts of suitable agents. Silver nanowires (AgNWs), are being investigated as a replacement for Indium Tin Oxide (ITO), which is the conventional, optically transparent conductive electrode material currently being used in the market place [36]. ITO has the advantage of being transparent, but is most often required to be applied using costly vacuum deposition and etching processes. ITO can be printed [37], however, there are still concerns pertaining to shortages and the high cost

associated with Indium. Nanoparticles from 1 nm to several hundred nanometers in diameter can be produced using solution-based processes. Brust et al. [38] first reported the ability to synthesize 1–3 nm Au particles in solution with a surface coating of thiol [3, 4]. It has been well established that Au forms strong chemical bonds with S (sulfur) in thiol molecules. This finding has been used by several researchers to produce stable Au nanoparticles [4–6]. The advantage of nanometallic particles is that they can be easily formulated into suitable inks that can be applied by multiple printing processes. Their low viscosity at 10-15% solids makes them especially suitable for inkjet, flexo, and offset-gravure printing [2]. In low viscosity ink, if solute particles are too large, they cannot be dispersed uniformly within the solvent. As a result, they easily settle out during storage, causing these inks to have poor shelf life. In contrast, small particles at the nanometer scale can be preserved in a solvent without significant sedimentation due to Brownian motion. Here, after an ink is made, it can be stored at room temperature for months.

The second attractive feature of nanoparticle inks is the high surface energy state of the particles. In general, the energy state of atoms within a crystalline body is the lowest, whereas atoms on the surface have a higher energy state than those inside the crystal due to dangling bonds on the material surface. As the size of particles decreases, the influence of the surface energy increases, resulting in a high-energy state of particles. Buffat et al. [39] measured this effect on the melting temperature of materials using electron diffraction spectroscopy with the aid of a simulation [2]. This work showed that the melting temperature evidently, decreases as the diameter of particles decrease. In particular, below 20 nm, melting temperatures rapidly decrease. On the other hand, size effects on sintering nanoparticles can be observed even for larger nanoparticles of up to 100 nm.

It is known that Ag nanoparticles have been used for many decades for their antimicrobial properties [8]. The solution process for manufacturing Ag nanoparticles has been well established [9, 10]. Ag nitrates are decomposed with a reducing agent into Ag ions in a temperature range of 150–200 °C. Amine-based molecules have been often used as a surfactant for Ag nanoparticles, which also plays the role of reducing agent in a solution process. It is easy to synthesize a single nanometer to several hundred

nanometers of Ag nanoparticles by controlling the reaction conditions. Nevertheless, the detailed mechanism of atomic bonding between alkylamine and Ag has not yet been clarified.

In comparison to metallic materials, organic materials such as different composites provide low electrical conductivity. While organic materials will not replace metals in applications requiring high electrical conductivity they are being used in some PE applications due to the ability to formulate them into inks. These materials are also attractive for PE use because they are soft and flexible, inexpensive, and compatible with aqueous and organic solvents. For these reasons, there is a great potential for their use as printed electrodes or wires with PE applications as TCF materials.

Among polymer-based conductive materials, superior electrical conductivity characteristics have been found for thiophene [PEDOT/PSS, poly(3,4-ethylenedioxythiophene) poly(styrenesulfonate). Although PEDOT is insoluble intrinsically, it becomes soluble in the presence of polystyrene sulfonic acid (PSS) as a colloidal dispersion in an aqueous solution. Further, the addition of an aqueous solution having the same charge system is also effective as a PEDOT/PSS mixture of polyvinylpyrrolidone (PVP). Recently, its conductivity characteristics have been improved [28]. Various types of doping have also been proposed both for conductivity improvement and for increasing stability. It has been shown that a conductivity of up to 1,000 S/cm (which is almost equivalent to that of ITO) can be achieved. PEDOT/PSS can be characterized as a very stable conductive polymer with respect to temperature and humidity. Nevertheless, environmental stability is one of the issues to consider with typical polymer materials.

Along with the requirements to formulate inks that will provide the desired electrical functionality, it is also required to formulate inks that will have proper runnability. For example, with high speed processing (e.g., printing), there is a possibility of ink foaming, which is a consequence of recirculation and high turbulence of ink in the inking pan. Bursting of trapped air bubbles upon drying can create defects in the resulting film and thus some ink formulations require the addition of de-foaming additives. Eliminating ink

foaming is especially important when processing functional layers where uniform and defect free layers are crucial for proper functioning. As can be seen, functional inks are slightly more complex in comparison to conventional graphic inks and require a great deal of tailoring to enable desired performance.

2.7 Substrates for Printed Electronics

Printed electronics also requires advanced materials technology for substrates. The requirements include flexibility, excellent transparency in many cases, surface smoothness, thin and lightweight, low thermal expansion, stiffness, heat resistance, low cost, and others. Several choices are available as substrates depending on the nature of the PE product. Substrates for PE may be flexible or rigid, and porous or nonporous. Table 6 lists materials commonly used in PE products.

Table 6. Materials commonly used as substrates in PE (Taken from [29]).

	Thickness (μm)	Density (g/cm^2)	Transparency (%)	Haze (%)	Tg (°C)	Process Temperature Limit (°C)
PET	16-100	1.4	90	Approx. 0.3	80	120
PEN	12-250	1.4	87	Approx. 0.8	120	155
PI	12-125	1.4	-	-	410	300
Glass	50-700	2.5	90	0.1	500	400
Paper	100	0.6-1.0	-	-	-	130
Transparent paper (made of nanocellulose)	20-200	Approx. 1	90	1-2	200	150
Steel	200	7.9	-	-	-	600

A glass substrate is an attractive transparent substrate and has been widely used for most optical purposes such as displays, photovoltaics, and lightings. Its transparency is greater than 90 %, with a haze far below 1 %. Thin glass substrates are now commercially available [40]. The thickness of glass substrates has already reached 30 μm. In contrast, the weakness of glass substrates is their brittleness, heavy weight compared with plastics,

and high cost. To provide flexibility and robustness to PE products, plastic, paper, or steel substrates are better.

PET film is the most popular and widely used plastic film within the PE industry. It has high optical transparency above 90 % and the great benefit of low cost compared with other substrates. A known drawback pertaining to the use of PET is its poor heat resistance. Due to its poor heat capability, all printing processes utilizing PET must be performed at low temperatures (below 130 °C), and under low tension. The heat resistance improves for polyethylene naphthalate (PEN), and improves further for polyimide (PI), however, with increasing these materials heat resistance their transparency decreases and costs increase. Though polymeric films are the first choice for PE products, several things must be carefully controlled to minimize distortion, especially for roll-to-roll printing. The factors that must be controlled are the atmosphere (temperature and humidity), tension, and drying. Printers must also have some level of distortion detection and high-resolution imaging with high-speed web handling.

2.8 PDMS

PDMS, poly(dimethylsiloxane), is a silicone elastomer with properties that make it desirable for use in many applications. PDMS is especially highly desirable for use with biomedical applications, and it has been used in such applications for the creation of implantable, as well as wearable devices. PDMS is desirable for use in such applications due to its many advantageous properties. These properties include biocompatibility, chemical inertness, thermal stability, gas permeability, flexibility, and transparency. These properties are a result of its molecular structure (Figure 10).

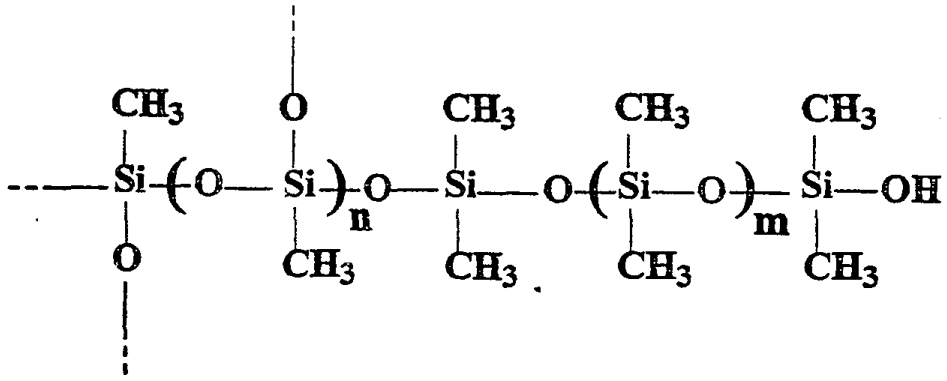

Figure 10. Molecular structure of PDMS [41].

However, as a consequence of this molecular structure, the ability to adhere functional inks to its surface is a challenge. Further, the implementation of its use for such biocompatible PE systems has been limited due to difficulties involved in integrating, embedding, and/or patterning of (metallic) inks onto its surface due to its weak adhesion to metals. As contemporary PE is accomplished using additive processes for deposition of materials, one of the main limitations to the use of these substrates (other than the functional characteristics of the created systems) is the ability to properly match ink-substrate properties to optimize interactions enabling desired functional and mechanical properties of the end-use system. The tailoring of substrate properties is essential to the viability of the future of PE. A few key substrate surface properties are porosity, permittivity, smoothness, hydrophobicity/hydrophilicity, surface-free energy, adhesion, water/chemical resistance, and cleanliness. Bulk properties of the substrate materials are also of great importance; these include biocompatibility, glass transition temperature, tensile strength, flexibility, electrical properties, resistance to electric-erosion, and dimensional stability, to name a few. By better characterizing these parameters and their interactions with inks (as they pertain to PDMS) their effects on the final output will be better understood and there will be a greater ability to properly match properties and interactions, enabling the creation of more efficient and robust solutions processed. This research aims to provide new information on the mechanisms and optimization of adhesion of conductive (metallic) inks to PDMS. As PDMS is a biocompatible, thin, flexible film, there is substantial interest in its application to PE for medical devices. However, due to the known processing concerns, it is currently unavailable for use with

roll-to-roll manufacturing. The desire to use PDMS as the substrate for biosensors is a driving motivation for much current research, including this dissertation.

2.9 PDMS for Biosensors

The properties of PDMS make it desirable for use in biomedical applications. It is especially attractive for use in the development of biocompatible MEMS and microfluidic sensors [42, 43]. Some of the benefits of PDMS aside from biocompatibility are flexibility, low cost, low toxicity, high oxidative and thermal stability, optical transparency, low permeability to water, low electrical conductivity, and ease of micro patterning [35]. PDMS also has the ability to be formed into large continuous films, allowing for its use in roll-to-roll processing techniques, which is an important attribute enabling high throughput and low cost production of devices and components. Historically, PDMS has been used in biomedical applications as a material for catheters, drainage tubing, insulation for pacemakers, membrane oxygenators, and ear and nose implants [44]. These applications implement the PDMS for its biocompatible properties and do not require the attachment of metals, as they are mainly non-electrically functional. However, the use of this material for the fabrication of biocompatible sensing devices requires good adhesion of metallic materials to PDMS; this is presently limited due to the known low surface energy of PDMS. Currently, the use of PDMS for creation of such biocompatible devices is accomplished using conventional etching processes, or soft-lithographic processes (Figure 11). This sensor was developed through the work of Yong-Hwan Choi, et al., [45] to enable the continuous monitoring of biochemical processes.

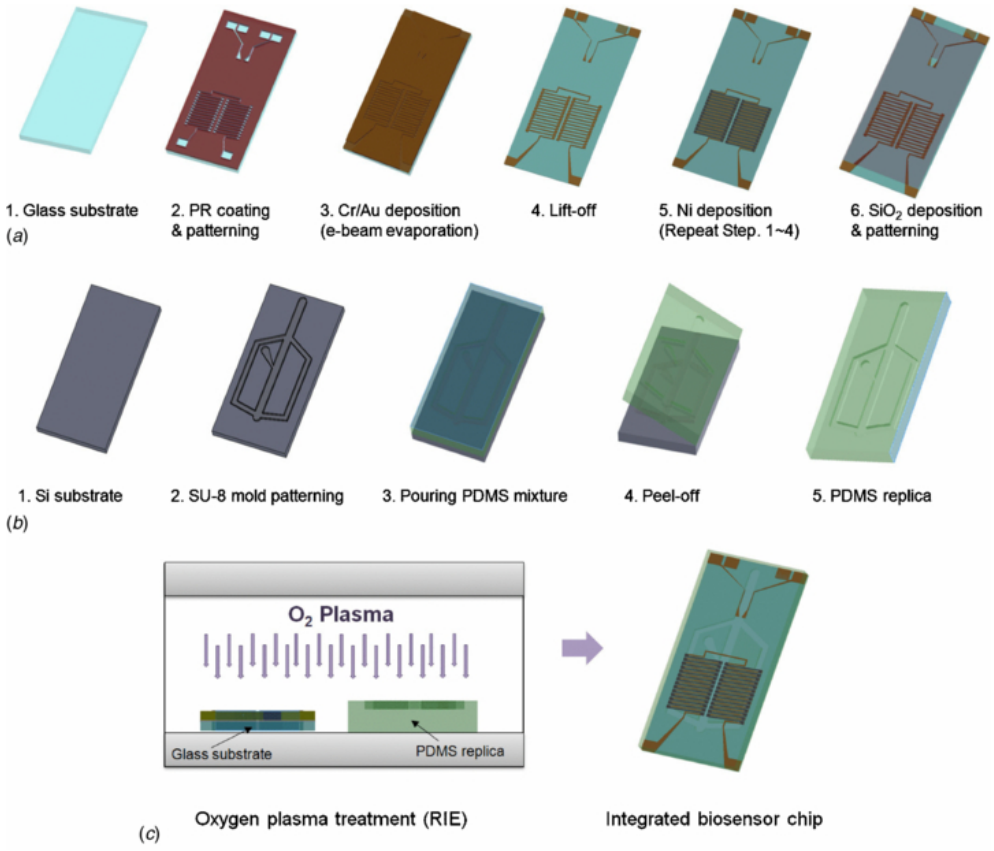

Figure 11. Typical method of creating biosensors utilizing PDMS [45].

The ability to use PDMS for the fabrication of such devices using roll-to-roll processing techniques is currently hindered by the need to use such processes, as depicted in Figure 11, to enable the creation of robust microelectrodes [46]. Therefore, the printing of metallic inks onto PDMS is one of the main challenges needing to be overcome to enable its use in roll-to-roll processing techniques for the creation of biocompatible sensing devices [20, 22].

Due to the current limitations of patterning microelectrodes on PDMS using roll-to-roll printing techniques, the use of PDMS in electronic applications has largely been driven by the use of soft lithography techniques, such as micro-contact printing, replica molding, micro-transfer molding, and solvent-assisted micro-molding [47]. These techniques often require the use of elastomeric stamps for the transfer of patterns onto subsequent substrates, which require additional processing steps, slowing production speeds and limiting throughput [3]. Additionally, these techniques often require the use of clean room facilities, and high energy processes such as vacuum deposition, further slowing

production and increasing production costs [48, 49]. Therefore, there is an increasing need to enable the use of PDMS with low cost, mass production processes.

Previous studies examining the fabrication techniques for the metal patterning of PDMS have been conducted using screen [50], inkjet [46], and flexographic printing processes [51]. However, these studies have either used additional processing steps, or created novel processing techniques, to optimize adhesion and resolution of the electrodes. This either limits the ability to incorporate these processes into roll-to-roll production or limits production speed negating its advantage in comparison to the soft lithographic techniques. For these reasons, there is a need for research pertaining to the processing techniques, such as UV-ozone and atmospheric plasma surface treatments that can be performed on press to improve the printability of metal electrodes on PDMS. It is especially important to conduct research on the optimization of surface treatment processing parameters for the promotion of adhesion of metallic inks to PDMS.

Numerous researchers have conducted studies implementing the use of flexographic printing for the creation of PE [52-54]. However, concerns still remain regarding the quality and performance of the product outcomes, especially as it pertains to the use of PDMS. Because PDMS is especially important for the enablement of the creation of printed biocompatible sensors, it has been the focus of much research as of late. For example, in the work of Maksud et al., [51] PDMS was used to create a stamp for micro-contact printing. This study found the process could be applied for the fabrication of components and devices for biomedical applications. Zheng, et al., [55] used PDMS to create an implantable self-powered pacemaker that was created using PDMS and placed into a rat for study. This work successfully demonstrated the use of the pacemaker and the ability to use PDMS for implantable biomedical devices. It further showed the material properties specific to PDMS (i.e., flexibility) were essential to the creation and success of the device. Here, the high flexibility of the PDMS was of utmost importance, allowing the device to move with the rat's movement, collecting energy to be used by the device, allowing the device to maintain power, and staying implanted. This work was of great significance as it demonstrated the *in vivo* application of a TENG (triboelectric

nanogenerator) device for harvesting biomechanical energy inside a living animal for the first time [55].

Further to the advancement of PDMS as a biocompatible material for sensing devices, Wu, et al., [46] studied the inkjet printing of silver inks onto PDMS. In this work the focus was on the optimization of the adhesive properties of silver ink on a PDMS surface. A ((3-mercaptopropyl) trimethoxysilane), MPTS, was used to modify the surface of the PDMS and improve surface wettability. A multilevel matrix deposition (MMD) method was also used to further avoid coalescence of the ink. With this procedure, it was found that the resulting silver pattern obtained excellent adhesion to PDMS, along with good uniformity and conductivity. As this is known to be an area of major concern, Kim, et al. [56], studied the influence of PDMS surface and ink characteristics on the screen printability of metallic prints. Here, the effects of contact angle and ink concentration were studied in relation to printability. It was found that, to optimize wettability, the gap spacing between lines had to be increased with an increase in the nominal line width. The printability then gradually increased as the line width increased.

Currently the use of PDMS as a substrate in printed electronic applications using R2R processing techniques is impeded by the inherent properties of PDMS leading to issues of adhesion and printability. Also, the use of PDMS is made difficult due to the difficulty in manufacturing the material as a substrate having the required characteristics (i.e., low caliper, high smoothness) to enable its use in R2R applications. Research is needed to advance the knowledge of the field to better enable to use of this substrate for use in R2R printed electronic applications.

The above-described works provide the groundwork for further research into the use of PDMS as a substrate material for use in PE applications. As discussed above PDMS is especially important for the development of biocompatible devices; therefore, continual research is of interest to material suppliers, device designers, and printers alike. As a consequence of the knowledge needed to use PDMS widely, this research aims to provide knowledge of surface treatment processing methods and material interactions pertaining

to the development of PE devices utilizing PDMS. To accomplish this goal, four studies were performed, and are discussed below.

CHAPTER 3

CHARACTERIZATION OF SURFACE TREATED SILICA-FILLED AND NON-FILLED POLY(DIMETHYLSILOXANE)

3.1 Abstract

In this work, various methods to enable the tailoring of poly(dimethylsiloxane) film surfaces were implemented and compared to determine their influence on surface energy and roughness. Films were prepared containing different levels of hydrophobic filler. Ultraviolet-ozone, and Piranha solution treatments were implemented and characterized. Lastly, the combination of both silica filler and treatments were utilized and characterized to understand their interactive effects. The influence of filler loading, and surface treatment on roughness, and surface energy of the films was examined. It was determined that regardless of surface treatment applied, the addition of silica had a significant influence on the total surface energy of the PDMS films alone and in combination with the Piranha and UV-ozone treatments. Through the application of these surface treatments, the total surface energy of the PDMS film was raised from 21.5 mN/m to 44.1 mN/m, a value that would make it wettable by more fluids. The highest surface energy was obtained through the combination of loading the PDMS with 10% silica filler and chemically treating the film in a Piranha solution for 30 minutes. The Piranha solution was found to change the macroscopic surface roughness of the films more significantly than the UV-ozone treatment, which had little effect on increasing the surface roughness of the films.

3.2 Introduction

PDMS, poly(dimethylsiloxane), is becoming of increasing interest for use with medical devices and applications [46, 57]. PDMS is highly desirable for such applications due to its high biocompatibility and flexibility enabling its use for both wearable and implantable devices [55, 58]. Properties that make it desirable for use in these applications also include chemical inertness, thermal stability, gas permeability, and transparency. These properties are a result of its molecular structure as seen in Figure 12.

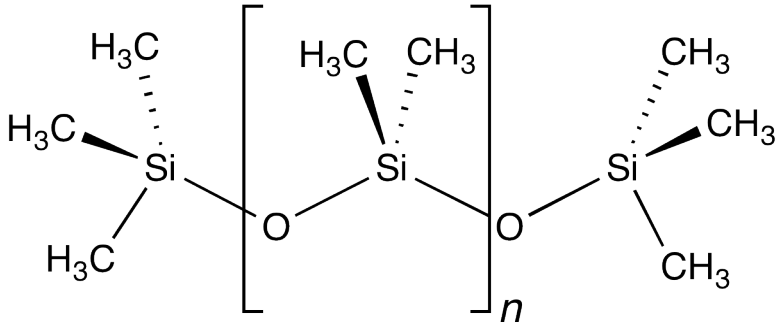

Figure 12. Molecular structure of PDMS [59].

However, as a consequence of this molecular structure, the ability of functional inks to wet and adhere to its surface is a challenge. Further, the implementation of its use for such biocompatible printed electronic (PE) systems has been limited, due to difficulties involved in the integration, embedding, and/or patterning of (metallic) inks onto its surface, due to their weak adhesion to its surface. As contemporary PE is accomplished using additive processes for deposition of materials, one of the main limitations to the use of these substrates (other than the functional characteristics of the created systems) is the ability to properly match ink-substrate properties to optimize interactions enabling desired functional and mechanical properties of the end-use system. The tailoring of substrate properties is essential to the viability of the future of PE. A few of these key substrate surface properties are: porosity, permittivity, smoothness, hydrophobicity/hydrophilicity, surface-free energy, adhesion, water/chemical resistance, and cleanliness. Bulk properties of the substrate materials are also of great importance; these include biocompatibility, glass transition temperature, tensile strength, flexibility, electrical properties, resistance to electric-erosion, and dimensional stability, to name a few. The use of PDMS for the development of functional electronic devices (i.e., sensors) has been of particular interest in recent years; especially, in such applications where implementation of printing techniques may be employed [42, 60, 61]. The use of PDMS in such applications is impeded heavily by complications pertaining to its wettability [62, 63]. This is especially true as it pertains to its utilization with high-speed processing techniques. A major challenge resultant of the inability to properly wet PDMS films is the inability to obtain the desired levels of adhesion of materials to the films surface [22, 64]. This inability to properly adhere materials, most notably metals, to the film surfaces

greatly reduces the ability to utilize high-speed processes (e.g., flexographic printing) in the development of functional (electronic) devices. The ability to deposit metallic materials is essential for the creation of the wiring required for such devices. As electrical conductivity is the most important property for wiring materials to have, metallic materials are most often the materials of choice. As the application of biocompatible printed sensors evolves, the need for high efficiency, robust PDMS sensors grows. As a result, there is an increasing need to improve the printability of PDMS, both as the active material in ink and as a substrate for other functional inks. This requires a more comprehensive understanding of the surface treatments and influence of filler loading on the surface energy and wetting characteristics of PDMS films. PE devices have been developed using screen [24], gravure [26, 31, 65], flexographic [27, 47-50], and inkjet [23, 25, 66, 67] processes. However, the printing of devices or components has been very limited with regards to the use of PDMS. This is in part due to the known complications pertaining to the wetting and adhesion of metallic particles to PDMS substrates.

One of the essential components for most PE devices is an effective functioning electrode; for which a continuous film is needed. Often silver is used due to its beneficial properties, such as high conductivity and low oxidation, as well as its lower cost in comparison to gold. Copper has also been utilized as it enables high conductivities, however, it does not posses some of the other characteristics desired for use in medical applications. With regards to its use in biomedical applications, it is advantageous to possess high antimicrobial characteristics, which silver delivers. The ability to encapsulate copper particles in silver shells [68] has recently been shown, and could be beneficial in cases where encapsulation of the device is not needed or desired. Although some researchers have shown the ability to print conductive inks onto PDMS, the need to encapsulate the device was required, to obtain the required robustness and efficiency throughout the lifetime of its use [55, 61].

By better characterizing surface treatments and their influence on the wettability of PDMS, their effects on the final output can be better understood resulting in a greater ability to properly match the properties between substrate and inks for the creation of more efficient and robust PE devices. While the effects of UVO and Piranha treatments

on non-filled PDMS have been reported, a comparison of these treatments in combination with various levels of modified silica filler loading has yet to be reported. In addition, the effects of these treatments on filled silica PDMS films where various treatment times have been applied are new. It is hoped that from these results, those working in the field of PE can advance the wetting and adhesion of conductive metallic films on PDMS. This work sought to advance the knowledge of PDMS surface treatment methods to enable its surface energy to be raised where by its wettability, and hence printability could be improved. The desire to use PDMS as a substrate for biosensors was the driving motivation for this study.

3.3 Experimental

PDMS films were prepared using Sylgard-184 (supplied by Dow Corning, Midland, MI), and hydrophobic fumed silica (Degussa, Jetsil® AK 15). PDMS Sylgard-184 is a heat curable PDMS supplied as a two-part kit consisting of pre-polymer (base) and cross-linker (curing agent) components. The manufacturer recommended that the pre-polymer and cross-linker be mixed at a 10:1 weight ratio, respectively. The hydrophobic fumed silica had a particle size of approximately 1.5 microns; as measured by Submicron Particle Sizer Model 370 (PSS Nicomp). Once mixed, the polymer mix was allowed to degas in ambient conditions for approximately 1 hour, after which time 30 grams was poured into a 0.7" x 0.4" (L x W) mold. The mold was leveled on a plate and placed onto a leveled shelf within an oven at approximately 140°C for 20 minutes to obtain films of uniform thickness. Once dried, the films were placed in a desiccator and allowed to sit for 24 hours prior to being removed from the mold. The films were then cut into strips (6" x 0.25", L x W) to enable their surface energies to be measured. The surface energy and roughness of the filled and non-filled PDMS films were characterized before and after being exposed to two different surface treatments for various periods of time. The two treatments applied were 1) ultraviolet ozone, UVO, ('Jelight' Irvine, CA model 144AX) and 2) submersion in Piranha solution (3:1 ratio of H_2O_2 and H_2SO_4). The surface energies of the films were measured using a FTA 200 (First Ten Angstrom Dynamic Contact Angle) measurement apparatus. The Owens-Wendt method was used for determination of the surface energies. It is one of the most common methods used for

estimating the surface free energy of solids and the two most frequently used measurement fluids used are water and methylene iodide (diodomethane). This method was used to estimate the surface energies of the films. The contact angles of water and methylene iodide were measured with a First Ten Angstrom dynamic contact angle measurement device, which captures the change in contact angle with time with a high-speed video camera [69] and [70]. The static contact angles (sessile drop method) of two liquids, ultra high filtered deionized water, and methylene iodide were measured. Contact angle measurements were taken on the topside of the PDMS films, that is, the side that was in contact with the air (not the side in contact with the mold). Once captured, the change in contact angle with time was plotted, and the equilibrium contact angle obtained and used in the estimation of the surface energy of the solid to which the liquids were applied. Five contact angles were obtained for each fluid from which five surface energy values were estimated. The average surface energies (total, polar and dispersive) for each sample are reported.

After completion of these measurements, new strips were taken from the same molded film and were UVO treated using a Jelight® (Irvine, CA) model 144AX UVO cleaner. Samples were subjected to UVO treatment times of 10, 20, 30, and 40, minutes allowing determination of treatment impact on surface energy. Samples also underwent treatment using a Piranha Solution (3:1 concentrated sulfuric acid to 30% hydrogen peroxide solution) soak. These samples were soaked for 10, 20, 30, and 40 minutes to determine treatment impact on surface energy.

The roughnesses of the PDMS films were measured using a Contour GT-K (Bruker Corporation) white-light interferometer. Topographical imaging was carried out in variable scanning interferometry (VSI) mode using a 5X objective giving a sample area of approximately 1.25 mm x 0.98 mm (L X W). The surface roughnesses of the samples were obtained in terms of the arithmetic mean of the surface roughness (Sa). The thicknesses of the films were found using a Mitutoyo (Absolute Digimatic) digital micrometer. Ten measurements from each sample set (% silica fill) were taken. Two different sample films per condition were used from which five measurements were taken from each.

3.4 Results and Discussion

The results of the thickness measurements are shown in Table 7. The results show a decreasing trend in thickness with the addition of silica filler. This is attributed to the silica filler being denser than the PDMS. Since the films were prepared on a weighted basis, the volume of PDMS fluid applied to the mold decreased for the higher density filled silica mixtures. Due to the care in making the films to ensure the molds and drying trays were level, as shown, the standard deviations of the PDMS films were low (0.1 mm) for all conditions.

Table 7. Average Thickness of PDMS Films.

PDMS Silica Fill (%)	*0*	*5*	*10*
Thickness (mm):	1.5 $\pm$ 0.1	1.4 $\pm$ 0.1	1.3 $\pm$ 0.1

The results of the roughness measurements for the untreated (control sample set) PDMS films are shown in Table 8. Topographic images of the surfaces of the untreated 0, 5, and 10% silica filled PDMS films are shown in Figures 13-15. The results show the roughness of the film to increase significantly upon addition of the 5% silica with no change between the 5% and 10% levels of addition (especially when considering the standard deviations). The lack of change in roughness between the 5 and 10% addition levels indicates a close packing of the silica particles at the film surface. This packing may also be seen in the Figures 13-15 where the additional roughness created by the silica can be seen. Some surface roughness can also be seen within the unfilled film, but this roughness is attributed to surface contaminants, such as dust, or entrapped air that was released during drying. The low standard deviations in roughness values indicate that the films are uniform, though rough.

Table 8. Average Roughness of PDMS Films (Control).

PDMS Silica Fill (%)	0	5	10
Roughness (μm)	0.04 $\pm$ 0.01	0.10 $\pm$ 0.02	0.10 $\pm$ 0.01

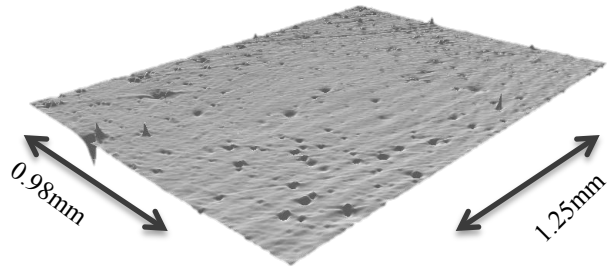

Figure 13. Topographic Image of 0% Silica Fill PDMS Film (Control).

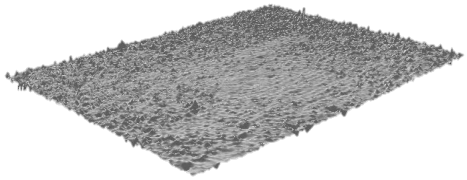

Figure 14. Topographic Image of 5% Silica Fill PDMS Film (Control).

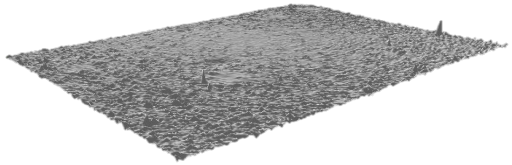

Figure 15. Topographic Image of 10% Silica Fill PDMS Film (Control).

The roughness values of the films after Piranha solution and UV-ozone treatments are shown in Table 9. The results show the roughness of the Piranha solution treated films to be quite high, in comparison to the untreated (control) and UV-Ozone treated samples, for all silica fill and treatment time conditions. The roughness of the Piranha treated unfilled (control) films were the highest of all samples tested, and showed a steady increase in roughness with time. The 5 and 10% silica filled samples showed an initial increase in roughness after 10 minutes of Piranha treatment, but did not show any significant increase with increased treatment time until the 40-minute treatment time for the 10% filled sample. This may be attributed to the silica filler slowing the interaction of the Piranha solution with the PDMS until a sufficient amount of the silica could be exposed. Once sufficiently exposed, the Piranha solution was likely able to penetrate the layer of PDMS entrapped below the silica, hence, enabling it to be affected by the solution. Topographic images of the surfaces of the 40 minute Piranha solution treated 0, 5, and 10% silica filled PDMS films are shown in Figures 16-18. These results and images show the ferocity of the Piranha solution, and its surface etching power.

In contrast to the Piranha treated film surfaces, the roughnesses of the UV-ozone treated samples are very low (Table 9) and are of similar values than those found for the control samples reported in Table 8. From the differences between the two results, it is clear that the two treatments modify the surface of the PDMS films differently. That is, the UV-ozone treatment modifies the surface by adding functional (polar) groups to the surface, while the Piranha solution roughens the macro surface. Each treatment works to increase the surface energy of the PDMS in its own way. There are no images of the UV-Ozone treated samples presented as there was no visible difference between these images and the ones presented for the untreated film surfaces.

Table 9. Average Roughness (μm) of PDMS Films with Treatments.

PDMS Silica Fill	***Piranha** Treatment Time (min)*			
	10	*20*	*30*	*40*
0%	0.94 ± 0.02	1.34 ± 0.05	1.46 ± 0.10	1.70 ± 0.02
5%	0.61 ± 0.01	0.67 ± 0.08	0.65 ± 0.01	0.65 ± 0.03
10%	0.49 ± 0.02	0.46 ± 0.08	0.48 ± 0.04	0.62 ± 0.04
	***UV-Ozone** Treatment Time (min)*			
	10	*20*	*30*	*40*
0%	0.039 ± 0.01	0.039 ± 0.01	0.039 ± 0.01	0.039 ± 0.01
5%	0.10 ± 0.02	0.10 ± 0.02	0.10 ± 0.02	0.10 ± 0.02
10%	0.10 ± 0.01	0.10 ± 0.01	0.10 ± 0.01	0.10 ± 0.01

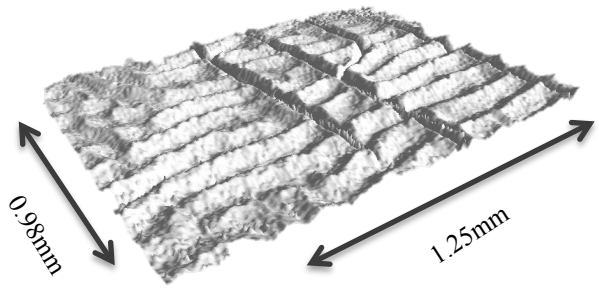

Figure 16. Topographic Image of 0% Silica Fill PDMS Film (40 min Piranha treated).

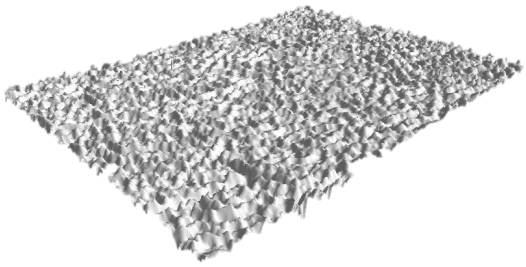

Figure 17. Topographic Image of 5% Silica Fill PDMS Film (40 min Piranha treated).

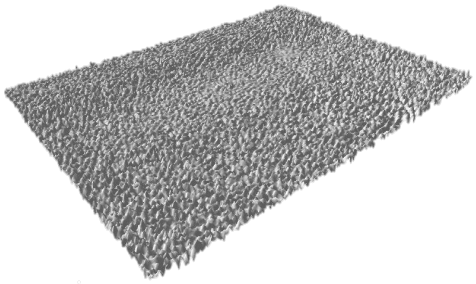

Figure 18. Topographic Image of 10% Silica Fill PDMS Film (40 min Piranha treated).

To analyze the results of the surface energies, a one-way ANOVA was performed using the Minitab® 17 software package (Minitab Inc.). ANOVAs were performed on the data pertaining to surface energies versus treatment type, treatment time, and level of silica filler added. The results are shown in Table 10. The analysis was performed both with and without the control group's data present. For all ANOVAs, the null hypothesis was that all means are equal, and the alternative hypothesis was at least one mean is different. A significance level of $\alpha = 0.05$ was used and equal variances were assumed.

Table 10. One-way ANOVA Data.

	With Control (p-value)	Without Control (p-value)
Total Surface Energy vs. Treatment Type	0.006	0.324
Total Surface Energy vs. Treatment Time (min)	0.009	0.223
Total Surface Energy vs. Silica Fill (%)	0.030	0.006
Polar Component vs. Treatment Type	0.001	0.477

Polar Component vs. Treatment Time (min)	0.000	0.092
Polar Component vs. Silica Fill (%)	0.256	0.063
Dispersive Component vs. Treatment Type	0.156	0.070
Dispersive Component vs. Treatment Time (min)	0.900	0.831
Dispersive Component vs. Silica Fill (%)	0.000	0.000

An examination of the p-values shows all factors to significantly impact the total surface energy of the PDMS films in the presence of the control. However, in the absence of the control data only the percent of silica fill addition is significant. There is no justification for omitting the control from any analyses. However, they are omitted in this case to show that much of the increase in surface energy occurs in the first ten minutes and the orders of magnitude of the values are the same regardless of treatment. This difference indicates that while treatment type and time significantly alters the total surface energy of the PDMS film, there is an insignificant difference between the total surface energies of the Piranha and UV-ozone samples. Regardless of the surface treatment, the addition of silica significantly influences the total surface energy. A comparison of the p-values for the polar and dispersive forces indicates that the changes in the observed total surface energies are the result of an increase in the polar component and the difference between polar components for both the UV-ozone and Piranha treatments are insignificant. The significance of these findings is further substantiated in Figures 19-21, which show the interactions between the main effect variables. From the total surface energy interaction plot, it is clear that there is a strong interaction between all three main effect variables.

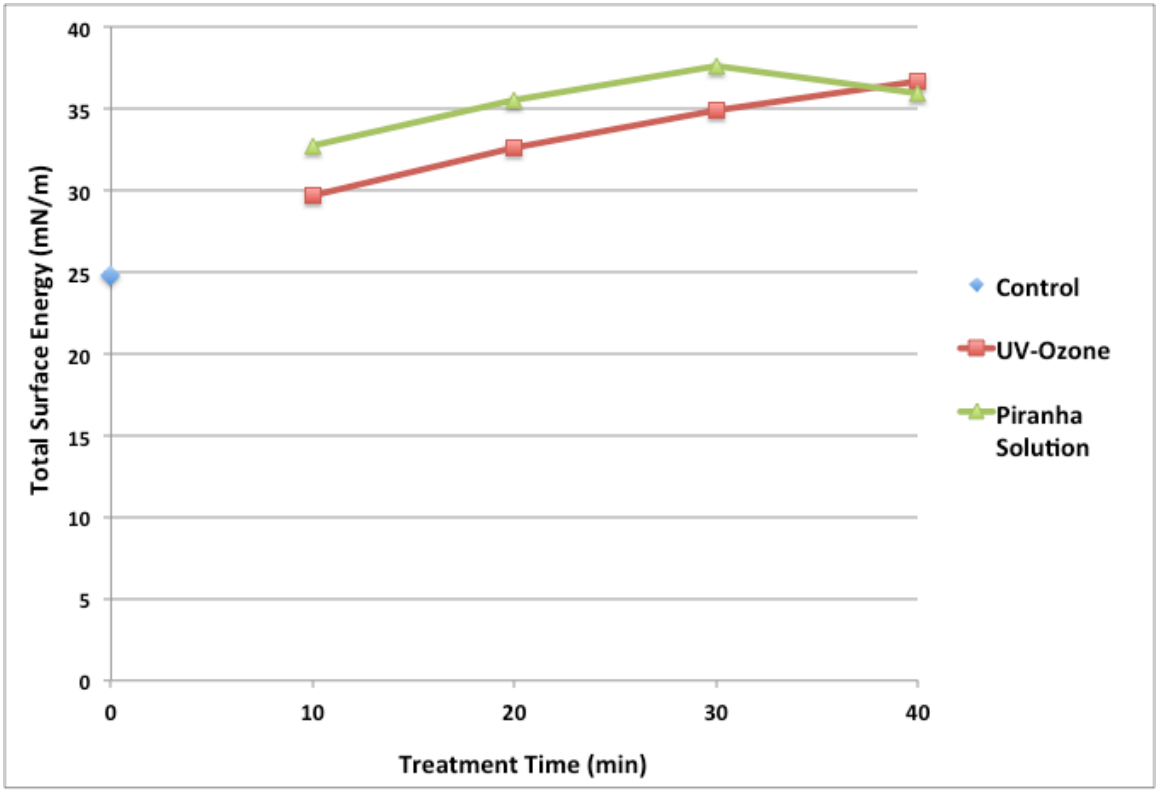

Figure 19. Interaction Plot Total Surface Energy vs. Treatment Type.

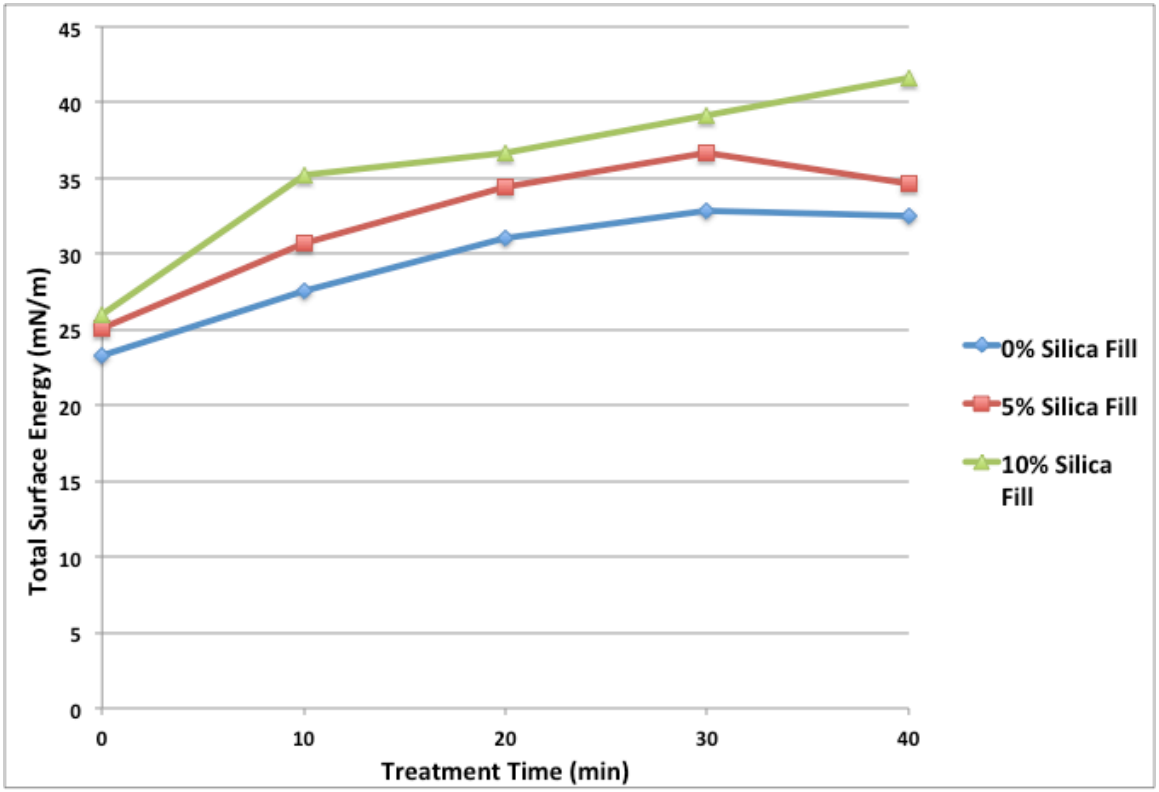

Figure 20. Interaction Plot Total Surface Energy vs. Time (min).

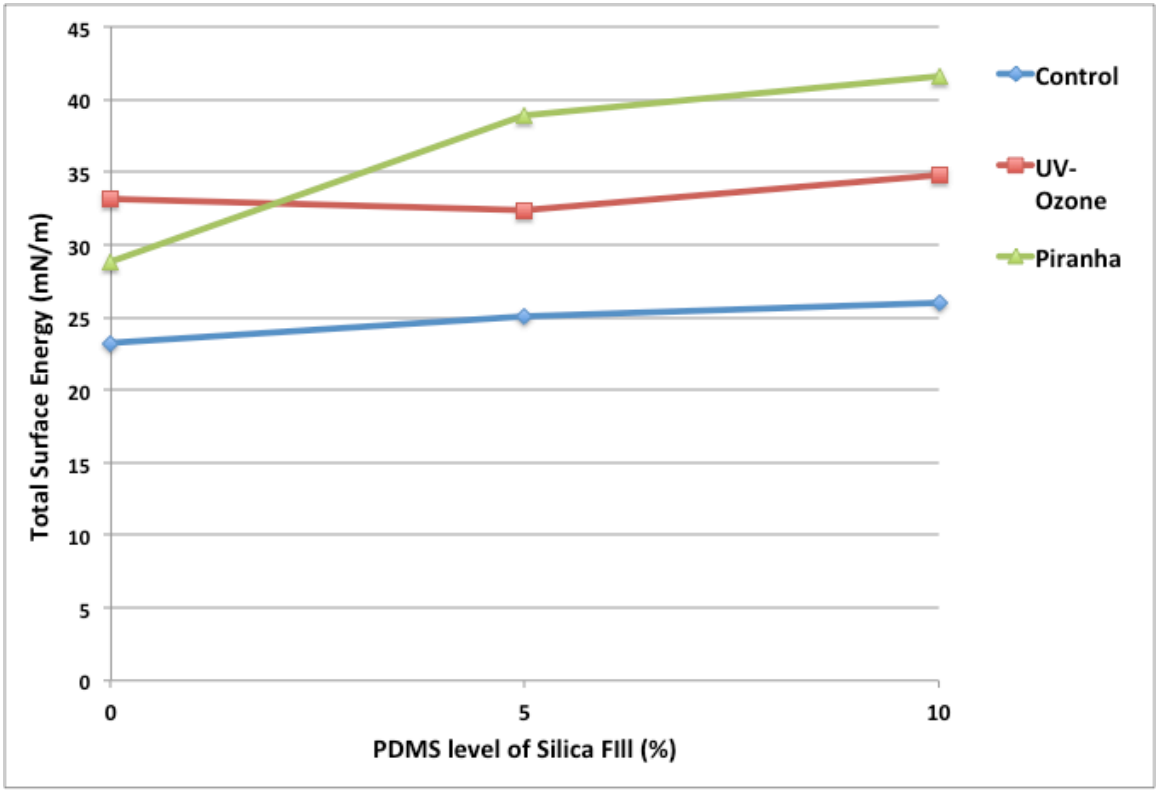

Figure 21. Interaction Plot Total Surface Energy vs. % Silica Fill.

After treatment, the surface energies of the films were again estimated. An aging study showed no immediate change within surface energies of the samples over a 20-minute period of time. After performing the surface energy estimation, the roughnesses of the films were then measured. Further ageing studies were performed after 24 hours (post treatment). These results showed the complete reversal of surface energy for the UVO treated samples, while there was no measureable impact on surface energy for the Piranha solution treated samples. A regression analysis was also performed for the surface energy versus treatment time, % silica fill, and treatment type. These results can be found in the Appendix.

3.5 Conclusions

By performing the two surface treatments, the total surface energy of a PDMS film was raised from 21.5 mN/m to 44.1 mN/m. The greatest increase in surface energy achieved was obtained through addition of 10% silica filler and 30 minute exposure to Piranha solution. The Piranha solution was found to change the macroscopic surface roughness

more significantly than the UV-ozone treatment, whose roughness was found to be close to that of the control (untreated) samples.

Both treatments influenced the total surface energy of the PDMS films by changing the polar component. The addition of silica influenced the total surface energy of the PDMS films by itself, and in combination with the Piranha and UV-ozone treatments. An aging study showed no immediate change within surface energies of the samples over a 20-minute period of time and the addition of the silica filler to have a slight positive impact on the influence of the treatments on surface energy over time.

The significance of this work is that a methodology that enables PDMS films of similar surface energies to be obtained both with and without roughening of the surface was revealed. This may be achieved by varying the treatment type and time in the presence of silica filler. These findings can be valuable to printers seeking to fabricate electronic sensors on PDMS films. Through the combination of roughness and surface energy variations the wetting and adhesion properties of functional inks can be altered to enhance sensor performance and durability. PDMS is a substrate of high interest for such applications due to its biocompatibility and this work demonstrates that with proper surface treatment or modification it may be possible to improve the wetting and adhesion of functional inks to PDMS to a level sufficient for use in PE applications where the biocompatibility is highly desired.

CHAPTER 4

THE USE OF ATMOSPHERIC-PLASMA TREATMENT TO ALTER THE SURFACE ENERGY OF PDMS FILMS

4.1 Abstract

The objective of this study was to advance the knowledge of the interaction between surface treated poly(dimethylsiloxane) (PDMS) films with flexographic conductive inks. The surface energies of PDMS films were altered by varying the length of time the surface of the films were exposed to an atmospheric O_2 plasma treatment After treatment, the films were printed with a water-based nano silver flexographic ink using a Harper QD flexographic printing press. While the surface energy of the films was successfully raised to be within 10 mN/m of the surface tension of the ink, the ink failed to wet and adhere to the PDMS film's surface. On the other hand, despite having surface energy significantly lower than the ink (> 20 mN/m lower), the untreated PDMS film printed better than the plasma treated films. XPS studies showed the treatment to be effective in replacing carbon groups with oxygen groups on the surface of the PDMS films indicating that the observed results were due to an interaction taking place between the ink and treated PDMS surface during printing Knowing that the ink viscosity was sensitive to pH, it was postulated that the oxidation of the PDMS surface could be causing enough of a shift in the pH of the ink to cause its destabilization. By neutralizing the surface of the film with NaOH prior to printing and through additional N_2 plasma treatment studies this hypothesis was confirmed and the print quality and adhesion of ink to the PDMS film was improved.

This work revealed that the generally accepted rule by graphic printers that a 10 mN/m difference between substrate and ink surface energy to achieve proper wetting, spreading, and adhesion for good print quality does not necessarily hold true for the printing of functional inks. The results show the importance of properly matching substrate surface (PDMS) and ink chemistries for good wetting, adhesion and print quality. These discoveries demonstrate the complexity of printing functional inks in comparison to graphic inks. While the general chemistries of graphic inks are well known, due to the maturity of these markets, the chemistry of functional inks is less known and can be quite

complex due to the need to balance functional performance, ink shelf-life stability and ink processability. In order for the field of printed electronics to advance, a greater understanding of functional ink chemistry and compatibility is needed. This work advances the functional printing of PDMS films and shows that innate differences between functional and graphic inks may require printers to create new general rules of practice.

4.2 Introduction

As the application of biocompatible printed sensors evolves, the need for high efficiency, robust PDMS sensors grows. As a result, there is an increasing need to improve the printability of PDMS, both as the active material in an ink and as a substrate for other functional inks. This requires a more comprehensive understanding of the surface treatments on the surface energy and wetting characteristics of PDMS films. Developments in PE have been reported with screen [16, 24, 61, 71, 72], gravure [15, 26, 73-75], flexographic [27, 51, 52, 76], and inkjet [14, 25, 46, 77, 78] processes enabling the creation of functional electronic devices. However, the implementation of high-throughput printing techniques for the development of devices or components has been limited with regards to the use of polymeric materials including PDMS [10, 31, 79, 80]. This is in part due to the known complications pertaining to the adhesion of metallic particles to these types of substrates [42, 62-64, 81]. Printed electrodes are one of the essential components of any electronic product, and to enable a high functioning electrode, a continuous film is needed. Often, Ag or Au are used due to their high conductivity. With regards to its use in biomedical applications, Ag is also advantageous due to its high antimicrobial characteristics. The commercialization of PE devices and components using naturally hydrophobic polymeric substrates, such as PDMS, will require advancements in knowledge of surface treatments, which promote wetting, allowing for higher levels of adhesion with metallic inks [82]. Although some researchers have shown the ability to adhere metal inks onto hydrophobic polymer substrates, often, the use of high-speed processing techniques has been complicated due to material compatibility issues, and process limitations. Due to these difficulties, the common practice is to direct print to film, e.g. PET, then embed the printed film within one or two

PDMS layers. The encapsulation of the film is required to obtain the required biocompatibility and to maintain robustness and efficiency during use [22].

To date the most popular printing processes for the development of hybrid/flexible electronics have been screen and inkjet printing techniques [14, 24, 61, 77, 83, 84]. Screen-printing has the advantage of depositing thick films, which is advantageous for obtaining high conductivities. However, thick films are more prone to delamination and cracking upon application of mechanical stresses. The use of these thick films also increases the cost of materials and requires longer curing times. Screen-printing also has the disadvantage that the amount of ink delivered to the substrate is dependent on the mesh size of the image carrier. With screen-printing, the mesh is both the ink metering system and the image carrier hence the mesh determines both the minimum feature size as well as the ink film thickness. Unlike the gravure and screen-printing processes, the amount of ink delivered to the substrate in the flexo process is not mainly dependent on the image carrier. This is because in the flexo process, an anilox roll is used to deliver a specified amount of ink to the flexible imaged plate, which then transfers the inked image to the substrate. To obtain ink films of different thicknesses for the same nominal resolution plate, anilox rolls of different cell volumes can be used. Hence, in comparison to the screen and rotogravure printing processes, ink films of varying thicknesses can be more readily achieved through this process. Inkjet printing provides high levels of variability to the printing process. That is, it allows printers to readily manipulate the desired print design, as well as, material and print attributes. The disadvantage to the inkjet method is the speed at which printing occurs and limitations of ink viscosities. The requirement to utilize low viscosity inks with inkjet printing subsequently limits ink solids, which can lower electrical performance. In the flexographic printing process, the amount of ink delivered to the substrate is controlled based on the selection of the anilox roll. Through anilox selection printers have the ability to achieve highly variable films thicknesses. Recent advancements in flexo plate materials and platemaking technology have greatly increased the resolutions, at which plates can be imaged. Anilox engraving technology has also improved, bringing flexo printing to the forefront of roll-to-roll (R2R) printing applications for printed electronics (PE). To achieve the desired printability and runnability, ink and process characteristics must be properly matched.

PDMS offers a challenge due to its low porosity and low surface energy. Thus, the ability to find solutions enabling these challenges to be overcome are a key to the enablement of PDMS as a substrate for use in PE applications.

For all printing processes, the properties of the ink are important to obtaining good print quality and functional performance. The flow and leveling properties, size of the ink particles, surface tension of the ink, and drying rate of the solvent carriers in the ink must all be matched to the process in order for the ink to print well on press. In addition to matching an ink to a process, the ink must also be matched to the substrate to which it is to be printed.

It has long been known that to obtain good adhesion and print quality the ink used must evenly wet the substrate. The greater the interfacial area between the liquid and substrate, the more likely an ink will sufficiently bond to a surface. For an ink to properly wet a surface, the primary forces of interest are the surface tension of the ink and the surface energy of the film. Surface tension results from intermolecular forces between molecules of liquids, while surface energy results from the reactivity of functional groups at the surface of a solid. Both terms, surface tension and surface energy are expressed in mN/m.

In order for a fluid to wet a surface the surface has to have a high enough surface energy in relation to the surface tension of the liquid. If the tension of the fluid is higher than the surface energy of the surface, the molecules of the liquid will cling together, and not wet-out. As a rule of thumb, the mN/m level of the substrate needs to be at least ten higher than the liquid in order for the liquid to wet the surface. Printers try to control the degree of wetting to achieve good print quality. If the ink spreads too much, then not only is too much line gain of concern, but thinning of the ink film (due to spreading) could result in a loss in functional performance and incomplete wetting will result in discontinuities and poor adhesion, which will also compromise functional performance.

Functional inks in use today include metallic flake, nanoparticle, and metal-organic-decomposition (MOD) conductive inks, dielectric inks, conductive polymeric inks, semi-conductive inks, resistive inks, and even those containing

biological materials such as DNA [29]. The critical attributes for a conductive ink to have for use in PE applications are shown in Table 11.

Table 11. Critical attributes for a conductive ink to have for flexible PE applications.

	Attributes
Conductor	• Metal or conductive organic polymer base • Transparency (For certain applications) • Bulk conductivity > 10^4 S/m • Low processing temperature (< 200 °C)

While knowledge from graphic ink formulations can be applied to functional inks, the effect of traditional ink ingredients on final electrical performance must be well appreciated due to their potential negative influence on final performance. Inks for conductive layers are typically based on dispersions of metal or graphite particles or intrinsically conductive polymers in an appropriate solvent/binder system. Metal particles can be of various shapes and sizes [33]. Nano-sized metal particle inks are also popular due to lower sintering temperatures [34] and ability to enable finer resolution features to be printed. However, the high surface area of nanoparticles leads to a tendency for increased agglomeration. Consequently, these inks are usually formulated with organic stabilizers (or oxide layer), which form a thin layer on the particles to keep the nanoparticles apart and stable [35]. Organic layers can be monomers or polymers suitable to each core metal. An appropriate surfactant or additive (Table 12) is then added to prevent their agglomeration at the nanometer scale. Metallic nanoparticles are usually formulated after stabilizing the particles with a thin organic layer (or oxide layer). Organic layers can be monomers or polymers suitable to each core metal. An appropriate surfactant or additive (Table 12) is then added to prevent their agglomeration at the nanometer scale.

Table 12. Common additives used with respective metallic particles (Taken from [29]).

Nanoparticles	Additive
Au	Dodecanethiol, octadecanethiol Triphenylphosphine Phthalocyanine Polyvinylpyrrolidone (PVP)

	Polyethylene glycol (PEG)
Ag	Dodecanamine Phthalocyanine Polyvinylpyrrolidone (PVP) Polyethylene glycol (PEG)
Cu	Polyvinylpyrrolidone (PVP) Polyethylene glycol (PEG)

Polymeric surfactants or additives usually work with most inorganic nanomaterials since they themselves cover nano objects well by forming networks. Since their networks are very strong, they are usually not easily removed during sintering. The solution process for manufacturing Ag nanoparticles has been well established [9, 10]. Ag nitrates are decomposed with a reducing agent into Ag ions in a temperature range of 150–200 °C. Amine-based molecules have been often used as a surfactant for Ag nanoparticles, which also plays the role of a reducing agent in the solution process. By this method, Ag particles of a single nanometer to several hundred nanometers can be synthesized by closely controlling the reaction conditions.

Numerous methods exist to increase the wettability of a naturally hydrophobic polymer [62, 63, 81, 85-90], and research continues in the advancement of methods to decrease costs and increase ease of their implementation. These methods include various chemical, plasma, and surface etching techniques. Of particular interest is the use of low-temperature atmospheric-pressure plasma treatment techniques. Atmospheric plasma offers several benefits such as simplicity, high productivity, and versatility. It does not require costly vacuum processes, which enable their use without placement into vacuum chambers. Therefore, there are fewer constraints on the size and shapes of materials that may be treated. Use of atmospheric-pressure plasma techniques provide the ability to greatly vary the surface energies of polymer films, and thus should enable greater levels of inks' or coatings' wettability to surfaces [91]. In particular the use of radiofrequency (RF) plasma treatment at atmospheric pressure enables a high level of variation to the surface energies of polymeric films [88, 89]. In these studies, contact angles below 20

degrees were readily achieved using the atmospheric plasma treatment techniques. To achieve proper wetting of inks to a substrate surface, graphic printers typically desire an interfacial energy approximately 10 mN/m lower than the surface energy of the substrate.

To create more robust, biocompatible devices, there exists a need for a better understanding of the interactions between functional inks and PDMS films in order to improve their printability, mechanical and functional properties. The objective of this study was to advance the knowledge of the material properties of PDMS films by altering their interactions with flexo conductive inks accomplished by tuning the surface energy of the films by altering the time of exposure and the intensity of the RF signal treatment received by the films to a low temperature atmospheric plasma source. By advancing this knowledge gains in print quality can be achieved, and more robust and higher performing biocompatible PE devices possibly realized.

4.3 Experimental

PDMS films were prepared using Sylgard-184 (supplied by Dow Corning, Midland, MI). PDMS Sylgard-184 supplied as a two-part kit consisting of pre-polymer (base) and cross-linker (curing agent) components. Films were prepared by mixing the manufacturer recommended 10:1 (weight ratio) of pre-polymer to cross-linker. Mixing was accomplished by hand using a 500 mL Pyrex beaker and a scientific stirring rod for approximately 5 minutes. Once mixed, the polymer mix was allowed to degas in ambient conditions for approximately 1 hour, after which time it was coated onto a 12 x 4 inch 70.3 gsm bleached DunUltra MG paper (Duncote Papers, Port Huron MI) using a 1.5 mil Byrd applicator. Paper was selected as the base substrate due to its ability to be recycled, as well as the roughness and absorption properties, which reduce the possibility for (PDMS) film separation during processing. Samples were then placed into an oven at 140°C for 20 min for curing. Once cured, the films were placed in a controlled environment (23°C, 50% R.H.) and allowed to condition for 24 hours prior to use. The PDMS was applied to paper to enable it to be printed on a Harper QD flexographic proofing press. The paper served as a good carrier for the thin films. From these samples, strips were cut (6" X 0.25" L X W) to enable their surface energies to be measured. The

surface energy and roughness of the samples were characterized before and after exposure to a Surfx® Atomflo™ 400 atmospheric plasma treater. The Surfx® system was equipped with a 7.6 cm linear beam source. The plasma was operated at both 120 and 180-Watts radio-frequency (RF) power, having 30.0 L/min of industrial grade helium (He), and 0.3 or 0.08 L/min of ultrahigh purity oxygen, respectively. The change in oxygen flow varied dependent on the manufacturers' recommended flow rates per operating frequency. A 4 mm source-to-substrate distance was used during the treatment of all samples. Sample exposure times were controlled by varying the speed of the conveyor belt on which the samples were placed, using speeds of 60 mm/s and 120 mm/s, and by altering the number of passes made under the plasma ejector nozzle (using either 1, 2 or 3 passes). The gas flow rates were delivered at a nominal temperature of 25° C and atmospheric pressure of 1 atm. The relative humidity in the environment was approximately 25% throughout the treatment of all samples. Samples were exposed to open air before, during, and after plasma treatment.

The thickness of the base sheet was measured with a Technidyne digital thickness gauge and compressibility was calculated from the difference in the roughness values measured on a Parker Print Surf Tester at clamping pressures of 500 and 1000 kPa. The ink used was a water-based nano silver ink (PFI-722, from NovaCentrix). The roughnesses of the PDMS films and the subsequently printed ink films were measured using a Contour GT-K (Bruker Corporation) white-light interferometer. Topographical imaging was carried out in variable scanning interferometry (VSI) mode using a 5X objective giving a sample area of approximately 1.25 mm x 0.98 mm (L X W). The surface roughnesses of the samples were obtained in terms of the arithmetic mean of the surface roughness, from which the RMS values were subsequently calculated. Ten measurements from each sample set were taken. Two different sample films per condition were used and five measurements taken from each.

A Harper QD flexo proofing press was used for printing. Print trails were conducted using various anilox rolls. Anilox rolls used were 1) 1000 lines per inch (lpi)/3.3 billion cubic meters (bcm) (5.1 μm), 2) 600 lpi/4.0 bcm (6.2 μm), and 3) 440 lpi/ 5.0bcm (7.8 μm). By varying the lpi of the anilox different resolutions of the prints could be achieved,

and by varying the bcm or unit volume per unit area of the cells (μm [92]) various ink volumes can be applied. The ink used was PFI-722 (water-based conductive silver ink from NovaCentrix). The properties of the ink are shown in Table 13. The proofer printing speed was set to its highest setting (400 inches/minute), using a 9lb spring set. The PFI-722 ink was cured in a thermal convection oven at 120 °C for 5 minutes after printing.

Table 13. PFI-722 Ink Properties.

Silver Content (wt%)	60% (±2%)
Density (wet)	2.2g/ml (18.4lb/gallon)
Viscosity @10s^{-1}	800 cP
Viscosity @1000s^{-1}	130 cP
pH	5.75
Volume Resistivity	7 μΩ-cm (2.8 mΩ/sq/mil)

The surface energies of the films were measured using an FTA 200 (First Ten Angstrom Dynamic Contact Angle) measurement apparatus. The static contact angles (Sessile Drop Technique) of two liquids, ultra high filtered deionized water, and methylene iodide were measured. Once drop images were captured, the change in contact angle with time was plotted, and the equilibrium contact angle (contact angle where no further change with time was observed) obtained and used in the estimation of the surface energy of the solid to which the liquids were applied. Five contact angles were obtained for each fluid from which five surface energy values were estimated. The average surface energies (total, polar and dispersive) for each sample are reported, and may be found in the Appendix. The surface tension of the ink was also measured using a Wilhelmy plate.

4.4 Results and Discussion

The properties of the base paper are shown in Table 14. After coating the base paper with PDMS, the roughness of the sample surface decreased slightly from 0.83 ± 0.03 (Duncote) to 0.50 ± 0.03 μm (PDMS coated on Duncote). A comparison of these results with those in Table 15 shows the plasma treatment to have significantly reduced the roughness of the PDMS surface**.**

Table 14. Paper Properties (Base Sheet Duncote Paper).

Surface Energy (mN/m)	**Roughness (μm)**	**Caliper (μm)**	**Compressibility (%)**

49.3 ± 0.5	0.83 ± 0.03	74.0 ± 1.5	0.3 ± 0.05

Although the plasma treatment significantly lowered the roughness of the PDMS film, it is clear from Table 15 that treatments beyond one pass were insignificant. This indicates that the plasma was sufficiently clean and removed containments by the plasma after one pass.

Table 15. Average PDMS Film Roughness (μm) 180W, 60mm/s Surfx Treated

1 Pass	**2 Pass**	**3 Pass**
0.10 ± 0.01	0.06 ± 0.02	0.07 ± 0.01

The roughnesses of the PFI ink films deposited on the untreated samples are shown in Table 16. Roughness measurements of the treated samples are not reported for reasons explained below. The difference in the conductive ink film roughnesses between the 600 and 1000 lpi printed samples was not significant for the untreated samples. This indicates that the ink film is sufficiently thick as to not be influenced by the roughness of the PDMS film layer.

Table 16. Average Ink Film Roughness (μm) Untreated Samples.

Average Roughness (μm)		
Anilox Roll	600 lpi 4bcm	1000 lpi 3.3 bcm
	0.47 ± 0.6	0.54 ± 0.07

Table 17 shows the line gains for the untreated printed samples in both the machine direction (MD) and cross direction (CD). Line gain is a printing term used to express the increase in the dimensions of the printed line over that of the nominal dimensions of the imaged line on the flexographic plate. The lines gains are extremely large for both anilox rolls and printing directions for all nominal line widths. The line gains were lower in the MD as compared to the CD as a result of less plate distortion occurring between plate and substrate. The best print (lowest gain) was found for the 50 micron line printed in the machine direction (MD) using the 600 lpi/ 4 bcm anilox roll The results show the importance of print direction and anilox selection on print quality.

Table 17. Line Gains of Untreated Lines.

MD Lines				
Anilox Roll	600 lpi 4bcm		1000 lpi 3.3 bcm	
Nominal Width	30 µm	50 µm	30 µm	50 µm
Gain (%)	210 ± 40	96 ± 40	137 ± 17	174 ± 28
CD Lines				
Anilox Roll	600 lpi 4bcm		1000 lpi 3.3 bcm	
Nominal Width	30 µm	50 µm	30 µm	50 µm
Gain (%)	260 ± 123	153 ± 35	327 ± 54	226 ± 74

The surface tension of the ink was found to be 30 ± 2 mN/m. Based on the surface energy data obtained for the PDMS treated samples (as can be seen in the Appendix), and surface tension values of the ink it was decided to treat samples using a power of 120W at a speed of 60mm/s with 1 pass for further print studies. This condition was selected based upon it providing the closest desired difference of 10 mN/m between the surface tension and surface energy of the ink. Based on graphic printing knowledge, it was thought these conditions would provide the expected proper wetting, adhesion and gain to obtain good print results for the print studies to be performed. However, the samples showed very surprising results. As shown in Figure 22, while the untreated samples were readily wetted by the ink and printed well, the treated samples failed to print at all.

Figure 22. Images of PFI-722 Ink on Plasma Treated (Top) and Untreated (Bottom).

So while the water from the contact measurements completely wetted the treated sample and beaded up on the untreated sample, the aqueous ink showed an opposite wetting characteristic. The aqueous PFI-722 ink wetted the untreated sample and failed to wet the treated PDMS film. To understand this finding additional tests were performed.

First the printing of a second aqueous conductive flake silver ink (CXT-0711, Sun Chemical) was performed on both treated and untreated PDMS films. This ink had a measured surface tension of 33.5 $\pm$ 1.33 mN/m, which was a bit higher than the PFI ink, and therefore further away from the 10 mN/m difference between ink and PDMS surface. This ink showed little difference between the amount of ink transferred to the treated and untreated PDMS samples and print attributes of the printed samples. These findings indicated that the PFI-722 ink findings were the result of its ink chemistry and suggested an incompatibility between the functional groups created on the surface of the plasma treated PDMS and components within the PFI-722 ink. To better understand these findings X-ray photoelectron spectroscopy (XPS) testing was performed to characterize the functional groups on the surface before and after treatment of the PDMS films. These results are shown Table 18, as well as, in the Appendix. The results show that the plasma treatment decreases the number of carbon groups at the surface and increases the number of oxygen groups at the surface.

Table 18. XPS Results for PDMS before and after Plasma Treatment.

Atomic Fraction (%)			
	Carbon	Oxygen	Silicon
Control	46.5	26.6	26.9
Plasma	23.7	48.9	27.4

Figure 23 shows some of the groups that could be present at the surface as a result of this treatment. As a result of the oxidation of the surface it is plausible that low molecular weight (LMW) fragments also exist on the surface of the PDMS. Considering the poor wetting behavior of the ink after treatment, it was reasoned that maybe the LMW fragments were interfering with the wetting and adhesion of the nano silver ink to the surface.

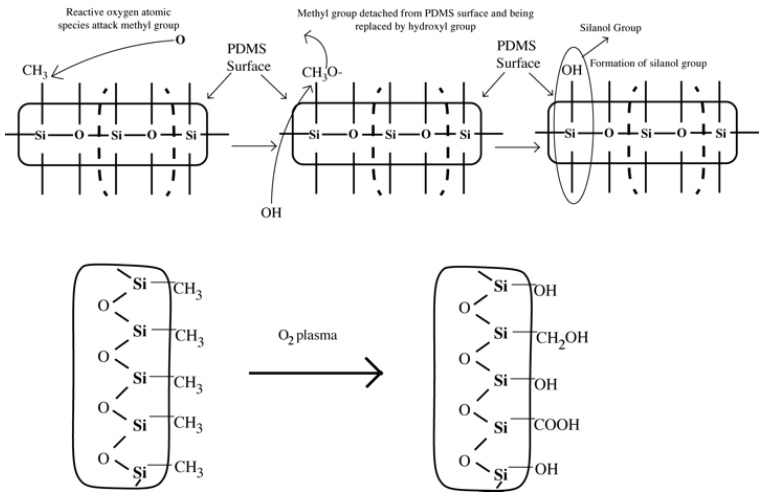

Figure 23. Oxidation of PDMS Surface.

Another reason for the observed behavior could also be that changes in the chemistry of the PDMS surface were causing the ink to become unstable resulting in poor in transfer. Knowing that aqueous based nano metallic inks contain fatty acid ligands in order to prevent the agglomeration of silver particles the mechanisms shown in Figures 24-25 were derived. Figure 24 shows the mechanism by which the ink wets the untreated PDMS surface.

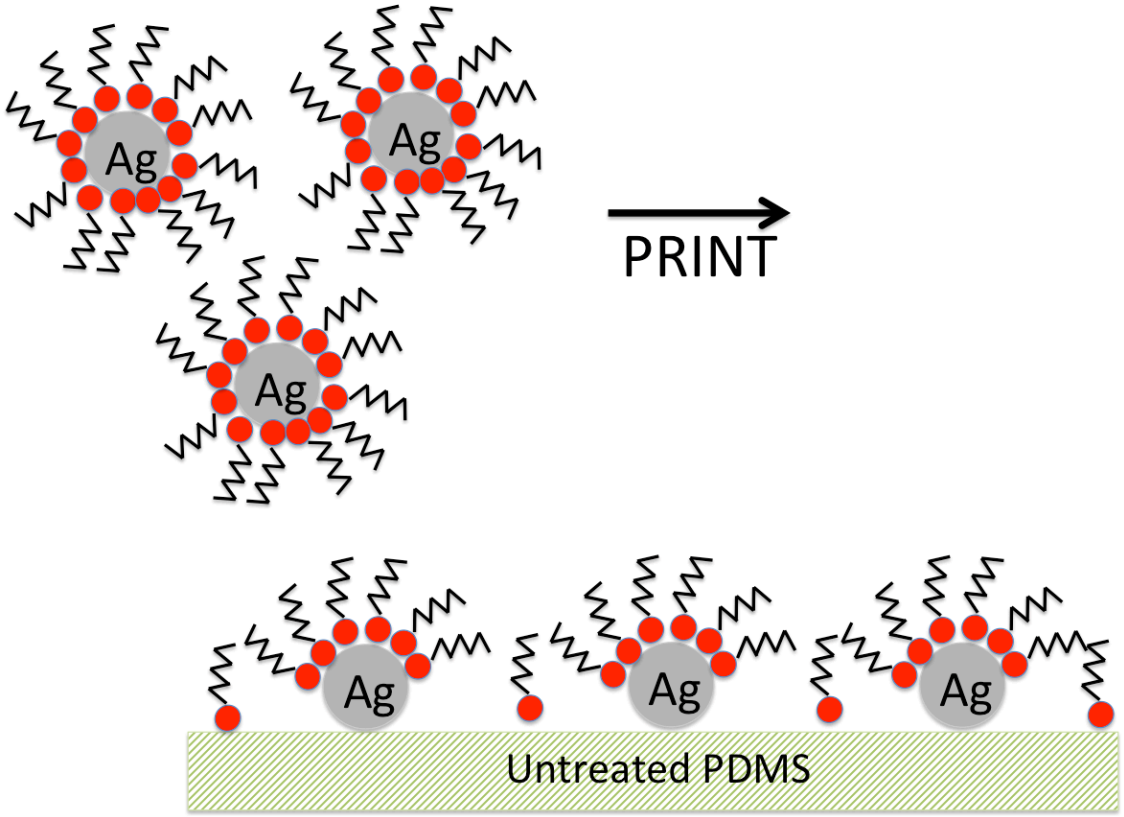

Figure 24. Proper Ink Wetting (Untreated PDMS).

Here it can be seen that the ink and pigment particles are wetting and adhering to the PDMS surface. However, as can be seen in Figure 25 the treated PDMS surface did not properly wet or enable adhesion of the ink. Based on this finding and through discussions held with the ink manufacturer it was hypothesized that a "surfactant (ligand) crash" was occurring. If true, the ink interaction with the hydroxyl rich surface was resulting in a reaction between the hydroxyl groups and carboxyl groups present in the ink (carboxylic acid groups in the aliphatic chains of the ligand), leading to a (pulling out) "crashing out" or separation of the ligand from the silver particles. This may also be described as a type of binder starving, where the separation of the two components of the ink rendered the two components incompatible, which prevented its wetting and adhesion to the PDMS surface.

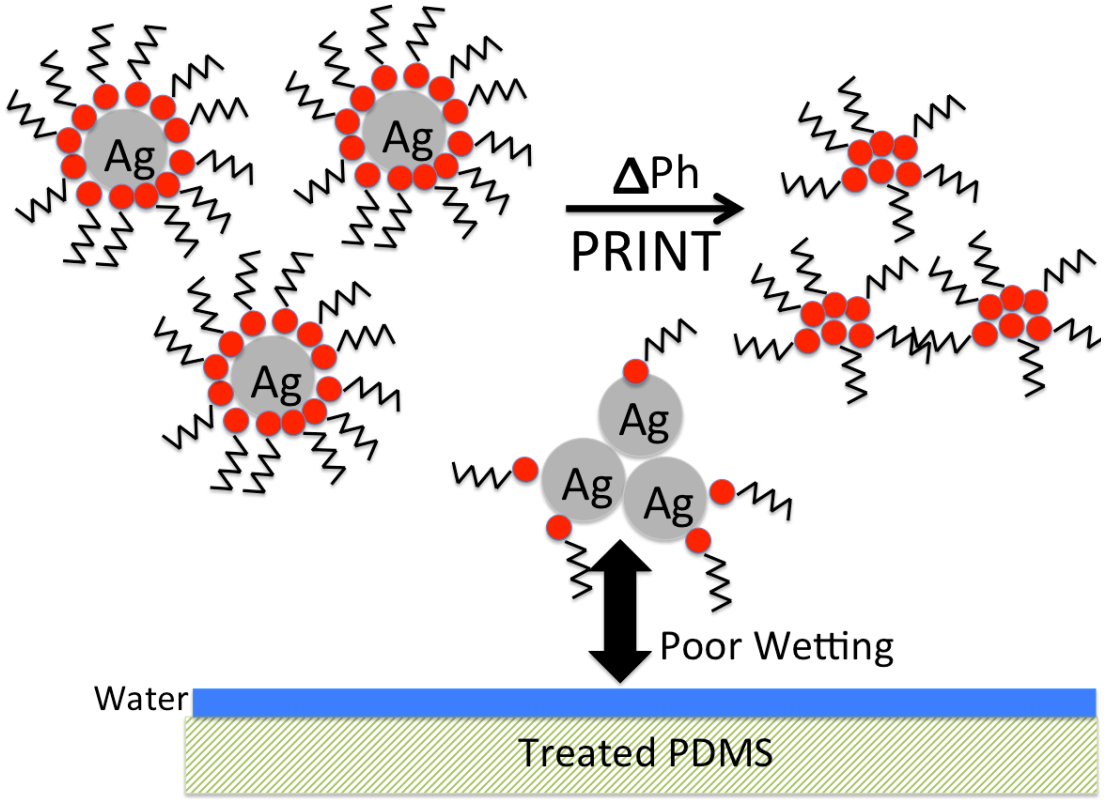

Figure 25. Mechanism of Ink Crash (Treated PDMS).

To support the proposed mechanism for poor wetting, additional contact angle measurements were performed on treated and untreated samples treated with a solution of NaOH to neutralize the pH of the surface. The resulting contact angles for these samples with water and PFI ink are shown in Figure 26.

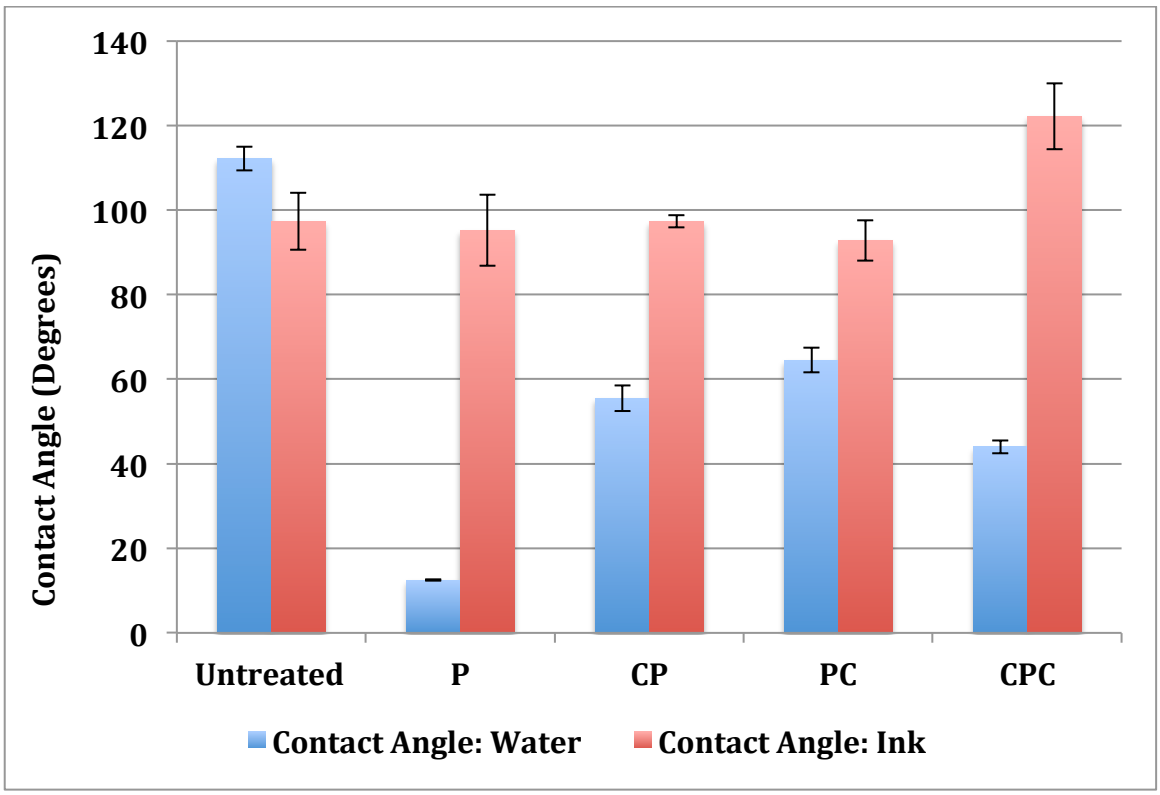

Figure 26. Contact Angles of Water and Ink on O_2 plasma Treated and Untreated PDMS.

The "P" denotes the application of plasma treatment and "C" denotes the application of the NaOH neutralization step. These labels are all utilized in chronological order with respect to their use, for example, the label "CPC" refers to the sample having first been neutralized (using NaOH) then plasma treated and again neutralized prior to contact angle measurement. The results show that the NaOH had a major impact on the contact angle (CA) of the water. However, there is little difference between the CA's of the untreated and plasma treated PFI ink samples for all conditions other than the before and after neutralization set, which actually shows an increase in CA in comparison to that of the untreated alone.

To further substantiate the proposed mechanism for the observed poor wetting results, an additional study in which PDMS films were treated with N_2 plasma was performed. Treatments were performed at an applied power of 120W and recommended 30 L/min of He and 0.35 L/min of N_2. After treatment, the contact angles of both water and PFI ink were performed before and after neutralization with NaOH, see Figure 27.

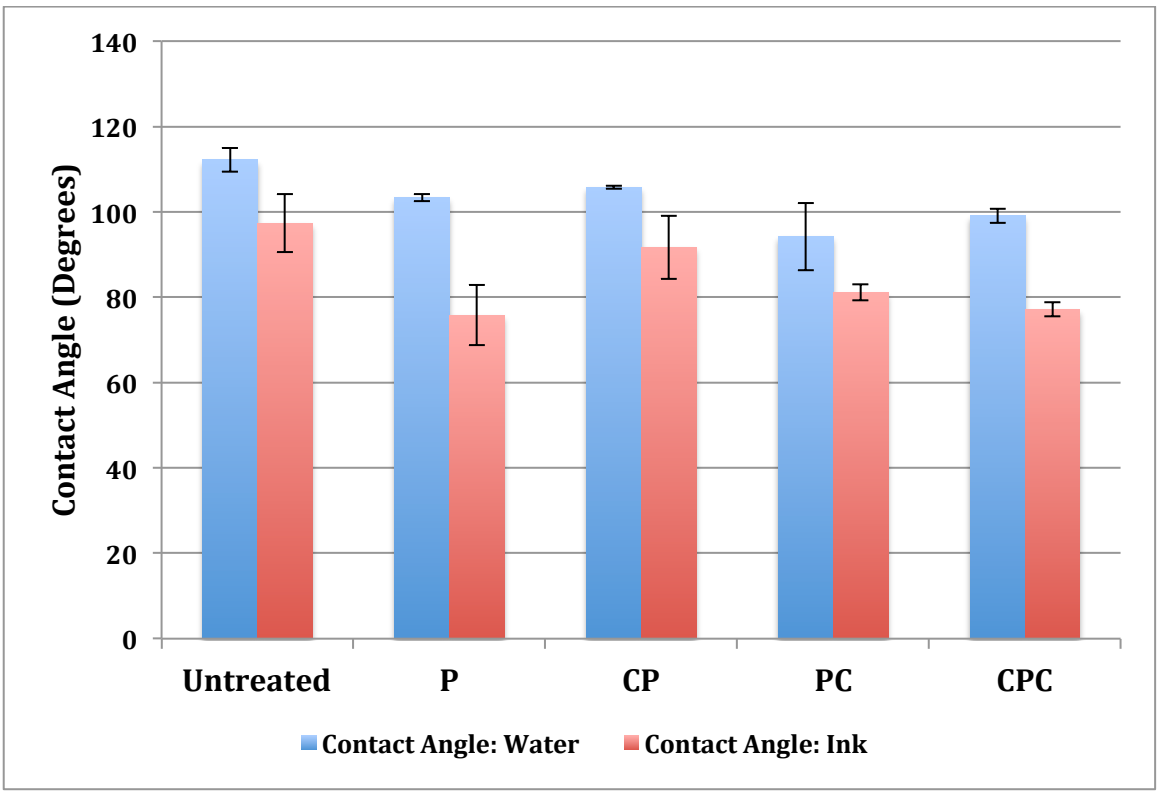

Figure 27. Contact Angle Results of N_2 Plasma Treated and Untreated PDMS Substrates.

It is clear from the results that the N_2 plasma treatment did not have the same impact on the water and ink contact angles as the O_2 plasma treatment. Only slight differences in water CA in comparison to the untreated sample, were observed. Regardless of the treatment with NaOH, the CA of the water and ink were nearly the same. Having gathered this information, the N_2 plasma treated samples were printed. A comparison of the printed PDMS samples before and after N_2 plasma treatment is shown in Figure 28. The samples were printed with1000 lpi, 3.3 bcm anilox roll.

The significant improvement in ink transfer and wetting observed for the N_2 plasma treated in comparison to the O_2 plasma treated samples supports the proposed mechanism and theory that the oxidation of the PDMS surface destabilized the nano silver ink, causing the silver particles to agglomerate, resulting in poor wetting and ink transfer.

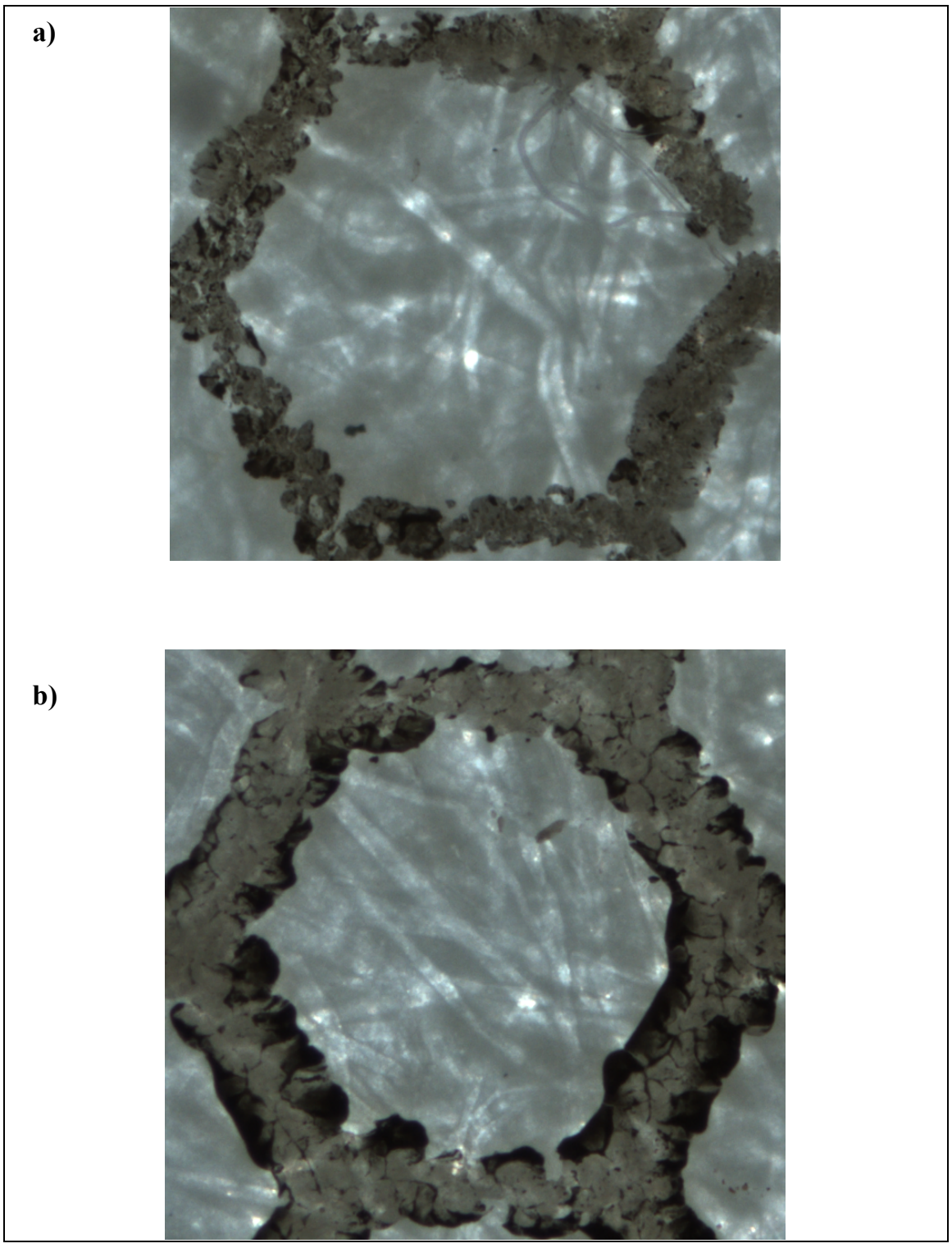

Figure 28. Printed PDMS samples a) No treatment b) N_2 treatment.

Having obtained a printable plasma treated surface with this ink, image analysis measurements were made. These results are provided in Table 19. The results show the

print quality of nitrogen treated samples to better than the untreated samples. While the line gains are greater, the standard deviations are much smaller due to the greater continuity in the lines in comparison to the untreated samples, as shown in Figure 28.

Table 19. Comparison of Flexo Printed Lines.

Nominal Line Width (μm)	Untreated	N_2 Treated
30	61.8 ± 8.3	91.9 ± 5.5
50	78.1 ± 32.1	127.6 ± 15.8
Rub Resistance	Poor	Good

It was also found that the rub resistance of the nitrogen treated samples were much better than the oxygen treated samples with the ink easily being removed when rubbed after drying. Though the results were not as first expected, studies to determine the cause for the unexpected results enabled the knowledge of printing PDMS with functional inks to be advanced. This work demonstrates the complexity of functional printing in comparison to graphic printing by having shown that the generally accepted 10 mN/m rule graphic printing rule did not hold true for the ink substrate pairings used in this study. From these results, it can be concluded that for successful functional printing printers must work closely with their ink suppliers to understand the chemistry of the inks to be used, which is not always willingly exchanged. More tests with generic ink formulations would greatly advance the knowledge of functional ink/substrate interactions and help guide manufacturers in the selection of their materials for their products.

4.5 Conclusions

Plasma treated PDMS films printed with a water-based Ag ink were shown to not properly wet or adhere well even though a 10 mN/m requirement was met. An

untreated and N_2 plasma treated PDMS films printed better than O_2 plasma treated PDMS films, even though its surface energy was significantly higher. The results from this work show the importance of properly matching substrate surface and ink chemistries for good wetting, adhesion and print quality. These discoveries demonstrate the complexity of printing functional inks in comparison to graphic inks. The results show that the generally accepted rule that a difference between the substrate and ink surface energy of 10 mN/m for good print quality does not necessarily hold true in the case of functional printing. In order for the field of printed electronics to advance, a greater understanding of functional ink chemistry and compatibility is needed. The innate differences between functional and graphic inks may require printers to create new general rules of practice.

CHAPTER 5

METHOD FOR HIGH THROUGHPUT PRODUCTION AND PRINTING OF THIN POLY(DIMETHYLSILOXANE) FILMS

5.1 Abstract

A method of producing and printing PDMS films of thicknesses down to 25μm was discovered. The method includes a) deposition and drying of a sacrificial layer of water-soluble polymer on a cellulosic substrate; b) deposition and curing of a crosslinkable PDMS polymer on top of the water-soluble polymer; c) removing the final electronic device by soaking the paper in water to dissolve the water-soluble polymer layer. This method enables the roll-to-roll production, patterning and/or printing of PDMS films. As a result of this work, Western Michigan University has moved forward in filing an application for a provisional patent.

5.2 Background

The technology described is especially suitable for applications where less time consuming and higher volume manufacturing methods for the production and printing of PDMS films is desired. Higher volume throughput for many applications is a cost benefit. The method enables the high through-put production of PDMS films of reduced caliper, which can be beneficial to product performance and/or costs. Large area films can be produced by this method, and PDMS film thicknesses down to 25μm can be achieved and roll-to-roll printed.

The most widely used fabrication method for preparing thin PDMS films (< 100μm) of different thicknesses is spin-coating, whereby the PDMS is spun onto a silicon wafer or glass and then the PDMS is manually peeled from the glass or silicon wafer after curing. Spin coating produces a thin uniform film, but its use for producing films is slow, is limited to size of films that may be produced, and it is a batch process. Another difficulty with current techniques used to produce thin PDMS films for subsequent processing is the fragile nature of the silicon wafer or glass base support layer. Due to their fragile nature, care must be taken not to break, scratch, or damage the glass or silicon wafer during subsequent processing steps. Care must also be taken to maintain the integrity of

the film should one choose to peel and move the film prior to subsequent processing, e.g., printing. Once peeled, there is the challenge of keeping the film free of wrinkles and contamination. The size of the film that can be produced is also limited by this method of production due to limitations in the size of the spin coating apparatus commercially available for use in this process. The ability to manufacture and print large area, thin PDMS films at higher processing speeds, with a reduced chance of damaging or contaminating the films during handling, would enable higher product yields and increased PDMS film throughput to be realized.

Thin PDMS films that are 100μm or less in thickness have several applications. One example is multi-layer microfluidic devices where thin patterned PDMS layers are aligned and stacked to create logic circuits. A second example is stencils for patterning biomolecules; this is accomplished by patterning the films with different surface active agents. In addition to these applications, such films are used as membranes to control the transport of molecules, as scaffolds for tissue engineering, and as biocompatible carrier films to support flexible and stretchable printed electronic sensors for medical and biological applications.

PDMS elastomers are also used to produce dielectric electroactive polymer (DEAP) films used in making actuators, generators and sensors. In the large-scale manufacture of DEAP films, PDMS is coated onto a carrier web, often PET, from which it is peeled, See Figure 29 [93]. During peeling considerable pre-strains can be induced along with some defects, which reduce performance of the DEAP film. To reduce the peel force required to remove the film, small quantities of perfluorether allyamide can be added as a release agent, but can not always be used where fluoro chemistries are of prohibited. The carrier web may also be coated with microscale corrugations of methylacrylate to reduce the point of contacts between the PDMS and carrier web [94].

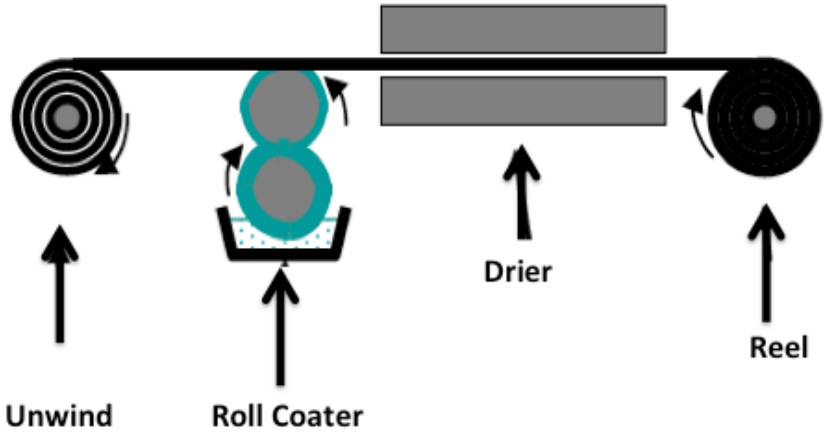

Figure 29. Schematic of coating process.

Flexible and stretchable printed electronics is an exciting new field of research and development. In this field, PDMS as a supporting base layer is of interest due to its stretchability, compressibility, biocompatibility, chemical inertness and ease of creating microfluidic channel in films created from it [95]. Another attractive property for some applications is its transparency. PDMS films for these applications are most commonly prepared by, spin coating, casting or molding a mixture of PDMS with crosslinker in the proportion of 10:1. The amount of crosslinker can be varied to alter the physical and mechanical properties of the final film. Once prepared, the PDMS mixture needs to be degassed, after which time it can poured into a patterned mold to create microfluidic channels, casted (poured into a non-patterned mold) or spin coated. Next, the PDMS filled mold or spin coated film (film usually spun onto glass or silicon wafer) must be placed into an oven to allow the film to cure. The amount of time required for complete cure depends on the thickness of the film and temperature of the drying oven. Once cured, the film can be peeled, transferred and bonded to another surface, which for thin films is difficult, for subsequent printing or processing. When it comes to bonding PDMS to another surface, there are at least four methods: [96] corona discharge treatment, UV/ozone treatment, gluing, and partial curing are used. All methods are time consuming and are not feasible for mass production.

Printing in comparison to traditional electronic fabrication methods is a high speed

manufacturing process. Printed electronics is a new application for the use of printing where conventional printing equipment such as screen printing, flexography, rotogravure and inkjet, is used to pattern one or more functional materials onto a substrate to create passive or active electronic devices. The use of many types of functional materials and substrates have been explored to create, rigid, flexible and stretchable devices. In the case of stretchable devices, both a stretchable substrate and functional ink layer is required. For these applications, PDMS films and conductive elastomers are desirable to use. Conductive elastomers can be produced by the mixing of PDMS with carbon nano-tubes (CNTs), silver nano wires or with metal powders [35]. The ability to print conductive elastomers has been demonstrated [97]. One problem with these elastomers is that they are of higher resistivity than the bulk metal due to blocking of conductive pathways by PDMS. However, in some applications the resistivity of these conductive elastomers is sufficient for use, as in the case where they are used for additional support in fracture sensitive zones, e.g., interconnects, or when constructing heaters [98-101].

The ability to mass produce biocompatible electronic and microfluidic devices is essential to bringing such devices to mass markets. PDMS has the needed properties for use in these applications. One of the commonly used PDMS products by researchers and industry is Dow Corning Sylgard Elastomer 184, which is mixed with a crosslinker and cured to produce a film.

When the two components are mixed, an organometallic crosslinking reaction cures the product to create a PDMS film. The curing agent contains a platinum based catalyst that aids in the formation of SiH bonds across vinyl groups within the Sylgard Elastomer product. As a result of this reaction, which is accelerated by heat, -Si-CH_2-CH_2-Si- linkages are formed. The presence of multiple bonding sites allows for the development of three-dimensional crosslinking throughout the cured PDMS, which results in a stretchable and pliable film [102] PDMS has several properties that make it suitable for application by various coating processes. Its viscosity allows it to be applied and metered over large areas as exemplified by its use in the production of PDMS membranes of thicknesses ranging from 127 - 1016 μm (.005-.040 inches) [103]. For thinner films (<

100 μm) spin coating is required and the PDMS mixtures are often diluted with compatible solvents such as hexane, cyclohexane and t-butyl alcohol.

When applying PDMS by spin coating to a silicon wafer or glass, a sacrificial layer is often applied to enable the thin PDMS film to be removed from the surface after being spun coated. A photoresist coating such as AZ4562 can be used to create the sacrificial layer. This material is dissolved by soaking the glass or silicon wafer in acetone to release the PDMS layer from its surface. While this method enables un-supported thin PDMS films to be produced, the method is not practical for the large scale manufacturing of thin sheets or rolls of PDMS films.

Paper is a biodegradeable, renewable material produced from cellulose pulp derived from wood and non-wood fiber resources. Paper is mass produced in a continuous process to produce products, which vary in caliper; basis weights (weight/unit area); and surface, mechanical and optical properties. These properties are varied to meet the end-use requirements of the customer. Being hydrophilic in nature, papers are commonly coated with aqueous coatings to improve their smoothness and uniformity for printing and functional performance. Thus methods to apply aqueous coatings to paper are well-understood and practiced on a large scale. Examples of high throughput roll-to-roll coating application and metering methods commercially practiced to coat paper are curtain coating, roll coaters, short dwell blade coaters, short dwell rod coaters, size press, and metered size press coaters (see Figure 30).

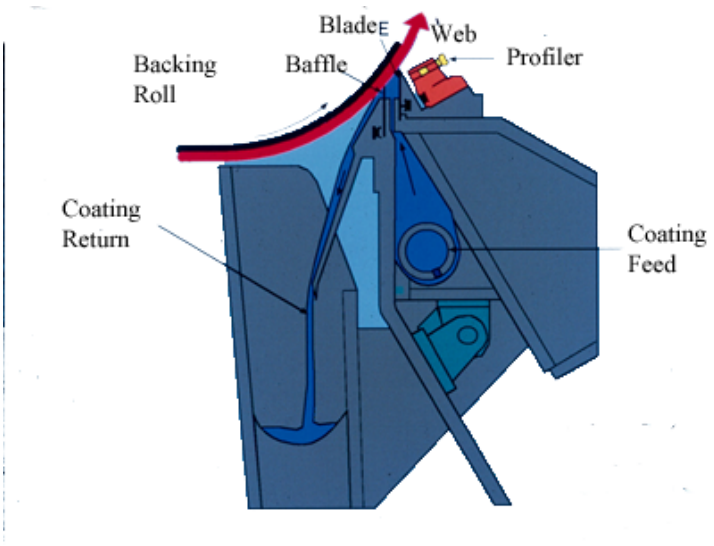

Figure 30. Schematic of Short Dwell Blade Coater (reproduced from U.S. patent #4,396,6481).

Printing is another high speed manufacturing process that can be performed on a moving web or sheet to reproduce a desired pattern from a master form to its surface. In the case where the master form contains an un-patterned (solid) image, coating methods rather than print methods are more commonly practiced. So printing equipment can be used to print or coat substrates. For printed electronic applications, the desire to pattern one or more functional layers to create passive or active electronic components towards the assembly of an electronic device is of high interest, because in comparison to traditional electronic fabrication methods, it can be done at faster speeds, with less waste, and on flexible and rigid substrates. Most certainly, the highest throughput is accomplished when the printing is performed continuously in a roll-to-roll fashion.

By first coating a paper substrate with a water soluble polymer, sufficient to completely cover any surface fibers, a sacrificial coating layer can be formed, which allows for the removal of subsequent applied non-water soluble layers by immersion in water to dissolve the water-soluble sacrificial coating. This method has been shown to be useful in the preparation of self-supported printed electronic sensors [104, 105]. While the ability to use a sacrificial layer to produce self-supported printed sensors has been demonstrated, the application of sacrificial layer as a release layers for PDMS films has not yet been reported or reduced to practice. Water soluble polymers previously reported as

appropriate materials for the production of sacrificial layer are all appropriate for use in this new application method. Examples of such materials include but are not limited to sodium alginate, carboxymethyated cellulose, ethylated starch, polyvinyl alcohol and carboxylated soy protein. The advantage of this technology to existing methods is the ability to produce thin PDMS films, down to 25μm using high throughput coating and printing processing methods to apply the alginate and PDMS solutions.

The thickness of PDMS film can be further reduced to less than 25μm by diluting the PDMS with solvents that do not dissolve the sacrificial layer, does not interfere with the PDMS crosslinker and in which the PDMS is miscible. The dilution should be done prior to application and metering of the PDMS onto the basepaper precoated with sacrificial coating layer. Examples of such solvents are acetone, benzene and toluene.

Films less than 50 μm can be difficult to handle once removed from the basepaper, and the addition of solvent to the PDMS requires the drying of such films to be initially performed at lower temperatures in order to enable the solvent to evaporate without blistering. Therefore the preferred method for highest throughput is to apply and meter an undiluted PDMS solution directly to a paper precoated with dried water soluble sacrificial coating layer. Once the alginate coated paper is obtained, the paper can be coated with the PDMS in a subsequent coating or off-line. If coated off-line, the finished product could then be printed with functional inks in subsequent printing stations in-line with the PDMS coating station. The use of the carrier base-paper with sacrificial layer enables <100 μm PDMS to be coated and printed at higher throughputs than current methods practiced.

5.3 Experimental

Two commercial basepapers were obtained and their properties characterized. The properties measured were basis weight, caliper, roughness and Cobb size. The properties of each paper and TAPPI standard test method used to perform the measurements are shown in Table 20. Prior to testing, the papers were equilibrated for 24 hours in an environmentally controlled TAPPI standard test lab (50% RH and 23 °C). The Wausau

paper was an unbleached Kraft MG Gumming Paper. The Dunn Paper was a bleached Kraft machine glazed paper. The properties of the paper used are reported in Table 20.

Table 20. Summary of Commercial Paper Properties.

Paper	Basis weight (gsm)	Caliper (µm)	PPS Roughness (µm)	Cobb Size (gsm)
Wausau Paper	65.0	86.4	4.31 ± .05	27
Dunn Paper	55.3	55.8	0.85 ± .06	35
TAPPI Test Method	T-410	T-411	T-555	T-441

After characterizing the properties of the papers, a water soluble sacrificial layer was prepared by first coating 15 sheets of the 65.0 gsm unbleached Kraft MG Gumming Paper (Wausau Paper) with a 6% solution of sodium alginate (S-50-C, SNP Inc.) with a #22 Meyer Rod. After coating, the papers were left overnight to dry in an enclosed chamber to prevent contamination by air borne particles. Once dried, the coat weights of the applied alginate layers were measured gravimetrically using a standard 100 cm^2 punch and Labwave CEM 4000 solids analyzer. A section from four of the 15 coated papers was punched and measured. The coat weight applied was determined to be 5.0 ± .3 gsm. Next, a de-aired 10:1 solution of Sylgard 184 and crosslinker was applied to the 15 alginate coated papers using 2.5 mil, 2.0 mil and 1.5 mil Bryd applicators (five per applicator). The PDMS coated papers where then dried in a forced air oven at a temperature of 140°C for 20 minutes. After drying, the samples were soaked in room temperature water (approx. 21°C). This enabled the alginate pre-coating layer to be dissolved to enable the PDMS films to be separated from the paper. The films were blotted dry and their thickness measured using a Mitutoyo electronic caliper. PDMS films below1.5 mil could be made by the same process but were difficult to handle. They easily folded back on themselves and could not be easily re-separated. For this reason, the results for only the films 1.5 mil or greater made are reported.

The next substrate to be coated was a 55.3 gsm machine glazed bleached Kraft (Dunn Ultra, Duncote Paper). Once again, 15 papers were coated with a 6% solution of sodium alginate (S-50-C, SNP Inc.) with a #22 Meyer Rod. The coated papers were dried and the coat weights measured as described above. A de-aired 10:1 solution of Sylgard 184 and

crosslinker was then applied to 15 of the dried alginate coated papers using 2.5 and 2.0, 1.5 mil Bryd applicator. The PDMS coated papers where then dried in a forced air oven at a temperature of 140°C for 20 minutes. After drying, the samples were soaked in room temperature water and the PDMS films separated from the paper. The films were blotted dry and their thickness measured using a Mitutoyo digital caliper. To confirm the thickness of the films were accurate, the thickness of these films were also measured with a SpecMetrix® coating thickness gauge. As shown the results were very close to those measured with the Mitutoyo instrument.

5.4 Results and Discussion

Table 21 shows the average thickness of the PDMS films. As shown, the measured values are in good correlation with the wet film applicator used. Since the PDMS is 100% active, the wet and dry film thicknesses are similar.

Table 21. Thickness of measured films.

Sample	Average Thickness of Film (μm)
Unbleached Kraft MG Gumming, 2.5 mil	65.2 ± 1.3 μm
Unbleached Kraft MG Gumming, 2.0 mil	52.2 ± 1.7 μm
Unbleached Kraft MG Gumming, 1.5 mil	38.4 ± 1.9 μm
Bleached Kraft MG glazed, 2.5 mil	64.0 ± 1.0 μm (62 μm)*
Bleached Kraft MG glazed, 2.0 mil	51.4 ± 1.3 μm (49 μm)
Bleached Kraft MG glazed, 1.5 mil	38.0 ± 1.2 μm (36 μm)

* SpecMetrix® coating thickness

5.5 Conclusions

A method of producing PDMS films of thicknesses down to 38μm was discovered. The method developed offers a way for PDMS films of less then 100 μm to be carried through a web-fed press for functional printing that would be beneficial to lowering the cost of flexible printed electronic devices.

CHAPTER 6

DEVELOPMENT OF A REPULPABLE SILICONE RELEASE PAPER

6.1 Abstract

A method to produce a silicone release paper that can be repulped and recycled to avoid the costs of sending scrap paper to landfill and to recover the value of the recycled fiber has been accomplished. The method comprises the application of a water-soluble coating to reduce the porosity of the paper surface, thus enabling the separation of a subsequently applied non-water soluble silicone release coating upon rewetting during the repulping process. The repulpable silicone release paper enables the recovery of paper fibers by conventional repulping and recycling processing methods.

6.2 Introduction

Paper is a porous material composed of cellulose fibers that can be readily penetrated by silicone coatings. For this reason, dense papers, such as glassine, parchment, and greaseproof papers, are used in order to minimize the amount of silicone that must be applied to obtain the required release characteristics of paper. Other low-porosity and smooth papers used as the base stock for release papers are: coated publishing papers, label face papers, non-coated supercalendered (SC) papers, and machine glazed (MG) papers [106, 107]. Due to the high cost of silicone, papers that require a minimal addition of silicone to their surface for release are most desired. Porosity and smoothness greatly impact the amount of silicone required.

Release papers play a vital role in the fabrication of pressure-sensitive adhesive (PSA) labels and tags where they serve as the disposable base layer to carry the labels through conversion and dispensing [108]. They are also used in the manufacturing of self-adhesive materials and components for tapes, industrial and graphic applications. The typical methods for obtaining release papers for adhesives are based on three chemistries: silicone [109], chrome complexes [110], and extruded PE (polyethylene) [111]. None of these allow the backing paper to be recycled [112]. A schematic of a typical silicone release paper is shown in Figure 26.

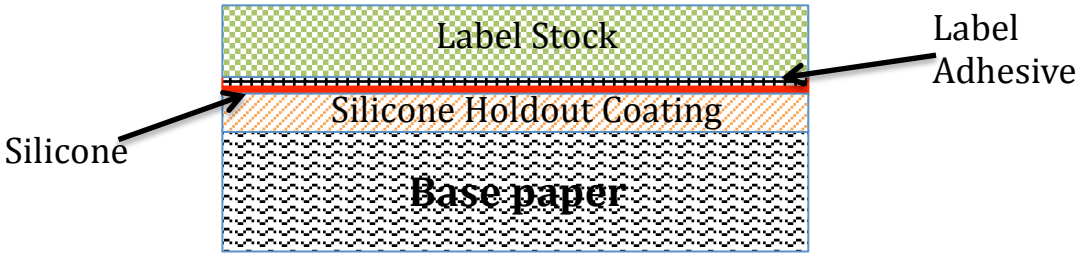

Figure 31. Side view of layers present in silicone release paper.

Most silicone release coating consists of a silicone polymer, crosslinker, and catalyst. A condensation reaction occurs between the catalyst and silicone polymer liberating hydrogen inducing the formation of a cross-linked silicone network (Figure X).

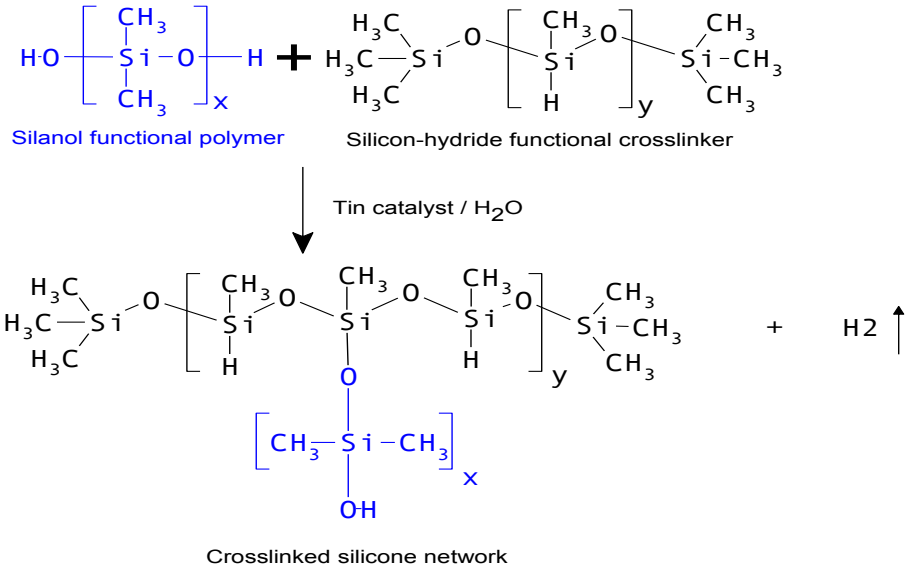

Figure 32. Condensation reaction between the polymer and the cross linker [113].

Silicone is used to produce release papers due to its very low surface tension. The silicone molecule also has a low molecular polarity, which is very important to the binding or crosslinking of the silicone to the cellulose fibers in paper. Three different types of silicones used for the manufacture of release papers are: solvent-based, water-based, and solvent-less. While the use of these materials provides performance for a broad range of adhesives, release liners produced from these materials are not repulpable or recyclable (as defined by the Recycled Paperboard Technical Association (RPTA), which requires less than 15% of silicone to pass through the recycling process). Chrome

complexes also represent a potential environmental hazard due to their chromium content and the resulting problems of heavy metals. PE extruded papers are also not recyclable because the PE polymer cannot be disintegrated in a typical repulper.

A considerable amount of waste paper is collected and recycled. This waste-paper contains reusable fiber if the fibers could be separated from their non-cellulosic impurities during the recycling process. For recycling, collected wastepaper and water is added to a pulper, that breaks apart (disintegrates) the paper by mechanical action into individual fibers. This is followed by various stages of cleaning and screening to obtain separate contaminants from the fibers. Fibers that are as pure as possible are recovered for re-use to prevent problems in the papermaking process. Contaminated fibers and contaminants are sent to landfill, which costs the papermaker in both cost of unrecovered fiber and landfill utilization costs.

The focus of this work was to determine if the application of a water-soluble sacrificial coating layer to a low porosity, smooth base paper, such as a MG paper would aid in the repulpability of such papers. The water-soluble coating layer should be of sufficient thickness to completely cover the surface of the paper to prevent penetration of the silicone into the network of paper fibers. Thickness doesn't necessarily imply coverage. By completely covering the surface of the fibers the sacrificial coating layer formed, allows the removal of subsequent applied silicone release coating upon immersion in water due to the resolubiliztion of the underlying sacrificial layer. While this method has been shown to be useful in the preparation of self-supported printed electronic sensors on thin PDMS films, it has not yet been reported for the fabrication of repulpable silicone release papers. Water-soluble polymers previously reported [104] as appropriate materials for the production of a sacrificial layer are all appropriate for use in this application. While a sodium alginate and partially hydrolyzed polyvinyl alcohol were used in this study, other water soluble polymers such as carboxymethylated cellulose, ethylated starch, and carboxylated soy protein could also be used. The advantage of this technology to existing methods is the ability to produce silicone release papers that can be repulped using conventional repulping processing equipment and no chemical additives, hence making recovery of the fibers economically feasible.

A non-recyclable release paper has a significant cost in that it has to be sent to a landfill or be incinerated. This becomes a cost to the producer who passes the costs onto the end-user, neither of which can re-sell the paper to a recycled paper mill. The reason why silicone coatings are not recyclable is that the silicone cannot be completely separated from the fibers; trace amounts of silicone in a recycle stream can cause spots on the resulting paper and/or build up on the paper machine that would result in expensive down time for cleaning [114].

6.3 Experimental

A commercial grade Duncote Ultra, Lightweight Coated, paper grade was used as the basepaper. The paper was coated with two different water-soluble polymers using #30 and #6 Myer rods to obtain approximately the same coat weight (3-4 gsm). The water soluble polymers used were sodium alginate, S-15-C (SNP Inc.) and polyvinyl alcohol (PVA), Selvol 203 (Sekisui). An 8% solution (by weight) of alginate was prepared by slowly adding the dry alginate powder to tap water and allowing it to mix for 30 minutes. The PVA was formulated to a 28% solution (by weight) by adding the dry powder into room temperature water under a mixer then heating the contents on a steam table to a temperature of 185°F (85°C), under agitation until the PVA was completely dissolved (30 minutes). It was found that using a #30 and #6 rod for the alginate and PVA, respectively enabled the desired target coat weight to be obtained for each. The actual coat weights applied were 3.84 (± 0.19) gsm for the alginate and 4.05 (± 0.14) gsm for the PVA. Coat weights were measured gravimetrically using a Labwave CEM solids analyzer. These samples were then coated with two different commercially available silicones using a 1.5 mil Byrd applicator. The silicones used were Sylgard-184 (Dow Corning) mixed in the recommended 10:1 ratio of silicone to cross-linker and Wacker 944 Dehesive 944 (Wacker) using a low SiH formulation consisting of 60.35% Dehesive 944, 37.59% toluene, 0.30% Crosslinker V90, and 1.76% Catalyst C 05. To cure the silicone coatings, the samples were dried in a thermal oven at 257°F for 20 minutes. After drying, a silicone cure test was performed by measuring the tape adhesion properties using Scotch brand cellophane tape 610 to ensure the complete cure. All samples showed no degree of detackification indicating that the silicone was completely cured. After being dried, the

samples were conditioned in a TAPPI standard control room (50% RH and 85°F) for 24 hours and the coat weight of the silicone applied was measured. The weights are given in Table 22. The high coat weight of the Sylgard in comparison to the Wacker product is due to its extremely high viscosity.

Table 22. Coat Weights of Various Coatings (gsm).

Alginate	3.84
Polyvinyl Alcohol (PVOH)	4.05
Sylgard	73.5
Wacker	44.5

The samples were then repulped using a Maelstrom laboratory hydrapulper. As a control, a commercial silicone release paper (label stock removed) was also repulped. The repulping studies were performed at a 6% consistency by tearing a known weight of each sample into an appropriate amount of water contained within the Maelstrom hydrapulper. During addition, the conditions of the hydrapulper were maintained at 300 rpm and 140°F. Approximately half way through the addition of sample to the hydrapulper (15 minutes), the mixing speed was increase to 400 rpm. Upon completion of sample addition, the speed of the hydrapulper was increased to 700 rpm and held at this speed for 20 minutes. After the 20 minutes the hydrapulper was discharged and its consistency remeasured. A portion of the sample was then taken and weighted for screening. Screening was performed using a Johnson 6-cut screen to separate and collect the acceptable and non-acceptable waste materials for weighing. The samples were allowed to run in the 6-cut until no apparent fibers were present in the accepted stream. To determine the weight of rejects, the collected sample was poured into a Buchner funnel containing a pre-weighed oven dried VWR 415 course filter paper. The sample and filter paper were then dried on a hot plate until bone dry, at which time its weight was taken and the %rejects calculated using the oven dried rejects (ODR) divided by the (consistency of the stock x total mass of stock into the 6-cut). Next, the consistency of the accepts were measured to enable the mass required to produce a 1.2g oven dried TAPPI standard hand sheet to be determined. TAPPI standard hand sheets were then made for each sample set, following TAPPI standard method T-205 procedure. After allowing the

hand sheets to condition for a minimum of 24 hours the weights of each samples were measured using a Mettler (AE 260) 3-point scale to enable the calculation of tensile index values. Tensile tests were performed according to TAPPI standard T-494 using an Instron Tensile Tester. Peak load and extension were tested. Ten tests were performed for each sample. The water absorptivity of each sample was also measured using a FTA dynamic contact angle apparatus. Both sides of the samples were tested.

Oxford Instruments Lab-X 3000 EDRF (X-Ray) unit calibrated for silicone coat weights. For this testing, each set of samples were corrected using the Duncote basepaper as the control to determine baseline of Si present, from clay, prior to silicone coating. The roughness and permeability of the samples prior to application of the silicone were measured using a Parker Print-Surf, Model No. ME-90 instrument. For roughness readings, a soft-backing plate was used at both 500 and 1000 kPa.

6.4 Results and Discussion

Contact angle measurements of the hand sheets made from the accepts stream failed due to water penetrating the substrate too quickly to enable image capture, and hence, analysis of contact angle changes from sample to sample. Results of the base sheet properties are shown in Table 23.

Table 23. Paper Properties (Base Sheet Duncote Paper).

Surface Energy (mN/m)	**Roughness (µm)**	**Caliper (µm)**	**PPS Porosity (mL/min)**	Permeability Coefficient ($x10^{-6}$ μm^2)
49.3 $\pm$ 0.5	0.83 $\pm$ 0.03	74.0 $\pm$ 1.5	2.11 $\pm$ 0.08	7.62*

* See reference [115] used for calculation of this value.

The results of the reject percentages collected from each repulping study are shown in the Figure 28.

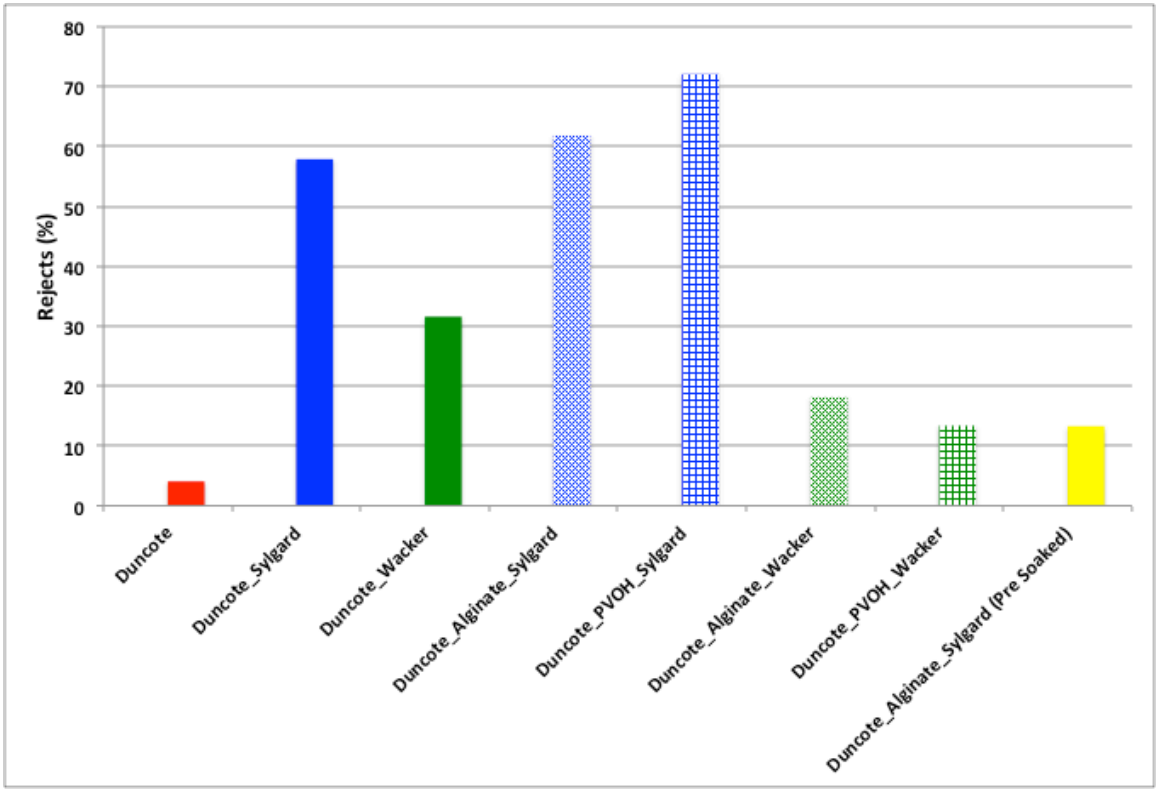

Figure 33. Rejects (%) from the repulping study.

The results show a decrease in the rejects for the Wacker silicone coated papers with sacrificial layer present. The % rejects was lower for the PVA pre-coated papers than the alginate pre-coated papers. This could be due to the higher roughness of the alginate samples caused by greater shrinkage during drying due to its lower solids. The results for the Sylgard were completely different. As shown, the % rejects increased for the samples pre-coated with alginate and PVA. Upon further investigation of these samples, it was observed that the majority of the rejects was silicone. The high coat weight of Sylgard in comparison to that of the Wacker was believed to be the cause of the differences obtained. To better understand these findings, an additional repulping study was performed. In this study a soaking step (1 hour) was added prior to adding the material into the hydrapulper. After soaking any materials floating on the surface were skimmed off, and the same pulping procedures were followed as previously performed. The significant reduction in rejects for the Sylgard pre-coated samples confirm that the majority of the rejects were from the higher amount of Sylgard addition level, in comparison to the Wacker. By pre-soaking the samples, the sacrificial layer performed as

desired, enabling the release of the silicone. The lower level of rejects obtained brought the percent rejects to a level to meet the Recycled Paperboard Technical Association (RPTA) requirements (less than 15%) to be considered a repulpable product.

The results of the tensile tests are shown in Figures 29 and 30, which show the tensile load and extension results respectively. The results show a decrease in load strength of the samples relative to the commercial silicone release paper. However, only the Sylgard sample shows a significant difference prior to the introduction of the sacrificial layer. With the introduction of the sacrificial layer all samples, with the exception of the alginate Sylgard sample, showed a significant decrease in load strength versus that of the commercial paper. The load strength of the pre-soaked and Duncote control shows that the addition of the pre-soaking step was effective in removing a majority of the silicone. The lowest load strength was found for the Wacker coated samples. These low strength values are attributed to the low coat weight and insolubility of the Wacker silicone, enabling the largest amount of silicone to make it through the accept stream and into the handsheets.

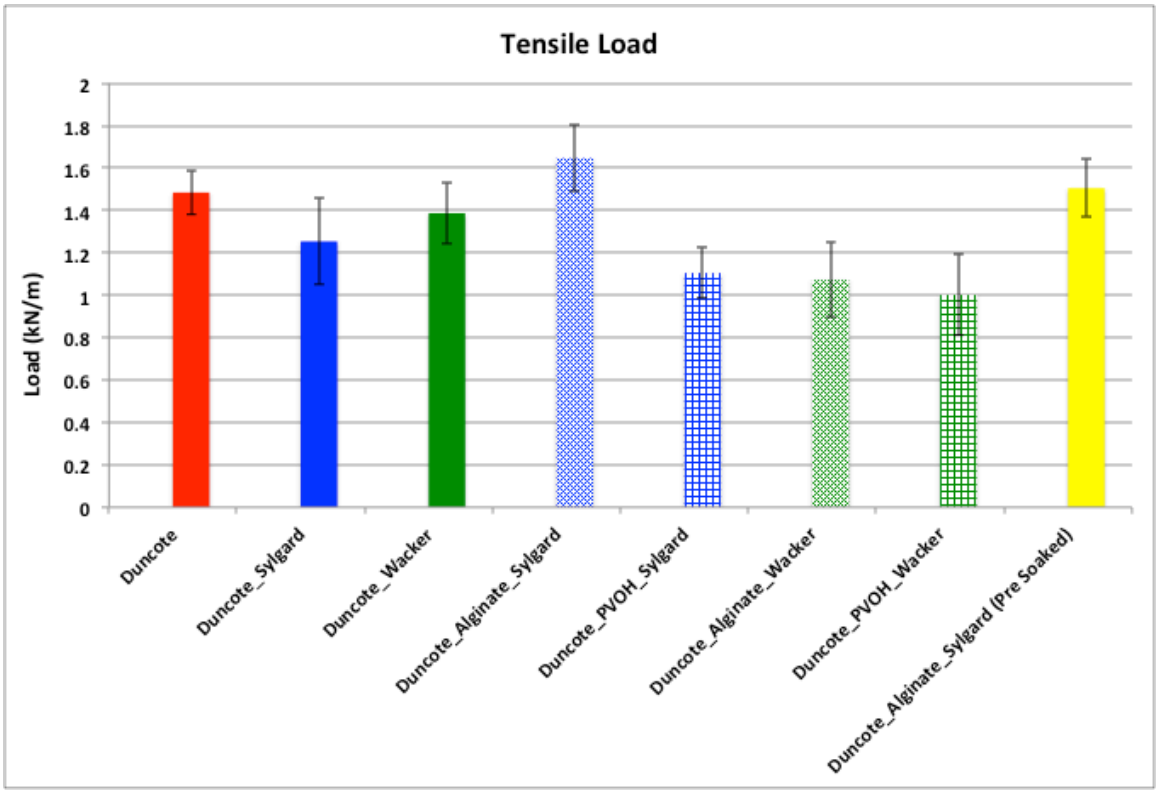

Figure 34. Tensile Load for Repulped Samples.

The tensile extension results, shown in Figure 44, show similar trends as the tensile load results. Here, however, all extensional values are lower in comparison to the commercial silicone paper. These results show the Sylgard coated samples having larger extensional values as compared to that of the Wacker samples, and the alginate/Sylgard samples having the highest average values of all the coated samples.

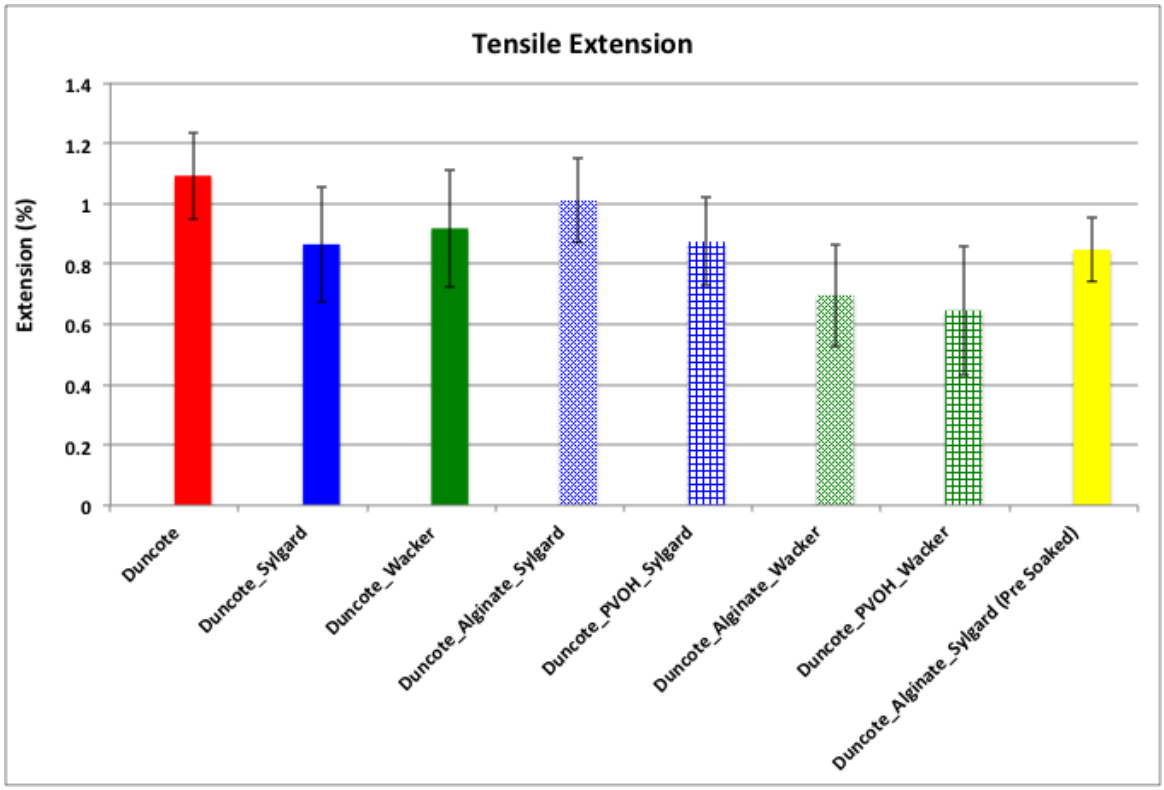

Figure 35. Tensile Extension vs. Sample Results.

From Figure 36 it may be seen that the Commercial silicone release paper has the highest silicone content present. The handsheets having the lowest silicone content are those of the Duncote/Wacker and Duncote/Alginate/Sylgard. A decrease in silicone content may be seen between the Duncote/Sylgard and Duncote/Alginate/Sylgard samples, showing the alginate sacrificial layer decreased the amount of silicone carried over into the accepts stream.

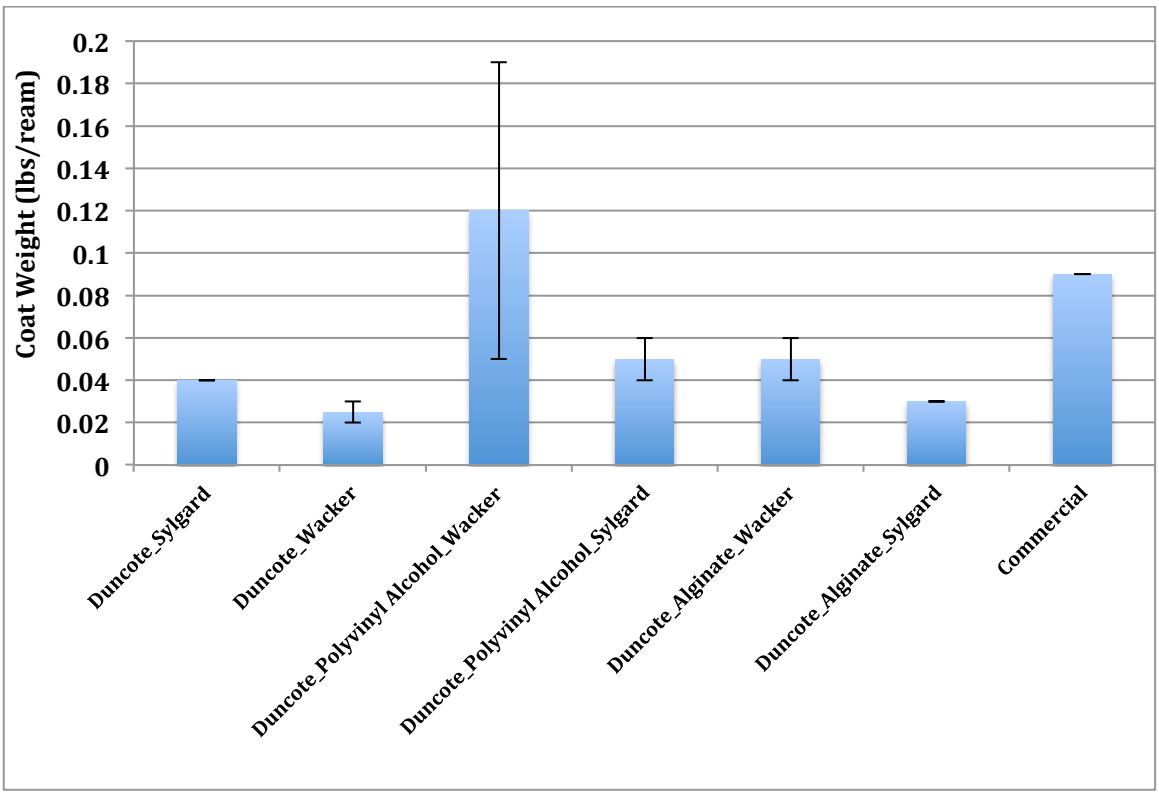

Figure 36. Oxford Twin X XRF Silica Content Results.

The large standard deviation seen with the Duncote/Polyvinyl Alcohol/ Wacker sample could be due to some sampling error, and additional testing should help to reduce this noise. It is believed that without this error the average value for this sample would align with that of the Duncote/Polyvinyl Alcohol/ Sylgard sample. The two lowest sample averages are that of the Duncote/Wacker, and Duncote/Alginate/Wacker. These samples are believed to have the lowest averages due to the lower coat weight and ability to flow through the waste stream presented from the Wacker coating. With the Duncote/Alginate/Sylgard sample it is believed that the sacrificial coating is completing the desired task of properly separating the PDMS from the paper fibers allowing the (PDMS) film to be removed during the recycling process.

6.5 Conclusions

The application of a water-soluble sacrificial pre-coat prior to the application of a silicone release coating resulted in the majority of the silicone being separated and removed during the repulping process. The lower level of rejects obtained by first applying the

sacrificial layer decreased the percent rejects to a level that meets the Recycled Paperboard Technical Association (RPTA) requirements (less than 15%) to be achieved. Based on this finding, the application of the water soluble layer was successful in enabling a newly constructed silicone release paper product to be repulped by use of conventional repulping and recycling processing methods. The sacrificial layer did not detrimentally impact the tensile strength or elongational properties of the repulped fibers indicating it was sufficiently removed during the repulping process.

CHAPTER 7

CONCLUSIONS AND FUTURE WORK

The results of this works advance the understanding of the use of surface treatment technologies to alter the surface energy and topography of PDMS films. In the first two papers presented, the ability to raise the surface energy of PDMS films by chemical and non-chemical methods was demonstrated. The chemical method utilized a mixture of a sulfuric acid and hydrogen peroxide (Piranha solution), to etch and oxidize the surface of PDMS. The non-chemical methods examined were UV-ozone and atmospheric oxygen plasma treatment methods. These methods also significantly raised the surface energy of PDMS, however, unlike the chemical treatment, the surface topography of the films were not significantly impacted. Regardless of the method used, the length of treatment time was important to controlling the extent to which the surface energy was increased. By filling the PDMS with a silica pigment, the extent of PDMS surface roughening with treatment time was reduced. The presence of filler also slightly reduced the caliper of the fabricated films.

Having gained an understanding on how to tune the surface energy of PDMS by controlling the time of treatment exposure, further works were performed to gain insight on the influences of PDMS surface energy on printability of the PDMS surface. Following the general guiding principle practiced by graphic printers that surfaces and inks that are within 10 mN/m of each other will wet and print well, the surface energy of PDMS was altered through oxygen plasma treatments to come within this desired difference of a water-based flexographic nano silver ink. However, the ink failed to print and adhere to the treated PDMS surface which does not agree with the 10 mN/m accepted practice, the untreated film print well, though the difference was approximately 20 mN/m lower than what would be considered printable. Examination of the film surfaces by XPS analysis confirmed the oxidation of the film surface. An extensive search and review of patent literature coupled with this information enabled a possible mechanism for this finding to be put forward. It is believed that the treatment of the PDMS surface with oxygen plasma altered the pH of the surface by creating

carboxylic and other acid functional groups through its oxidation. The low pH of the surface decreased the solubility of the ligand used within the ink to prevent the silver particles from sticking to one another. The loss of ligand solubility resulted in the aggregation of silver particles and increase in ink viscosity. In addition, the silver particles, being highly hydrophobic failed to wet the hydrophilic treated PDMS surface, resulting in the poor ink quality observed. While the results were not as expected, with a aqueous ink wetting and printing well on a low surface energy substrate and printing poorly on a high surface energy substrate, the findings strongly demonstrate the complexity of printing functional inks in comparison to graphic inks. From the knowledge gained, it may be possible to develop new aqueous nano metallic inks for printing PDMS films.

In the remaining three works technologies that improve the manufacture and processability of PDMS were presented. One of these works resulted in the award of an international patent for the development of a novel process technology to produce self-supportive printed sensors by using a sacrificial coating as a base layer onto which a functional device could be printed. The use of use water-soluble polymers as a release coating was then further extended into the next two works to create a roll-to-roll method for producing sub 100 micron PDMS films, which could be then be roll-to-roll printed and a repulpable silicon release paper. The novelty of these works resulted in the filing of two provisional patents.

By providing a greater understanding of the impact of material interactions on the printability of silver conductive inks on PDMS and creation of novel methods to high throughput print thin PDMS films this work has contributed to the advancement of PDMS as a biocompatible material for use in PE and non-PE applications.

Future work should focus on broadening the ink materials applied to treated PDMS films. Copper flake, nano copper, grapheme, silver coated copper inks are just a few examples of inks that could be printed in combination with treated PDMS films to advance material options for future use. Printability and adhesion studies for each of these inks should be preformed. Plasma treatments could also be extended to include interlayer treatments

towards building multilayer devices. The mechanical properties of the PDMS films before and after treatment should also be studied, since these properties would be important to the end-use performance of PE devices. Roll-to-roll coating and print trials could be attempted to work through the process requirements for manufacturing thin printed and unprinted PDMS films. It would be interesting to also study the mechanical properties of thin PDMS films produced by this method. Finally, repulping studies could be extended to include more substrates and could be performed on a larger pilot plant scale to determine the commercial viability of this technology. These studies could be performed on printed and unprinted PDMS films.

REFERENCES

1. Hi Nagatsu, et al., *Printed wiring board fabrication by offset gravure printing*, N.T.a.T.P.C. Report, Editor. 1959
2. Alexander Kamyshny, Joachim Steinke, and S. Magdassi, *Metal-based Inkjet Inks for printed electronics.* The Open Access Applied Physics, 2011. **4**: p. 19-36.
3. Younan Xia and G. Whitesides, *Soft Lithography.* Annual Review of Material Science, 1998. **28**: p. 153-184.
4. Kovalsky, A., *Biomimetic Adhesion for Transfer Printing Via Microstructured Surfaces*, in *Materials Science and Engineering*. 2011, University of Illinois at Urbana-Champaign: University of Illinois at Urbana-Champaign.
5. Xiuling Li and P. Bohn, *Metal-assisted chemical etching in HF/H_20_2 produced porous silicon.* Applied Physics Letters, 2000. **77**(16): p. 2572-2574.
6. Hyonik Leea, et al., *Selectively grown vertical silicon nanowire p-n+ photodiodes via aqueous electroless etching.* Applied Surface Science, 2013. **274**: p. 79-84.
7. Macaran. *Typical Print Station of a Flexo Press*. 2016 May 8, 2016]; Available from: http://www.macaran.com/flexo1.html.
8. Sheahan, T., *Future proofing: prepress technology in the converting sector has come on in leaps and bound in recent months. Advancements in proofing and visualisation software have been complemented by a wealth of launches in the platesetter arena*, in *Converting Today*. 2012, Progressive Media Markets Ltd.
9. Harper. *Plate Dot vs Anilox Cell.* 2016 May 8, 2016; Available from: http:// www.harperimage.com/AniloxRolls/Anilox-Guides/Plate-Dot-vs-Anilox-Cell.
10. Donovan Sung, Alejandro de la Fuente Vornbrock, and V. Subramanian, *Scaling and Optimization of Gravure-Printed Silver Nanoparticle Lines for Printed Electronics.* IEEE Transactions on Components and Packaging Technologies, 2010. **33** (1): p. 105-114.
11. Dae-Hyeong Kim, et al., *Epidermal electronics.* Science 2011. **12**: p. 838–843.
12. Vivek Subramanian, et al., *Printed organic transistors for ultra-low-cost RFID applications.* IEEE Packaging Technology, 2005. **28**(4): p. 742-747.
13. Jau Ding, et al., *Patternable polymer bulk heterojunction photovoltaic cells on plastic by rotogravure printing.* Solar Energy Materials and Solar Cells, 2009. **93**(4): p. 459-464.
14. Arias, A.C., et al., *All jet-printed polymer thin-film transistor active-matrix backplanes.* Applied Physics Letters, 2004. **85**(15): p. 3304.
15. Sai Reddy, et al., *Gravure Printed Electrochemical Biosensor.* Procedia Engineering, 2011. **25**: p. 956-959.
16. Abhinav Gaikwad, et al., *A flexible high potential printed battery for powering printed electronics.* Applied Physics Letters, 2013. **102**(23): p. 233302.
17. Tse Nga Ng, et al., *Organic inkjet-patterned memory array based on ferroelectric field-effect transistors.* Organic Electronics, 2011. **12**(12): p. 2012-2018.
18. Sunho Jeong and Jooho Moon, *Low-temperature, solution-processed metal oxide thin film transistors.* Journal of Materials Chemistry, 2012. **22**(4): p. 1243-1250.
19. Jolke Perelaer, et al., *Printed electronics: the challenges involved in printing devices, interconnects, and contacts based on inorganic materials.* Journal of Materials Chemistry, 2010. **20**(39): p. 8446-8453.

20. Jiang Yusheng, et al., *Applications of micro/nanoparticles in microfluidic sensors: a review.* Sensors (Basel), 2014. **14**(4): p. 6952-6964.
21. Mark Leenen, et al., *Printable electronics: flexibility for the future.* physica status solidi (a), 2009. **206**(4): p. 588-597.
22. Jovanche Trajkovikj, J-F Zürcher, and A.K. Skrivervik, *Soft and Flexible Antennas on Permittivity Adjustable PDMS Substrates*, in *Loughborough Antennas & Propagation Conference*. 2012, IEEE: Loughborough, UK. p. 1-4.
23. Dan Soltman, et al., *Methodology for inkjet printing of partially wetting films.* Langmuir, 2010. **26**(19): p. 15686–15693.
24. Namsoo Lim, et al., *Screen printed resonant tags for electronic article surveillance tags.* IEEE Transactions on Advanced Packaging, 2009. **32**(1): p. 72-76.
25. Sooman Lim, et al., *Inkjet Printing and Sintering of Nano-Copper Ink.* Journal of Imaging Science and Technology, 2013. **57**(5): p. 50506-1-50506-7.
26. Veronika Hrehorova, et al., *Gravure Printing of Conductive Inks on Glass Substrates for Applications in Printed Electronics.* Journal of Display Technology, 2011. **7**(6): p. 318-324.
27. Michael Joyce, et al., *Contribution of Flexo Process Variables to Fine Line Ag Electrode Performance.* International Journal of Engineering Research & Technology 2014. **3**(8): p. 1645-1656.
28. Kay Reuter, et al., *Influence of process parameters on the electrical properties of offset printed conductive polymer layers.* Progress in Organic Coatings, 2007. **58**(4): p. 312-315.
29. Suganuma, K., *Introduction to Printed Electronics(Book)*. Springer Briefs in Electrical and Computer Engineering. 2014, Springer Science+Business Media New York Springer. 1-124.
30. Young, *An Essay on the Cohesion of Fluids.* Philosophical Transactions Royal Society of London, 1805. **95**: p. 65-87.
31. Noh Dongsun Yeom, et al., *Scalability of Roll-to-Roll Gravure-Printed Electrodes on Plastic Foils.* IEEE Transactions on Electronics Packaging Manufacturing 2010. **33**(4): p. 1-9.
32. Erika Hrehorova, et al. *The Properties of Conducting Polymers and Substrates for Printed Electronics*. in *NIP & Digital Fabrication*. 2005. Society for Imaging Science and Technology.
33. Erika Hrehorova, et al. *Polymeric Materials for Printed Electronics and Their Interactions with Paper Substrates*. in *23rd International Conference on Digital Printing Technologies, and Digital Fabrication*. 2007.
34. Vivek Subramanian, et al., *Progress Toward Development of All-Printed RFID Tags- Materials, Processes, and Devices*, in *IEEE*. 2005. p. 1330-1338.
35. Khosla, A., *Nanoparticle-doped Electrically-conducting Polymers for Flexible Nano-Micro Systems.* The Electrochemical Society, 2012(4): p. 67-70.
36. Madaria Anuj, et al., *Uniform, highly conductive, and patterned transparent films of a percolating silver nanowire network on rigid and flexible substrates using a dry transfer technique.* Nano Research, 2010. **3**(8): p. 564-573.
37. Dania Alsaid, et al., *Gravure Printing of ITO Transparent Electrodes for Applications in Flexible Electronics.* Journal of Display Technology, 2012. **8**(7).

38. Mathias Brust, et al., *Synthesis of Thiol-derivatised Gold Nanoparticles in a Two-phase Liquid-Liquid System.* Journal of the Chemical Society, Chemical Communications, 1994(7): p. 801-802.
39. Ph Buffat and J.-P. Borel, *Size effect on the melting temperature of gold particles.* Physics Review 1976. **13**: p. 2287-2298.
40. Chien-Yi Peng, et al. *Flexible CZTS Solar Cells on Flexible Corning® Willow® Glass Substrates*. in *Photovoltaic Specialist Conference*. 2014. Denver, CO: IEEE.
41. Malik Abdul and W. Dongxin, *Solid phase microextraction fiber structure and method of making*, U.S.P. Office, Editor. 2000, Malik Abdul, Univ South Florida, Wang Dongxin: United States.
42. Alvaro Mata, A. Fleischman, and R. Shuvo, *Characterization of Polydimethylsiloxane (PDMS) Properties for Biomedical Micro/Nanosystems.* Biomedical Microdevices, 2005. **7**(4): p. 281-293.
43. Eric Leclerc, Yasuyuki Sakai, and T. Fujii, *Cells culture in a three-dimensional network of PDMS (PolyDiMethylSiloxane) microchannels.* Biomedical Microdevices, 2003. **5**(2): p. 109-114.
44. Buddy Ratner, et al., *Biomaterials Science*. An Introduction to Materials in Medicine. 1996, New York: Academic Press. 484.
45. Yong-Hwan Choi, et al., *An electrodynamic preconcentrator integrated thermoelectric biosensor chip for continuous monitoring of biochemical process.* Journal of Micromechanics and Microengineering, 2012. **22**(4).
46. Jianwei Wu, et al., *Inkjet-printed microelectrodes on PDMS as biosensors for functionalized microfluidic systems.* Lab Chip, 2014. **15**: p. 690-695.
47. Whitesides, X.a., Angewandte Chemie International Edition 1998. **37**: p. p. 550–575
48. Jasbir Patel, et al., *PDMS as a sacrificial substrate for SU-8-based biomedical and microfluidic applications.* Journal of Micromechanics and Microengineering, 2008. **18**(9): p. 1-12.
49. Donghak Byun, Cho Sung Joon, and S. Kim, *Fabrication of a flexible penetrating microelectrode array for use on curved surfaces of neural tissues.* Journal of Micromechanics and Microengineering, 2013. **23**: p. 1–10.
50. Hermann Brischwein, et al., *Electric cell-substrate impedance sensing with screen printed electrode structures.* Lab on a Chip, 2006. **6**: p. 819-822.
51. M I Maksud, et al., *A Study on Printed Multiple Solid Line by Combining Microcontact and Flexographic Printing Process for Microelectronic and Biomedical Applications.* International Journal of Integrated Engineering, 2013. **5**(3): p. 36-39.
52. M I Maksud, et al., *Study on Finite Element Analysis of Fine Solid Lines by Flexographic Printing in Printed Antennas for RFID Transponder.* International Journal of Integrated Engineering, 2012. **5**(3): p. 36-39.
53. Mohd Yusof, Z Said, and M.I. Maksud, *Exploration of Fine Lines Profile Effects in Flexographic Printing.* Journal of Appied. Mechanical Mater, 2013. **315**: p. 458–462.

54. Mohd Yusof and D. Gethin, *Investigation of Carbon Black Ink on Fine Solid Line Printing in Flexography*, in *10th World Scientific and Engineering Academy and Society (WSEAS) international conference*. 2011. p. 138–142.
55. Qiang Zheng, et al., *In vivo powering of pacemaker by breathing-driven implanted triboelectric nanogenerator.* Adv Mater, 2014. **26**(33): p. 5851-5856.
56. Kim Seunghwan, et al., *Effect of hydrophobic microstructured surfaces on conductive ink printing.* Journal of Micromechanics and Microengineering, 2011. **21**(9): p. 1-8.
57. Paal Klykken, Margaret Servinski, and X. Thomas, *Silicone Film-Forming Technologies for Health Care Applications*. 2004, Dow Corning: Dow Corning.
58. Khairudin Mohamed, Nazrin Kooy, and K. Ibrahim, *Development of a low cost roll-to-roll nanoimprint lithography system for patterning 8-inch wide flexible substrates.* International Journal of Nanotechnology 2014. **11**(5/6/7/8): p. 520-528.
59. Smokefoot. *PDMS Molecular Structure*. 2015 January 2, 2016]; Available from: href="https://commons.wikimedia.org/wiki/File:PmdsStructure.png -/media/File:PmdsStructure.png>"
60. Binu Narakathu, et al., *Development of a Novel Printed Flexible Microfluidic Sensing Platform Based on PCB Technology*, in *13th IEEE Sensors Conference*. 2014: Valencia, Spain. p. 665-668.
61. Ali Eshkeiti, et al., *Screen Printed Flexible Capacitive Pressure sensor*, in *13th IEEE Sensors Conference*. 2014: Valencia, Spain. p. 1192-1195.
62. Shantanu Bhattacharya, et al., *Studies on Surface Wettability of Poly(Dimethyl) Siloxane (PDMS) and Glass Under Oxygen-Plasma Treatment and Correlation With Bond Strength.* MicroElectro Mechanical Systems, 2005. **14**(3): p. 590-597.
63. Maji Debashis, S Lahiri, and D. Soumen, *Study of hydrophilicity and stability of chemically modified PDMS surface using piranha and KOH solution.* Surface and Interface Analysis, 2012. **44**(1): p. 62-69.
64. Attila Oláh, H. Hillborg, and J. Vancso, *Hydrophobic recovery of UV/ozone treated poly(dimethylsiloxane): adhesion studies by contact mechanics and mechanism of surface modification.* Applied Surface Science, 2005. **239**(3-4): p. 410-423.
65. Veronika Hrehorova, et al., *Polymeric Materials for Printed Electronics and Their Interactions with Paper Substrates*, in *23rd International Conference on Digital Printing Tech* 2007, NIP.
66. Nir Dov Zamir, et al., *Electrically conductive inks for inkjet printing* in *The chemistry of inkjet inks*, S. Magdassi, Editor. 2010, New Jersey-London Singapore: World Scientific. p. 225-254.
67. Erica Coenen, et al., *Photonic sintering of inkjet printed current collecting grids for organic solar cell applications.* Organic Electronics, 2013. **14**(1): p. 38-46.
68. Michael Grouchko, Alexander Kamyshnya, and S. Magdassi, *Formation of air-stable copper–silver core–shell nanoparticles for inkjet printing.* Journal of Materials Chemistry 2009. **19**: p. 3057-3062.
69. Angstroms, F.T. *Owens-Wendt Surface Energy Calculation*. 1998 [cited 2015 August 16, 2015]; Available from:

http://www.firsttenangstroms.com/pdfdocs/OwensWendtSurfaceEnergyCalculation.

70. D. K. Owens and R. C. Wendt, *Estimation of Surface Free Energy of Polymers.* Journal of Applied Polymer Science, 1969. **13**: p. 1741-1747.
71. Sari Merilampi, T. Laine-Ma, and P. Ruuskanen, *The characterization of electrically conductive silver ink patterns on flexible substrates.* Microelectronics Reliability, 2009. **49**(7): p. 782-790.
72. Tong Ge, et al., *Fully-Additive Printed Electronics on Flexible Substrates- A Fully-Additive RFID Tag*, in *IEEE 57th International Midwest Symposium on Circuits and Systems (MWSCAS)*. 2014.
73. Pak Lau, et al., *Fully printed, high performance carbon nanotube thin-film transistors on flexible substrates.* Nano Lett, 2013. **13**(8): p. 3864–3869.
74. Wayman N.M. Wong, e.a., *Gravure Printed Hydrophobic Templates onto PET Films for Guiding the Assembly of Nanowires: Towards the Ultralow-Cost Transparent Conductive Electrodes*, in *Electronic Components and Technology Conference*, IEEE, Editor. 2011.
75. Aijazi, A.T., *Printing Functional Electronic Circuits and Components*, in *Chemical and Paper Engineering*. 2014, Western Michigan University.
76. Davide Deganello, et al., *Impact of metered ink volume on reel-to-reel flexographic printed conductive networks for enhanced thin film conductivity.* Thin Solid Films, 2012. **520**(6): p. 2233-2237.
77. Jongwoo Lim, et al., *All-inkjet-printed Metal-Insulator-Metal (MIM) capacitor.* Current Applied Physics, 2012. **12**: p. e14-e17.
78. Seamus Burns, et al., *Inkjet Printing of Polymer Thin-Film Transistor Circuits.* Mrs Bulletin, 2003: p. 829-834.
79. Matthew Fahlman and W. Salaneck, *Surfaces and interfaces in polymer-based electronics.* Surface Science, 2002(1-3): p. 904-922.
80. Appelt, B., *Advanced Substrates: A Materials and Processing Perspective*, in *Materials for Advanced Packaging*, D. Lu, Editor. 2009, Springer. p. 243-271.
81. Kirill Efimenko, William Wallace, and J. Genzer, *Surface Modification of Sylgard-184 Poly(dimethyl siloxane) Networks by Ultraviolet and Ultraviolet/Ozone Treatment.* Journal of Colloid and Interface Science, 2002. **254**(2): p. 306-315.
82. Brown, H., *Adhesion-Between-Polymers-and-Other-Substances-A-Review-of-Bonding-Mechanisms-Systems-and-Testing.* Materials Forum, 2013. **24**: p. 48-58.
83. Seung Ko, et al., *All-inkjet-printed flexible electronics fabrication on a polymer substrate by low-temperature high-resolution selective laser sintering of metal nanoparticles.* Nanotechnology, 2007. **18**(34): p. 1-8.
84. Ahmed Aijazi, et al., *Evaluation of Screen Printed Inductive Coils for Wireless Power.* International Journal of Science and Advanced Technology, 2012. **2**(10): p. 6.
85. Dhananjay Bodas and C. Khan-Malek, *Hydrophilization and hydrophobic recovery of PDMS by oxygen plasma and chemical treatment—An SEM investigation.* Sensors and Actuators B: Chemical, 2007(123): p. 368-373.
86. Andreas Schutze, et al., *The Atmospheric-Pressure Plasma Jet: A Review*

and Comparison to Other Plasma Sources. IEEE Transactions on Plasma Science, 1998. **26**(6): p. 1685-1694.
87. Arpita Bhattacharyy and C. Klapperich, *Mechanical and chemical analysis of plasma and ultraviolet-ozone surface treatments for thermal bonding of polymeric microfluidic devices.* Lab Chip, 2007. **7**(7): p. 876-82.
88. Donghee Leea and S. Yang, *Surface modification of PDMS by atmospheric-pressure plasma-enhanced chemical vapor deposition and analysis of long-lasting surface hydrophilicity.* Sensors and Actuators B: Chemical, 2012. **1**(62): p. 425-434.
89. Hui Taek Kim and O.C. Jeong, *PDMS surface modification using atmospheric pressure plasma.* Microelectronic Engineering, 2011(88): p. 2281-2285.
90. Lance Kersey, et al., *The effect of adhesion promoter on the adhesion of PDMS to different substrate materials.* Lab on a Chip, 2009. **9**: p. 1002-1004.
91. Eleazar Gonzalez II, et al., *Remote Atmospheric-Pressure Plasma Activation of the Surfaces of Polyethylene Terephthalate and Polyethylene Naphthalate.* Langmuir, 2008. **24**(21): p. 12636-12643.
92. Ramesh Kattumenu, et al., *Evaluation of Flexographically Printed Conductive Traces on Paper Substrates for RFID Applications.* Technical Association for the Graphic Arts (TAGA), 2011. **5**(1): p. 1-18.
93. Sindhu Vudayagiri, Michael Daniel Junker, and A.L. Skov, *Factors affecting surface and release properties of thin Polydimethylsiloxane films.* Polymer Journal, 2013. **45**: p. 871–878.
94. Hans-Erik Kiil and M. Benslimane. *Scalable industrial manufacturing of DEAP*. in *Electroactive Polymer Actuators and Devices (EAPAD)*. 2009. San Diego, California, USA: The International Society for Optical Engineering.
95. Johana Kuncova-Kallio and P. Kallio. *PDMS and its suitability for analytical microfluidic devices*. in *Engineering in Medicine and Biology Society, 28th Annual International Conference of the IEEE*. 2006. New York, New York: IEEE.
96. Mark Eddings, Michael Johnson, and B. Gale, *Determining the optimal PDMS–PDMS bonding technique for microfluidic devices.* Journal of Micromechanics and Microengineering, 2008. **18**(6): p. 1-4.
97. Alexandre Larmagnac, et al., *Stretchable electronics based on Ag-PDMS composites*. 2014, Biomedical Engineering: Nature.com. p. 1-7.
98. Han-Sheng Chuang and S. Wereley, *Design, fabrication and characterization of a conducting PDMS for microheaters and temperature sensors.* Journal of Micromechanics and Microengineering, 2009. **19**(4): p. 1-5.
99. Xize Niu, et al., *Characterizing and Patterning of PDMS-Based Conducting Composites.* Advanced Materials, 2007. **19**(18): p. 2682-2686.
100. Hailin Cong and T. Pan. *Microfabrication of Conductive PDMS on Flexible Substrates for Biomedical Applications*. in *International Conference on Nano/Micro Engineered and Molecular Systems*. 2009. Shenzhen: IEEE.
101. Liyu Liu, et al., *Microheaters fabricated from a conducting composite.* Applied Physics Letters, 2006. **89**(22): p. 223521-3.

102. Dean Campbell, et al., *Replication and Compression of Surface Structures with Polydimethylsiloxane Elastomer.* Journal of Chemical Education, 1999. **76**(4): p. 537.
103. Inc., S. *Thin Silicone Membranes*. 2016 May 8, 2016]; Available from: http://sspinc.com/products/Thin_Silcone_Membranes_4_category.htm.
104. Margaret Joyce, et al., *Self-Supported Electronic Devices*, W.I.P. Organization, Editor. 2016. p. 33.
105. Michael Joyce, et al., *Self-supported printed multi-layer capacitors.* Journal of Print and Media Technology Research, 2015. **4**(4): p. 241-316.
106. Dohler, H., *Low-cost Paper Applications.* Paper Film and Foil Converter, 2005. **79**(11).
107. Reardon, C., *Paper or Plastic?* Paper, Film and Foil Converter, 2009. **83**(12).
108. munksjo. 2016; Available from: http://www.munksjo.com/products/release-liners/release-papers/.
109. Andriot, M., *Silicones in Industrial Applications*, in *Inorganic Polymers*, M.G. Roger De Jaeger, Editor. 2007, Nova Science: New York. p. 61-161.
110. Benedek, I., *Buildup and Classification of Pressure-Sensitive Products*, in *Development in Pressure-Sensitive Products*, I. Benedek, Editor. 2005, Taylor and Francis: Boca Raton.
111. Benedek, I., *Manufacture of Pressure-Sensitive Products*, in *Development and Manufacture of Pressure-Sensitive Products*, I. Benedek, Editor. 1999, Marcel Dekker: New York.
112. Robert Scott Vonfelden and J. Kokoszka, *Release Coating*, U.S.P. Office, Editor. 2014, Sustainable Fiber Solutions, LLC. p. 4.
113. Noll, W., *Chemistry and Technology of Silicones*. 1983, New York: Academic Press.
114. Roland Gong, et al. *Elimination of Pressure Sensitive Label and Deinkability of Water Based Flexographic and NIP Inks in One Recycling Step*. in *Technical Association of the Graphic Arts (TAGA)*. 2012.
115. Lokendra Pal, Margaret Joyce, and P.D. Fleming, *A Simple Method for Calculation of the Permeability Coefficient of Porous Media.* TAPPI, 2006. **5**(9).

APPENDIX

Regression Analysis: Surface Energy versus Treatment Time, % Silica Fill, Treatment Type

Method: Categorical predictor coding (1, 0)

Analysis of Variance

Source	DF	Adj SS	Adj MS	F-Value	P-Value
Regression	4	566.94	141.74	13.78	0.000
Treatment Time	1	91035	91035	8.88	0.007
% Silica Fill	1	200.67	200.67	19.52	0.000
Treatment Type	2	72.71	36.36	3.54	0.470
Error	22	226.20	10.28		
Total	26	793.15			

*Computed using alpha = 0.05

Model Summary

S	R-sq	R-sq(adj)	R-sq(pred)
3.20656	71.48%	66.29%	57.43%

Coefficients

Term	Coef	SE Coef	T-Value	P-Value	VIF
Constant	21.39	2.00	10.70	0.000	
Treatment Time	0.1745	0.0585	2.98	0.007	1.56
% Silica Fill	0.668	0.151	4.42	0.000	1.00
Treatment Type					
Piranha	6.34	2.54	2.50	0.200	4.17
UV-Ozone	4.35	2.54	1.71	0.101	4.17

Treatment Type	Regression Equation
None	Surface Energy= 21.39 + 0.1745(Treatment Time) + 0.668(% Silica Fill)
Piranha	Surface Energy = 27.73 + 0.1745(Treatment Time) + 0.668(% Silica Fill)
UV-Ozone	Surface Energy = 25.74 + 0.1745(Treatment Time) + 0.668(% Silica Fill)

Contact Angles of PDMS Films

Water Contact Angle		Methylene Iodide Contact Angle		Treatment Type	Treatment Time (min)	Silica Fill (%)
STD (±)	*Average*	STD (±)	*Average*			
2.3	98.5	1.8	66.5	Control		0
1.4	92.4	1.2	65.8	Control		5
3.7	96.2	1.3	64.6	Control		10
3.1	84.8	1.2	63.6	Uv-Ozone	10	0
0.0	80.1	0.1	63.3	Uv-Ozone	10	5
2.7	80.7	0.6	62.3	Uv-Ozone	10	10
1.0	70.2	1.7	66.6	Uv-Ozone	20	0
0.1	79.5	0.1	61.4	Uv-Ozone	20	5
1.0	76.7	0.6	61.5	Uv-Ozone	20	10
0.7	70.3	3.2	63.9	Uv-Ozone	30	0
0.1	73.6	0.1	55.8	Uv-Ozone	30	5
1.3	72.5	2.2	53.2	Uv-Ozone	30	10
0.9	69.3	2.5	65.1	Uv-Ozone	40	0
0.2	81.7	0.1	55.9	Uv-Ozone	40	5
1.8	62.4	1.8	53.4	Uv-Ozone	40	10
2.5	85.1	3.1	67.7	Piranha Solution	10	0
1.2	81.3	2.3	59.3	Piranha Solution	10	5
7.5	69.2	2.5	48.0	Piranha Solution	10	10
2.9	80.3	5.4	70.3	Piranha Solution	20	0
3.3	72.3	2.9	51.3	Piranha Solution	20	5
3.8	65.6	1.7	51.5	Piranha Solution	20	10
2.9	77.6	3.7	64.4	Piranha Solution	30	0
2.9	74.1	2.4	50.1	Piranha Solution	30	5
3.7	67.3	2.7	38.8	Piranha Solution	30	10
3.2	78.9	4.3	66.9	Piranha Solution	40	0
3.0	73.9	1.6	52.2	Piranha Solution	40	5
6.2	65.9	8.7	50	Piranha Solution	40	10

Contact Angle vs. Time Plot of 40 minute Piranha Treated Film

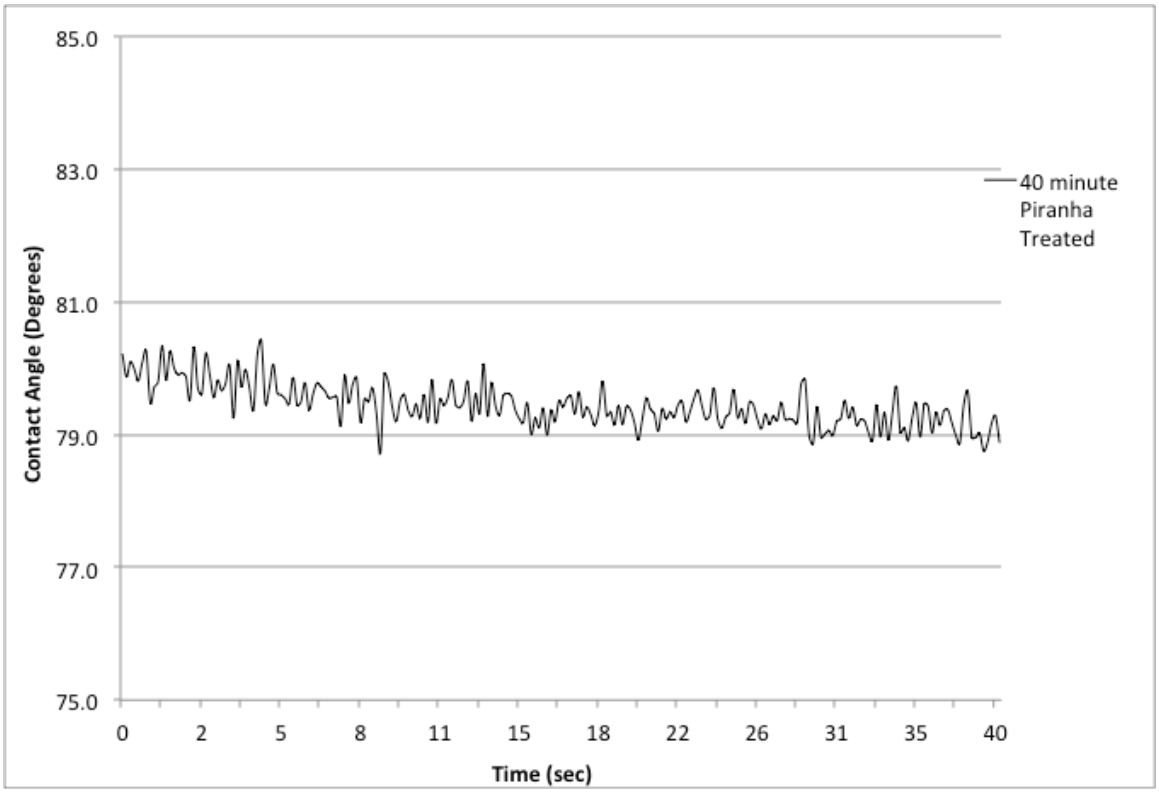

Surface Energies of PDMS Films

Total Surface Energy			Polar Component			Dispersive Component			Treatment Type	Treatment Time (min)	Silica Fill (%)
(-) Average	*Average*	*(+) Average*	*(-) Average*	*Average*	*(+) Average*	*(-) Average*	*Average*	*(+) Average*			
22.0	21.5	21.2	0.7	0.6	0.4	21.3	21.0	20.8	Control		0
25.9	25.0	25.6	3.3	2.9	3.1	22.6	22.2	22.6	Control		5
27.0	26.0	25.2	2.7	1.8	1.0	24.2	24.2	24.2	Control		10
29.9	28.5	27.1	7.4	6.1	4.8	22.5	22.4	22.3	Uv-Ozone	10	0
30.2	30.2	30.2	8.6	8.6	8.6	21.7	21.6	21.6	Uv-Ozone	10	5
31.6	30.3	29.2	9.5	8.0	6.7	22.1	22.3	22.5	Uv-Ozone	10	10
35.3	34.3	33.3	16.8	16.6	16.4	18.5	17.7	16.9	Uv-Ozone	20	0
31.2	31.1	31.1	8.5	8.5	8.5	22.7	22.6	22.6	Uv-Ozone	20	5
32.9	32.3	31.8	10.7	10.3	9.6	22.1	22.0	22.2	Uv-Ozone	20	10
34.7	34.8	33.7	17.1	15.6	16.2	17.5	19.3	17.6	Uv-Ozone	30	0
35.6	35.6	35.4	10.8	10.8	10.7	24.8	24.8	24.9	Uv-Ozone	30	5
38.3	34.3	35.6	11.1	13.1	10.5	27.2	21.1	25.1	Uv-Ozone	30	10
36.3	35.2	34.1	16.6	16.8	17.0	19.7	18.4	17.1	Uv-Ozone	40	0
43.6	32.6	32.6	6.2	6.1	6.0	26.5	26.6	26.6	Uv-Ozone	40	5
28.8	42.1	40.6	19.0	18.1	17.3	24.6	23.9	23.2	Uv-Ozone	40	10
32.6	26.7	24.7	7.5	6.8	6.2	21.3	19.9	18.5	Piranha Solution	10	0
44.6	31.3	30.0	7.3	7.0	6.9	25.5	24.3	23.1	Piranha Solution	10	5
30.8	40.2	36.4	16.2	11.7	7.6	28.4	28.6	28.8	Piranha Solution	10	10
40.2	27.8	25.0	10.8	10.4	10.1	20.0	17.4	14.8	Piranha Solution	20	0
43.4	37.7	35.3	11.9	10.5	9.1	28.2	27.3	26.2	Piranha Solution	20	5
33.4	41.0	38.7	16.9	14.6	12.6	26.6	26.4	26.1	Piranha Solution	20	10
39.5	30.9	28.4	11.4	10.5	9.7	22.1	20.4	18.8	Piranha Solution	30	0
46.5	37.0	35.4	10.3	9.3	7.9	29.2	27.7	27.6	Piranha Solution	30	5
32.4	44.1	41.8	33.8	10.8	9.1	12.7	33.3	32.7	Piranha Solution	30	10
32.4	29.5	26.8	11.2	10.4	9.5	21.1	19.2	17.3	Piranha Solution	40	0
38.6	36.8	35.0	11.2	9.7	8.2	27.4	27.1	26.8	Piranha Solution	40	5
46.8	41.1	35.3	16.6	14.5	12.6	30.2	26.7	22.7	Piranha Solution	40	10

Contact Angles of Films

Water Contact Angle				Methylene Iodide Contact Angle				Treatment Type	# of Passes
(-) Average	STD	Average	(+) Average	(-) Average	STD	Average	(+) Average		
96.2	2.3	98.5	100.8	64.7	1.8	66.5	68.3	Control	0
63.3	5.5	68.8	74.3	60.9	2.5	63.4	65.9	P120/60mm-s	1
43.4	2.8	46.2	49.0	42.6	6.2	48.8	55.0	P120/60mm-s	2
17.7	3.0	20.7	23.7	43.0	3.9	46.9	50.8	P120/60mm-s	3
72.5	8.9	81.4	90.3	61.7	1.3	63.0	64.3	P120/120mm-s	1
68.8	1.2	70.0	71.2	61.5	1.1	62.6	63.7	P120/120mm-s	2
32.0	1.1	33.1	34.2	56.3	2.5	58.8	61.3	P120/120mm-s	3
6.2	13.5	19.7	33.2	47.1	5.3	52.4	57.7	P180/60mm-s	1
5.8	14.9	20.7	35.6	39.8	2.3	42.1	44.4	P180/60mm-s	2
10.6	7.3	17.9	25.2	33.0	3.3	36.3	39.6	P180/60mm-s	3
52.9	3.5	56.4	59.9	58.5	1.4	59.9	61.3	P180/120mm-s	1
36.6	4.5	41.1	45.6	40.4	6.1	46.5	52.6	P180/120mm-s	2
13.3	4	17.3	21.3	42.2	5.8	48.0	53.8	P180/120mm-s	3

Surface Energies of Films

Total Surface Energy			Polar Component			Dispersive Component			Treatment Type	# of Passes
(-) Average	*Average*	*(+) Average*	*(-) Average*	*Average*	*(+) Average*	*(-) Average*	*Average*	*(+) Average*		
22.0	21.54	21.2	0.7	0.56	0.4	21.3	20.98	20.8	Control	
39.96	36.56	33.30	20.16	17.06	14.32	19.81	19.50	18.98	P120/60mm-s	1
56.15	54.12	50.89	27.85	27.49	25.88	28.29	26.63	28.35	P120/60mm-s	2
71.01	69.89	63.45	48.10	48.54	42.80	22.95	21.35	20.65	P120/60mm-s	3
32.64	29.98	27.81	10.77	7.88	5.55	21.87	22.10	22.28	P120/120mm-s	1
40.09	37.12	35.05	19.18	16.99	15.07	20.68	20.13	19.99	P120/120mm-s	2
65.44	60.80	55.55	48.26	44.03	38.80	17.18	16.76	16.72	P120/120mm-s	3
69.89	69.11	66.22	49.44	50.24	48.73	19.18	18.70	17.49	P180/60mm-s	1
71.41	68.71	63.07	46.27	44.81	39.88	23.88	23.90	23.18	P180/60mm-s	2
71.42	69.33	66.67	43.56	42.71	41.19	26.86	26.61	25.48	P180/60mm-s	3
48.37	46.60	44.81	28.17	26.94	25.68	20.19	19.67	19.12	P180/120mm-s	1
61.55	57.03	52.35	35.35	32.77	30.08	26.20	24.27	22.26	P180/120mm-s	2
70.24	68.68	67.41	47.61	47.70	47.89	22.63	20.98	19.52	P180/120mm-s	3

XPS Results

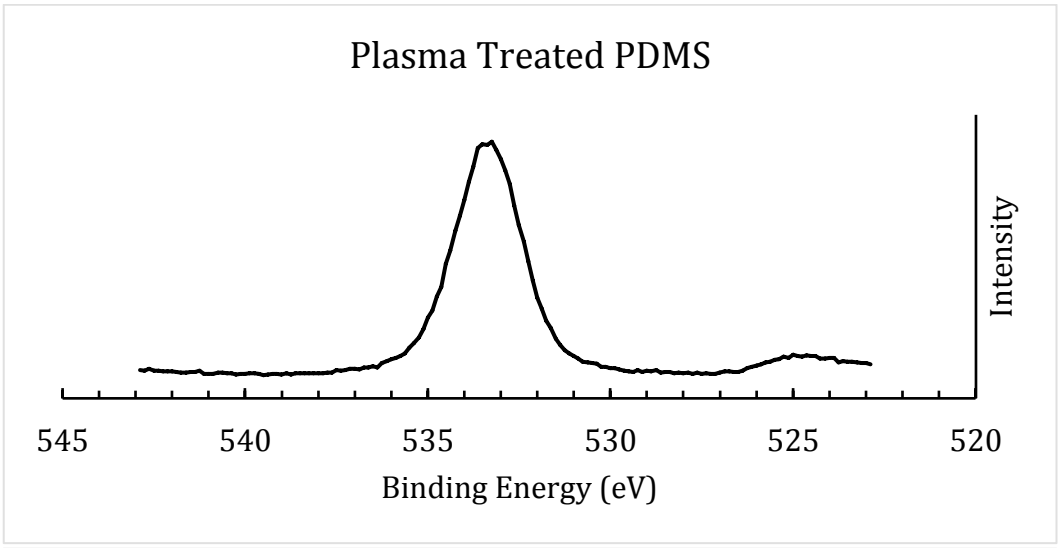
Plasma Treated PDMS
Intensity
545
540
535
530
525
520
Binding Energy (eV)

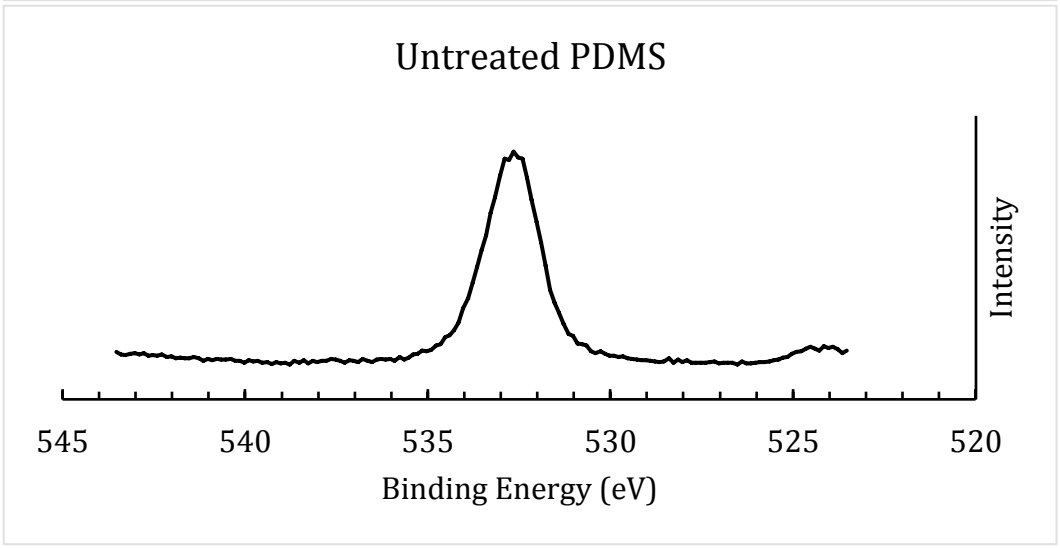
Untreated PDMS
Intensity
545
540
535
530
525
520
Binding Energy (eV)

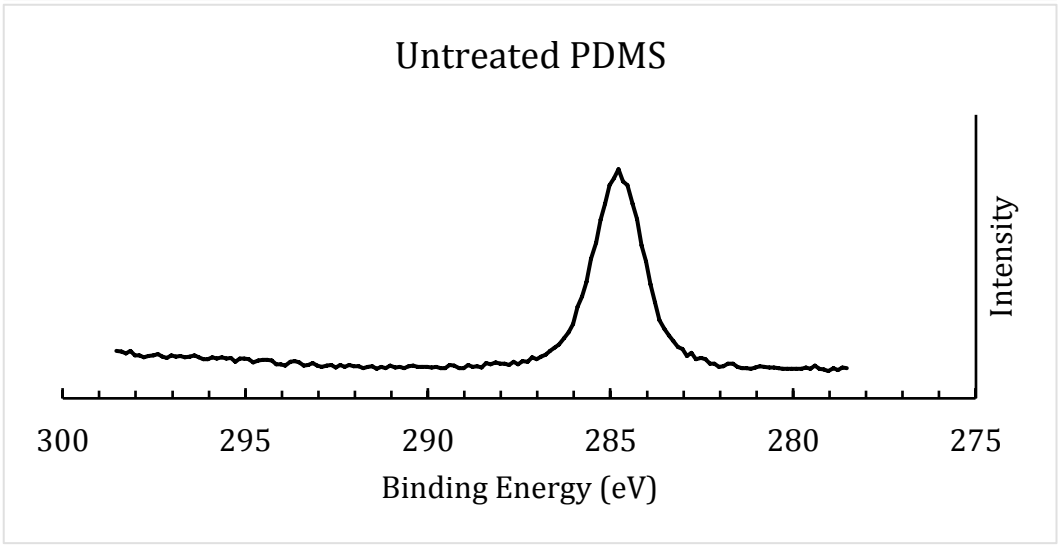
Untreated PDMS
Intensity
300
295
290
285
280
275
Binding Energy (eV)

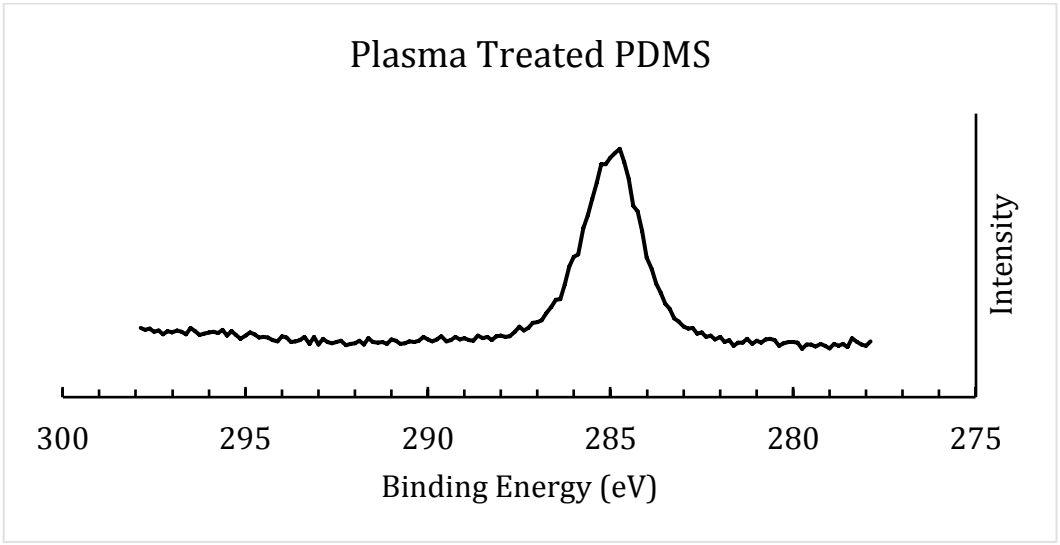
Plasma Treated PDMS
Intensity
300
295
290
285
280
275
Binding Energy (eV)

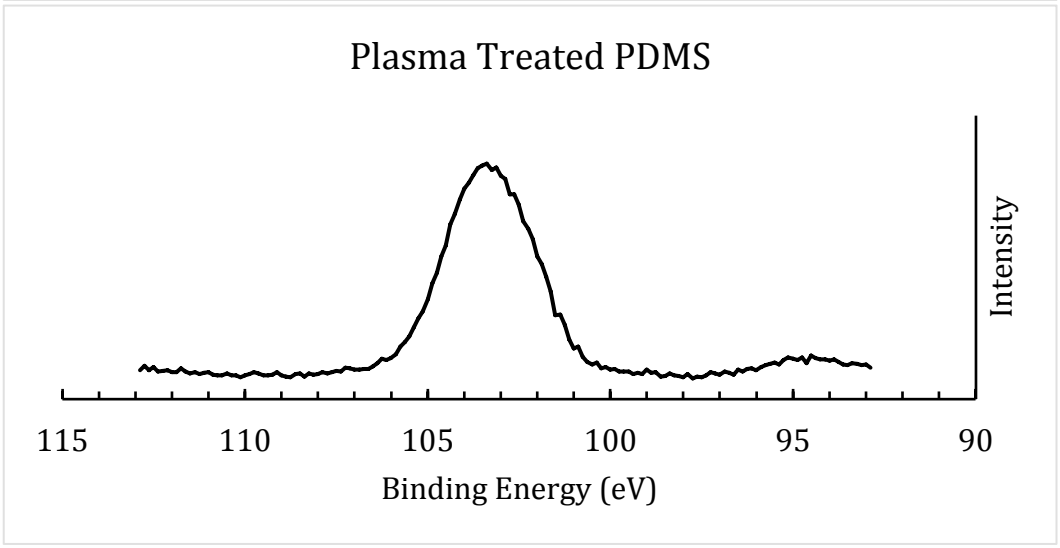
Plasma Treated PDMS
Intensity
115
110
105
100
95
90
Binding Energy (eV)

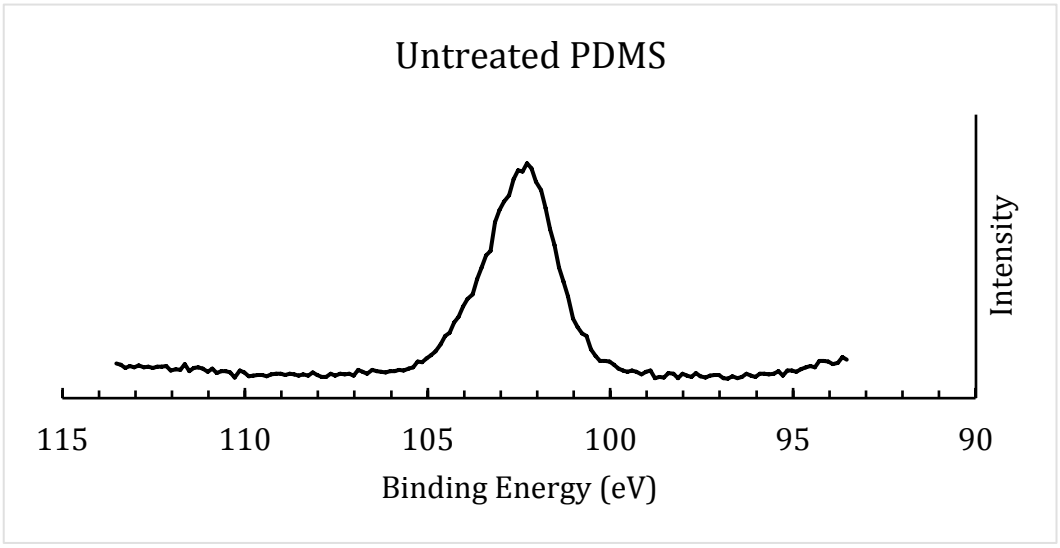
Untreated PDMS
Intensity
115
110
105
100
95
90
Binding Energy (eV)

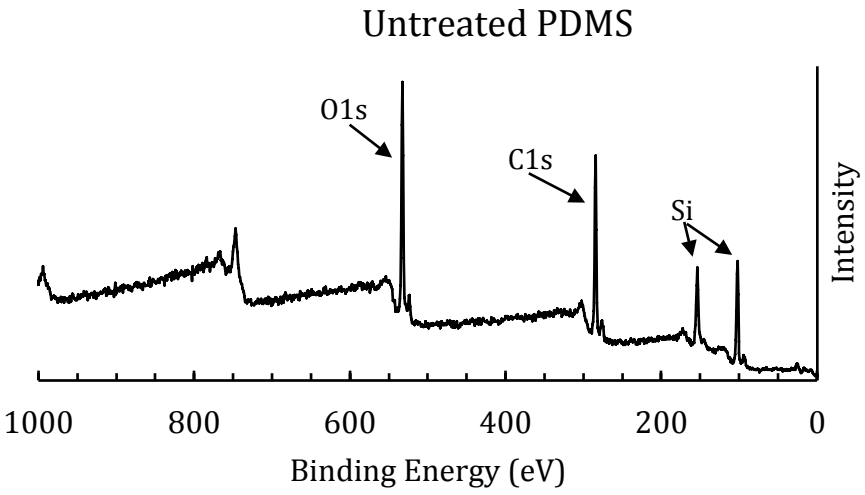
Untreated PDMS
O1s
C1s
Si
Intensity
1000
800
600
400
200
0
Binding Energy (eV)

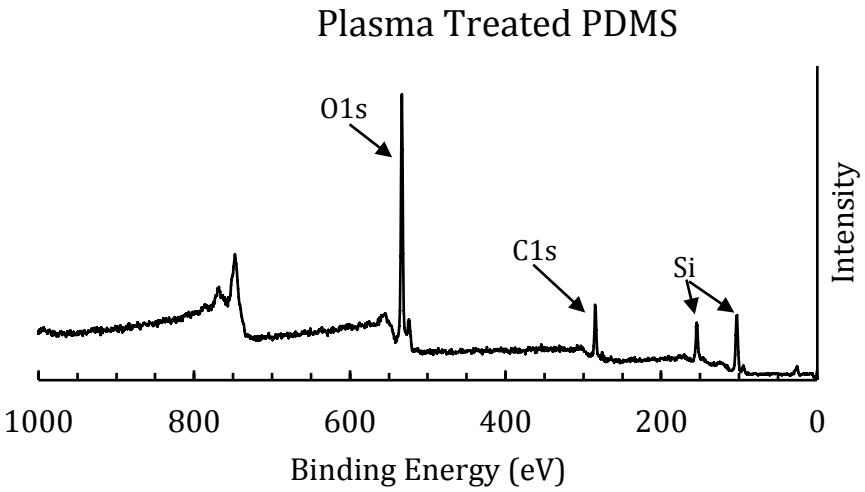
Plasma Treated PDMS
O1s
C1s
Si
Intensity
1000
800
600
400
200
0
Binding Energy (eV)

Published Works

Patents

1. Michael Joyce, M. K. Joyce, A. Eshkeiti, M.Z. Atashbar, P.D Fleming III, 2016. *Self-Supported Electronic Devices*. PCT/US2015/043076. 04.02.2016.
2. Michael Joyce, M.K. Joyce, *Feasibility for the Development of a Repulpable Silicone Release Paper.* Provisional Patent in Process
3. Michael Joyce, M.K. Joyce, *Method for the High Throughput Manufacture of Poly-Dimethylsiloxane (PDMS) Films,* Provisional Patent in Process.

Publications

1. Michael Joyce, et. al., *Contribution of Flexo Process Variables to Fine Line Ag Electrode Performance,* International Journal of Engineering Research & Technology, **3**(8): p. 1645-1656. (2014).
2. Ali Eshkeiti, et. al., *Screen Printing of Multilayered Hybrid Printed Circuit Boards on Different Substrates*. IEEE Transactions on Components, Packaging and Manufacturing Technology, 5(3): 415-421. (2015).
3. Michael Joyce, et. al., *Self-supported printed multi-layer capacitors.* Journal of Print and Media Technology Research, **4**(4): 241-316. (2015).
4. Jason Kleiner, et. al., *Low Melting Glass Frit as an Adhesion and Resistivity Promotor: Photonically Sintered Silver Nanoparticle Ink on Indium Tin Oxide Coated Glass*. International Journal of Engineering Research & Technology **5**(3): 785-795. (2016).
5. Michael Joyce, Paul D. Fleming, Alexandra Pekarovicova, *The Characterization of Surface Treated Silica-Filled and Non-Filled Polydimethylsiloxane Films*.

Presentations (published in conference proceedings)

1. Azem K. Yahamed, et. al., *Biopolymers for 3D Printed Bone Structure and Testing*, Paper Presented at Digital Fabrication and Digital Printing/ NIP31, Retrieved October 25, 2015, from Imaging.org.
2. Ali Eshkeiti, et. al., *A Novel Self-Supported Printed Flexible Strain Sensor for Monitoring Body Movement and Temperature*. *IEEE* Conference Proceedings, Nov. 2-5, pp. 1615-1618. Valencia, Spain. (2014).
3. Michael Joyce, et. al., *The Characterization of Surface Treated Silica-Filled and Non-Filled Polydimethylsiloxane Films*, Paper Presented at TAGA Annual Technical Conference, Memphis, TN, March 20-23, 2016.

(12) INTERNATIONAL APPLICATION PUBLISHED UNDER THE PATENT COOPERATION TREATY (PCT)

(19) World Intellectual Property Organization
International Bureau

(43) International Publication Date
4 February 2016 (04.02.2016)

WIPO | PCT

(10) International Publication Number
WO 2016/019223 A1

(51) International Patent Classification:
H01G 4/33 (2006.01) *H01F 5/00* (2006.01)
H01L 21/64 (2006.01) *H01Q 9/00* (2006.01)

(21) International Application Number:
PCT/US2015/043076

(22) International Filing Date:
31 July 2015 (31.07.2015)

(25) Filing Language: English

(26) Publication Language: English

(30) Priority Data:
62/032,024 1 August 2014 (01.08.2014) US

(71) Applicant: **WESTERN MICHIGAN UNIVERSITY RESEARCH FOUNDATION** [US/US]; 1903 West Michigan Ave., Kalamazoo, MI 49008 (US).

(72) Inventors: **JOYCE, Margaret K.**; 2506 Chippendale Drive, Kalamazoo, Michigan 49009 (US). **JOYCE, Michael James**; 2506 Chippendale Drive, Kalamazoo, Michigan 49009 (US). **ESHKEITI, Ali**; 1020 Bretton, Lansing, Michigan 48917 (US). **ATASHBAR, Massood Zandi**; 4265 Squire Heath Road, Portage, Michigan 49024 (US). **FLEMING, Paul D., III**; 1119 Wickford Drive, Kalamazoo, Michigan 49009 (US).

(74) Agent: **CALLAGHAN, Terry S.**; Price Heneveld LLP, 695 Kenmoor, S.E., P.O. Box 2567, Grand Rapids, Michigan 49501-2567 (US).

(81) Designated States *(unless otherwise indicated, for every kind of national protection available)*: AE, AG, AL, AM, AO, AT, AU, AZ, BA, BB, BG, BH, BN, BR, BW, BY, BZ, CA, CH, CL, CN, CO, CR, CU, CZ, DE, DK, DM, DO, DZ, EC, EE, EG, ES, FI, GB, GD, GE, GH, GM, GT, HN, HR, HU, ID, IL, IN, IR, IS, JP, KE, KG, KN, KP, KR, KZ, LA, LC, LK, LR, LS, LU, LY, MA, MD, ME, MG, MK, MN, MW, MX, MY, MZ, NA, NG, NI, NO, NZ, OM, PA, PE, PG, PH, PL, PT, QA, RO, RS, RU, RW, SA, SC, SD, SE, SG, SK, SL, SM, ST, SV, SY, TH, TJ, TM, TN, TR, TT, TZ, UA, UG, US, UZ, VC, VN, ZA, ZM, ZW.

(84) Designated States *(unless otherwise indicated, for every kind of regional protection available)*: ARIPO (BW, GH, GM, KE, LR, LS, MW, MZ, NA, RW, SD, SL, ST, SZ, TZ, UG, ZM, ZW), Eurasian (AM, AZ, BY, KG, KZ, RU, TJ, TM), European (AL, AT, BE, BG, CH, CY, CZ, DE, DK, EE, ES, FI, FR, GB, GR, HR, HU, IE, IS, IT, LT, LU, LV, MC, MK, MT, NL, NO, PL, PT, RO, RS, SE, SI, SK, SM, TR), OAPI (BF, BJ, CF, CG, CI, CM, GA, GN, GQ, GW, KM, ML, MR, NE, SN, TD, TG).

Declarations under Rule 4.17:

— *as to applicant's entitlement to apply for and be granted a patent (Rule 4.17(ii))*

— *as to the applicant's entitlement to claim the priority of the earlier application (Rule 4.17(iii))*

Published:

— *with international search report (Art. 21(3))*

(54) Title: SELF-SUPPORTED ELECTRONIC DEVICES

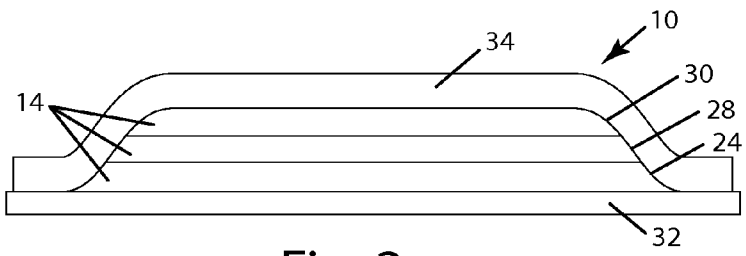

Fig. 2

(57) Abstract: A method of forming a self-supported electronic device, including depositing a sacrificial layer on a first surface substrate, wherein the sacrificial layer is substantially soluble in a first solvent. At least one device layer is deposited in a desired pattern on top of the sacrificial layer. The at least one device layer is substantially insoluble in the at least one device layer. The sacrificial layer is at least partially dissolved in the first solvent to release at least a portion of the first device layer from the substrate. The at least one device layer removed from the substrate forms a self-supported electronic device, which is a thin film electronic device having at least a portion thereof that is not supported by a material carrier.

WO 2016/019223 A1

SELF-SUPPORTED ELECTRONIC DEVICES

BACKGROUND

[0001] The present disclosure relates to self-supported electronic devices, and methods for manufacturing the same.

SUMMARY

[0002] One aspect of the present disclosure is a self-supported electronic device, including a thin film electronic device, wherein at least a portion of the electronic device is not supported by a material carrier.

[0003] In another aspect, the present disclosure includes an assembly for producing a self-supported electronic device, including a substrate and a sacrificial layer disposed on a top surface of the substrate, wherein the sacrificial layer is soluble in a first solvent. At least one device layer is disposed on a top surface of the sacrificial layer. The at least one device layer has a thickness greater than about 10 nm and is substantially insoluble in the first solvent. The sacrificial layer is substantially insoluble in the at least one device layer.

[0004] In yet another aspect, the present disclosure includes a method of forming a self-supported electronic device, including depositing a sacrificial layer on a first surface of a substrate, wherein the sacrificial layer is substantially soluble in a first solvent. At least one device layer is deposited in a desired pattern on a top surface of the sacrificial layer, and the sacrificial layer is substantially insoluble in the at least one device layer. The sacrificial layer is at least partially dissolved in the first solvent to release at least a portion of the first device layer from the substrate.

[0005] Self-supported electronic devices, as described herein, are especially suitable for applications where a carrier substrate is undesired due to increased material costs, increased thickness, reduced flexibility, reduced conformability or incompatibility with a surface that the electronic device will be placed in contact with. The method of manufacturing the self-supported electronic devices allows formation of the self-supported electronic devices on a substrate, and the subsequent removal of the device from the substrate, which means that the substrate can be re-used for production of multiple self-supported electronic devices. Additionally, removal of the substrate allows processing of the self-supported electronic devices at higher temperatures once removed

from the substrate, or prior to removal (up to the degradation temperature of the sacrificial layer), and allows the use of substrate materials that are not compatible with the final product or even the materials of the self-supported electronic device.

[0006] Another aspect of the present invention is a stretchable and wearable printed sensor for human body motion monitoring. The sensor may comprise a strain sensor that is fabricated by screen printing carbon nanotube (CNT) ink on a water-soluble polymer-based polyvinyl alcohol (PVA) substrate. The printed sensor may be transferred onto the forearm of a human, and water may be used to dissolve the sacrificial PVA layer. The sensor may be subjected to flexion and extension movements of the elbow, and the sensor may be utilized to monitor body movement. In one example, the average resistance of the sensor increased by approximately 10% for multiple flexion movements. In addition, for extension movements, a 2% increase was observed in the base resistance after 10 cycles.

[0007] These and other features, advantages, and objects of the present device will be further understood and appreciated by those skilled in the art upon studying the following specification, claims, and appended drawings.

BRIEF DESCRIPTION OF THE DRAWINGS

[0008] Fig. 1 is a side elevation schematic view of one embodiment of an assembly of a substrate, a sacrificial layer, and a self-supported electronic device;

[0009] Fig. 2 is a side elevation schematic view of one embodiment of a self-supported electronic device;

[0010] Fig. 3 is a top view of one embodiment of a self-supported inductance coil;

[0011] Fig. 4 is a top view of one embodiment of a self-supported RFID antenna;

[0012] Fig. 5 is a top view of one embodiment of a self-supported heavy metal ion sensor;

[0013] Fig. 6 is a top exploded view of one embodiment of a self-supported capacitor;

[0014] Fig. 7 is a top view of the embodiment of the self-supported capacitor shown in Fig. 6;

[0015] Fig. 8 is a top exploded view of one embodiment of a supercapacitor;

[0016] Fig. 9 is a top view of the supercapacitor shown in Fig. 8;

[0017] Fig. 10 is a side elevation view of one embodiment of a rolled supercapacitor.

[0018] Fig. 11 is a top perspective view of one embodiment of a self-supported capacitive pressure sensor;

[0019] Fig. 12 is a side elevation view of one embodiment of a cantilevered sensor as formed on a substrate;

[0020] Fig. 13 is a schematic view of a stretchable and wearable sensor for monitoring human body motion according to another aspect of the present invention;

[0021] Fig. 14 shows the sensor of Fig. 13 printed on a sacrificial substrate prior to mounting the sensor on the skin of a human subject;

[0022] Fig. 15 is a partially fragmentary view showing the sensor of Figs. 12 and 13 disposed on the skin of a human forearm;

[0023] Fig. 15A is a partially fragmentary view showing the sensor of Figs. 12 and 13 disposed on the skin of a human upper arm (bicep); and

[0024] Fig. 16 is a graph showing the response of the sensor when a subject's elbow is flexed.

DETAILED DESCRIPTION

[0025] For purposes of description herein the terms "upper," "lower," "right," "left," "rear," "front," "vertical," "horizontal," and derivatives thereof shall relate to the assembly as oriented in Fig. 1. However, it is to be understood that the device may assume various alternative orientations and step sequences, except where expressly specified to the contrary. It is also to be understood that the specific devices and processes illustrated in the attached drawings, and described in the following specification are simply exemplary embodiments of the inventive concepts defined in the appended claims. Hence, specific dimensions and other physical characteristics relating to the embodiments disclosed herein are not to be considered as limiting, unless the claims expressly state otherwise.

[0026] Figs. 1 and 2 depict one embodiment of a self-supported electronic device 10 and an assembly 12 for forming the self-supported electronic device 10. Self-supported electronic device 10, as described herein, is a thin film electronic device wherein at least a portion of the electronic device is not supported by a material carrier. Generally, thin film electronic devices as used herein include printed electronic devices, or other

similarly produced electronic devices having at least one device layer 14, each device layer 14 contributing to a functional electronic device 10, with each device layer 14 preferably ranging in thickness from 10 nanometers to 60 nanometers. Examples of electronic devices that can be produced as self-supported electronic devices 10 herein include without limitation, an inductance coil, an antenna, an RFID antenna, a heavy metal ion sensor, a capacitor, a supercapacitor, a pressure sensor, a thin film transistor, a resistor, a diode, an organic light emitting diode, an accelerometer, or any other electronic device that is unsupported by a material carrier. Self-supported electronic devices 10 can also include a combination of electric devices that form a functional circuit. As used herein, the term self-supported electronic device 10 also includes electronic devices such as cantilever sensors which are only partially unsupported by a material carrier, as described in greater detail below.

[0027] As shown in the embodiment of the assembly 12 shown Fig. 1, the assembly 12 (produced during manufacturing of the self-supported electronic device 10) includes a substrate 16 with a sacrificial layer 18 disposed on a top surface 20 of the substrate 16. The sacrificial layer 18 is soluble in a chosen solvent. A first device layer 24 is disposed on a top surface 26 the sacrificial layer 18, and a second device layer 28 and third device layer 30 are disposed over the first device layer 24 to form the self-supported electronic device 10. In alternate embodiments, the self-supported electronic device 10 includes only one device layer 14, or includes a plurality of device layers 14 as useful to carry out a desired electrical function. To remove the self-supported electronic device 10 from the substrate 16, the chosen solvent is used to at least partially dissolve the sacrificial layer 18, resulting in the separation from the substrate 16 of the self-supported electronic device 10, which optionally incorporates a portion of the sacrificial layer 18, one embodiment of which is illustrated in Fig. 2.

[0028] Generally, the substrate 16 used in production of the self-supported electronic device 10, as shown in the embodiment depicted in Fig. 1, can be chosen from any material suitable for the processing steps to form the self-supported electronic device 10 thereon, wherein the material of the substrate 16 is also is compatible with at least the sacrificial layer 18 which is applied thereto. Substrates 16 can be rigid or flexible, and optionally include rigid or flexible traditional electronic device substrates, such as PET, PEN, glass, polyimide, polycarbonate, Mylar, polyethylene, aluminum, stainless steel, or

silicon wafer. Alternative substrates 16 can also be used in the methods disclosed herein, because the substrates 16 are not directly in contact with the self-supporting electronic device 10, and because the substrates 16 are removed before use of the self-supported electronic devices 10, and optionally before final processing steps for producing the self-supported electronic device 10 or positioning the device 10 in its final position for use. Therefore, substrates 16 that would otherwise be unsuitable for use in an electronic device can be used as long as they are compatible with the sacrificial layer 18 and the processing steps of forming the self-supported electronic device 10.

[0029] The sacrificial layer 18, which is disposed on the top surface 20 of the substrate 16, serves to separate the substrate 16 from the self-supported electronic device 10, and allows removal of the self-supported electronic device 10 from the top surface 20 of the substrate 16. The sacrificial layer 18 is a material, which is substantially soluble in the chosen solvent, and which is preferably substantially insoluble in the first device layer 24, or any device layer 14 that will come into direct contact with the sacrificial layer 18. In one preferred embodiment, the sacrificial layer 18 is a water-soluble polymer. Examples of such polymers are sodium alginate, hydroxyethylated cellulose, carboxymethylated cellulose, guar gum, carboxymethylated starch, ethylated starch, polyvinyl alcohol, plant and animal proteins, gum arabic, carrageenan gum, hydroxypropylcellulose, hydroxypropylmethyl cellulose, and methylcellulose. The water-soluble polymer is preferably applied to the top surface 20 of the substrate 16 as a film to form the sacrificial layer 18. In another preferred embodiment, the water-soluble polymer includes a hydrocolloid, protein, polysaccharides or derivatives of the foregoing. Alternatively, solvent soluble polymers can be used as the sacrificial layer 18, including without limitation, ethylcellulose, polylactic acids, and polyhydroxyalkaonates.

[0030] The composition of the sacrificial layer 18 determines the appropriate solvent to use in any given embodiment of the method for preparing the self-supporting electronic devices 10 disclosed herein. For example, where a water-soluble polymer is used for the sacrificial layer 18, water is one appropriate solvent to be used to solubilize the solvent. When using ethylcellulose as the sacrificial layer 18, the solvent chosen to solubilize the ethylcellulose is preferably a mixture of aromatic hydrocarbons and lower molecular weight aliphatic alcohols such as toluene, xylene or ethylbenzene with ethanol, methanol, isopropanol or n-butanol. Polylactic acids are preferably used in conjunction

with chlorinated solvents, hot benzene, tetrahydrofuran or dioxane as the solvent. Polyhydroxyalkaonates are preferably used in conjunction with halogenated solvents such as chloroform, dichloromethane, or dichloroethane.

[0031] In certain preferred embodiments, a plasticizer is added to the sacrificial layer 18, to improve characteristics of the sacrificial layer 18 such as increasing elasticity, flexibility, and toughness; reducing brittleness; and preventing cracking. Low molecular weight, non-volatile plasticizers are preferred for addition to sacrificial layers 18 which are made of polysaccharide films, including, without limitation, propylene glycol, glycerol, sorbitol, and glycerin. These plasticizers create a greater distance between polar groups within the polysaccharide molecules of the sacrificial layer 18, which reduces the attraction between adjacent polymeric chains. The preferred amount of plasticizer added into hydrocolloid solutions used for the sacrificial layer 18 can vary between about 10% and 60% by weight of the hydrocolloid. Water can also be used as a plasticizer in the sacrificial layer 18, and therefore the moisture content or relative humidity of the environment will potentially affect the properties of the sacrificial layer 18. Addition of plasticizers to the sacrificial layer 18 also decreases the ability of the sacrificial layer 18 to attract water, and slows the time to solubilize the sacrificial layer 18 if water is used as the solvent, and may also decrease the tensile strength and increase the tackiness of the sacrificial layer 18.

[0032] In certain embodiments, the sacrificial layer 18 is not completely solubilized in the solvent. In some embodiments, it is preferable to completely remove the sacrificial layer 18 from the self-supported electronic device 10. In other embodiments, it is preferable to only partially remove the sacrificial layer 18 from the self-supported electronic device 10. In embodiments where the sacrificial layer 18 is not entirely removed, the sacrificial layer 18 is preferably solubilized enough to separate the self-supported electronic device 10 from the top surface 20 of the substrate 16, with a residue or portion 32 of the sacrificial layer 18 remaining on the self-supported electronic device 10. Where a portion 32 of the sacrificial layer 18 remains on the self-supported electronic device 10, the portion 32 is optionally used as an adhesive to secure the self-supported electronic device 10 in its final desired location. For example, the portion 32 of the sacrificial layer 18 remaining on the self-supported electronic device 10 can be used as an adhesive to secure the self-supported electronic device 10 to skin where the self-supported electronic device 10 is

desired for use in an application where it is applied to a subject's skin. In alternate embodiments, a separate adhesive can be applied to the self-supported electronic device 10 to secure the self-supported electronic device 10 in its desired location of use.

[0033] The self-supporting electronic device 10 includes one or more functional materials which are applied in one or more device layers 14. The functional materials of the device layers 14 are preferably formulated as inks which are printed onto the sacrificial layer 18 (or onto one of the previously applied device layers 14). Printing is a preferred method of application of the device layers 14 because printing is an additive process, which allows the functional materials to be applied in the specific design intended, minimizing the amount of material that must be used and the number of processing steps in manufacturing. The inks used, and their functional materials, are preferably substantially insoluble in the solvent that will be used to dissolve the sacrificial layer 18. In one preferred embodiment, all of the device layers 14 are insoluble in the solvent to be used. In another preferred embodiment, at least an outer device layer 14 is insoluble in the solvent and will protect the device layers 14 underneath the outer device layer 14 from dissolving in the solvent. Preferably, any device layers 14 that are soluble in the solvent are encapsulated with other device layers 14 that are substantially insoluble in the solvent.

[0034] The self-supported electronic devices 10 preferably include one or more device layers 14 which have predetermined electrical properties to perform as the desired electronic device. For example, the first device layer 24 in the embodiment depicted in Figs. 1 and 2 can be a conductive layer and the second device layer 28 can be a dielectric layer, with a conductive ink used to print the first device layer 24 and a dielectric ink used to print the second device layer 28. Alternatively, the first device layer 24 can be a dielectric layer, to electronically insulate the self-supported electronic device 10 from any underlying surface to which the self-supported electronic device 10 may ultimately be affixed, allowing the self-supported electronic device 10 to function properly when affixed to a range of different materials. In yet another embodiment, the first device layer 24 is optionally a barrier layer, such that the first device layer 24 is a material in which the sacrificial layer 18 is substantially insoluble. This allows for the printing of subsequent device layers 14 in the self-supported electronic device 10 that may otherwise solubilize the sacrificial layer 18. Some embodiments of self-supported

electronic devices 10 as described herein are flexible enough to be rolled or bent, allowing the creation of electronic devices with enhanced features, such as rolled supercapacitors, as described in greater detail below.

[0035] The ink chosen for printing the device layers 14 of the self-supported electronic device 10 will depend at least partially on the composition of the sacrificial layer 18. The sacrificial layer 18 is preferably substantially insoluble in the inks used in the device layers 14. Additionally, the inks used in the device layers 14 are preferably film-forming when applied over the sacrificial layer 18. Solvent-based, water-based, and UV-curable inks can be used for printing the device layers 14 on the sacrificial layer 18, including without limitation, semiconductors, resistive, and emissive polymer inks, which can be applied to the sacrificial layer 18 using various printing methods such as screen printing, inkjet printing, flexographic printing, gravure printing, offset gravure printing, rotogravure printing, offset rotogravure printing, offset lithography, or other printing processes that are suitable for use with the solvent-based, water-based, or UV-curable inks used for the device layers 14. Additionally, each device layer 14 can be applied to the self-supported electronic device 10 independently, allowing the use of different printing methods for different device layers 14. Each device layer 14 preferably has a thickness from about 0.1 μm to about 60 μm, depending on the printing method used and the viscosity of the ink. The viscosity of the ink used for printing the device layers 14 preferably varies depending on the printing method to be used. For screen printing, the ink preferably has a viscosity of between 1,000 centipoise (cP) and 10,000 cP. For rotogravure or offset rotogravure, the viscosity of the ink is preferably between 50 cP and 1,000 cP. For flexographic printing, the viscosity of the ink is preferably between 100 cP and 5,000 cP, and for offset lithography, the viscosity of the ink is preferably between 1,000 cP and 50,000 cP. For inkjet printing, the viscosity of the ink is preferably between 5 cP and 100 cP, and for aerosol jet printing the viscosity of the ink is preferably between 1 cP and 1000 cP. For microplotter printing the viscosity of the ink is preferably between 1 cP and 450 cP.

[0036] Non-limiting examples of suitable conductive inks for use in the device layers 14 include, without limitation, flake silver inks, nano silver inks, flake copper inks, nano copper inks, inks containing carbon nanotubes, carbon inks, gold inks, graphene inks, and nickel inks. Several non-limiting examples of presently available UV-curable conductive inks suitable for screen printing device layers 14 include, without limitation, UHF ™ ink

available from Polychem, and ELECTRODAG PD-054 ™ ink available from Henkel and AST 6200™ solvent-based flake silver ink, available from Sun Chemical Co. Several non-limiting examples of presently available UV-curable dielectric inks suitable for screen printing the device layers 14 include, without limitation, UV-1006S™ available from Conductive Compounds, UV-2530™ available from Conductive Compounds, UV-2560™ available from Conductive Compounds, UV-2531™ available from Conductive Compounds, EDAG 1020A™ available from Henkel; EDAG 452SS™ available from Henkel, and EDAG PF455B™ available from Henkel. Other inks having appropriate functional properties for the device layers 14 can be used.

[0037] Direct printing of the device layer 14 on the sacrificial layer 18 can achieve resolutions as low as 10 microns if the properties of the ink used for the device layer 14, such as viscosity and wetting properties, are matched to the surface energy of the sacrificial layer 18. In some preferred embodiments, the device layers 14 include ink printed over a large area, and in others fine resolution of printed device layers 14 are desirable.

[0038] In traditional electronic devices, the properties of the substrate 16, such as the temperature resistance, solvent compatibility, smoothness, cost, surface energy, thickness, rigidity, and functional properties, can limit the functional materials used in the creation of the traditional electronic device and the printing methods or other formation methods available. In contrast, with self-supported electronic devices 10, the self-supported electronic device 10 will be removed from the substrate 16, and is separated therefrom by the sacrificial layer 18. Therefore, the substrate 16 can be selected based in its mechanical properties to allow the use of desired functional materials in the production of the self-supported electronic devices 10, even if the substrate 16 would not be suitable for the desired end use of the self-supported electronic device 10 or for all processing steps of the formation of the self-supported electronic device 10. For example, in a flexible electronic device, where the electronic device is not removed from the substrate 16, the substrate 16 chosen must have sufficient flexibility for the desired end use of the electronic device. However, flexible substrates tend to have limited temperature processing ranges, requiring the balancing of flexibility with the desired temperature processing parameters of the functional materials being applied to form the electronic device. According to the present

disclosure, where the self-supported electronic device 10 is removable from the substrate 16, the substrate 16 chosen can be a rigid substrate 16 that is capable of handling high temperature processing as desired for the preferred functional materials. In this case, the processing temperatures achievable would still be bounded by the degradation temperatures of the sacrificial layer 18 and the self-supported electronic device 10. Additionally, substrates 16 are preferably re-usable in the formation of the self-supported electronic devices 10, allowing for the use of substrates 16 that would otherwise be cost prohibitive.

[0039] An encapsulating layer 34 is optionally deposited over the device layers 14 to seal the self-supported electronic device 10. The encapsulating layer 34 is optionally applied prior to solubilizing the sacrificial layer 18, after removing the self-supported electronic device 10 from the underlying substrate 16, or after applying the self-supported electronic device 10 to its final use position. The encapsulating layer 34 is preferably a film-forming layer that creates a barrier when applied to the self-supported electronic device 10. In one preferred embodiment, the encapsulating layer 34 is a silicone-based material that desirably imparts water-resistant properties to the self-supported electronic device 10. If the encapsulating layer 34 is applied prior to solubilizing the sacrificial layer 18, it is preferable to coat a smaller surface area with the encapsulating layer 34 than the area covered by the sacrificial layer 18. This allows a wicking action to solubilize the sacrificial layer 18 to release the self-supported electronic device 10 from the substrate 16. If the encapsulating layer 34 is applied after removing the self-supported electronic device 10 from the underlying substrate 16 or after applying the self-supported electronic device 10 to its final use position, then the encapsulating layer 34 preferably has a surface area equal to or larger than the area of the self-supported electronic device 10 to better seal the self-supported electronic device 10. In another preferred embodiment, the encapsulating layer 34 can be a passivation layer, such as a silicone spray, to protect the device layers 14 from corrosive effects.

[0040] In certain embodiments of the self-supported electronic device 10 described herein, the sacrificial layer 18 or the substrate 16 can be used to add three-dimensional shape to the self-supported electronic device 10, or to allow a portion of the self-supported electronic device 10 to be released from the substrate 16.

[0041] Generally, a method of manufacturing self-supporting electronic devices 10 as described herein includes the steps of applying the sacrificial layer 18 to the top surface 20 of the substrate 16, and applying at least one device layer 14 over the sacrificial layer 18 in a predetermined pattern to form the self-supporting electronic device 10. The chosen solvent, in which the sacrificial layer 18 is soluble, is then contacted with the sacrificial layer 18, to at least partially dissolve the sacrificial layer 18 and allow separation of the self-supported electronic device 10 from the substrate 16. In an alternate embodiment, the sacrificial layer 18 and the self-supported electronic device 10 can be peeled or otherwise separated from the substrate 16 for storage, and dissolution of the sacrificial layer 18 is carried out at a later time (e.g., at the time of application of the self-supporting electronic device 10 to its use position).

[0042] The sacrificial layer 18 can be applied to the substrate 16 using a variety of methods, including without limitation casting, curtain coating, spraying or printing the sacrificial layer 18 onto the top surface 20 of the substrate 16. In some embodiments, the sacrificial layer 18 is dried or cured after application to the top surface 20 of the substrate 16.

[0043] The device layer 14 or layers 14 can also be applied to the sacrificial layer 18 using a variety of methods, though the least one device layer 14 is preferably printed on the sacrificial layer 18 in the predetermined pattern to form the desired self-supported electronic device 10. Where multiple device layers 14 are incorporated, the different layers 14 optionally include functional materials with different properties, allowing the creation of various types of self-supported electronic devices 10, several examples of which are discussed in greater detail below. Each device layer 14 is optionally dried or cured after its application.

[0044] Following formation of the self-supported electronic device 10 on the sacrificial layer 18 and the substrate 16, the solvent is applied to dissolve the sacrificial layer 18. In some embodiments it may be preferable to submerge the substrate 16 with the self-supported electronic device 10 thereon in the solvent. In other embodiments, the solvent may be sprayed, coated, painted or otherwise applied to the sacrificial layer 18 to dissolve the sacrificial layer 18. In some preferred embodiments, the sacrificial layer 18 is only partially removed, with the dissolution sufficient to release the self-supported electronic device 10 from the substrate 16. When the self-supported electronic device 10

is not placed immediately in its position of use following removal from the substrate 16, the self-supported electronic device 10 can be placed on a silicone release sheet or other non-stick sheet until the desired time of use.

[0045] One embodiment of a self-supported electronic device 10, as illustrated in Fig. 3, is a self-supported inductance coil 40. The self-supported inductance coil 40 includes at least one continuous spiral device layer 42, with a terminal 44 at each end thereof. The inductance coil 40 is formed by coating the sacrificial layer 18 on the substrate 16, and printing the spiral device layer 42 using conductive ink. The sacrificial layer 18 is then dissolved in the solvent to remove the inductance coil 40 from the substrate 16.

[0046] Another embodiment of a self-supported electronic device 10 is illustrated in Fig. 4. The self-supported electronic device 10 illustrated in Fig. 4 is an RFID antenna 50. Similarly to the inductance coil 40, the RFID antenna 50 is formed by coating the sacrificial layer 18 on the substrate 16, and printing the RFID antenna 50 on sacrificial layer 18 using conductive ink. The sacrificial layer 18 is then dissolved in the solvent to remove the RFID antenna 50 from the substrate 16. RFID antenna 50 may include one or more layers of flexible or rigid polymer material (not shown) or other suitable material formed on sacrificial layer 18 and/or above the conductive layer forming antenna 50 to structurally support the conductive layer that forms antenna 50.

[0047] Another embodiment of a self-supported electronic device 10 is illustrated in Fig. 5, as a heavy metal ion sensor 60. The embodiment of the heavy metal ion sensor 60 shown in Fig. 5 is formed by coating the sacrificial layer 18 on the substrate 16 and then printing a first rectangular dielectric ink layer 62. Conductive counter electrodes 64 and 68 are printed, as are two conductive layers of a working electrode 66. The sacrificial layer 18 is then dissolved in the solvent to remove the heavy metal ion sensor 60 from the substrate 16.

[0048] Another embodiment of a self-supported electronic device 10 is illustrated in Figs. 6 and 7, as a capacitor 70. The embodiment of the capacitor 70 shown in Figs. 6 and 7 is formed by coating the sacrificial layer 18 on the substrate 16, and then printing a first device layer 72 in generally rectangular form with contacts 74 using conductive ink. A second device layer 76 is printed in rectangular form using a dielectric ink overlapping the first device layer 72. The third device layer 78 is printed in generally rectangular form with contacts 80 using conductive ink, overlapping the first and second device layers 72,

76, to form two conductive layers 72, 78 separated by a dielectric layer 76. The sacrificial layer 18 is then dissolved in the solvent to remove the capacitor 70 from the substrate 16.

[0049] In one specific example, a self-supporting electronic device 10, which functions as a capacitor 70, was formed using the substrate 16 of Melinex ST 506 PET, available from DuPont. The sacrificial layer 18 was formed by adding dried alginate into a pre-weighed amount of distilled water under agitation to obtain a 6% aqueous solution of alginate. The alginate solution was allowed to mix for 20 minutes. 25% glycerol by weight of alginate was added and the alginate solution was allowed to further mix for 40 minutes to hydrate the alginate. The glycerol was added as a plasticizer to improve the flexibility of the sacrificial layer 18 formed from the alginate solution and prevent cracking of the sacrificial layer 18 upon drying. The alginate solution was then placed in a closed container and held overnight to degas. The alginate solution was then applied by pipette to the substrate 16, which was cleaned with isopropyl alcohol just prior to application of the alginate solution. Drawdowns were performed by use of Meyer rods or Byrd applicators to coat the alginate solution on the substrate 16. The substrate 16 with the coated alginate solution was placed in a TAPPI standard test room at drying conditions of 50% relative humidity and 23 °C to form the sacrificial layer 18 on the substrate 16.

[0050] The first device layer 72, comprising a conductive solvent-based silver flake ink, AST 6200 from Sun Chemical, was screen printed over the sacrificial layer 18 using an AMI MSP-485 semi-automated screen printer and a 230 LPI mesh 0.0011" wire diameter at 45° wire angle screen and an emulsion layer of 10 µm thickness produced by Microscreen of South Bend, Indiana. The conductive solvent-based ink of first device layer 72 was thermally dried at 135F for 5 minutes until fully dried (no significant change in resistivity with time). After drying the conductive ink to form the first device layer 72, the second device layer 76 was printed using a UV dielectric ink, Electrodag PF-455B from Henkel, and the same screen printer and the same type of screen as used for the conductive ink. The dielectric ink second device layer 76 was cured using a Fusion UV drier equipped with a D60 bulb by passing the substrate 16 with the sacrificial layer 18, first device layer 72 and second device layer 79 through the drier 3 to 4 times until completely cured (no longer tacky to the touch). The third device layer 78 was printed over the second device layer 76, the third device layer 78 including another layer of the

conductive solvent based silver flake ink. The third device layer 78 was also thermally dried. The resulting self-supported capacitor 70 includes three layers, the conductive first layer 72, the dielectric second layer 76, and the conductive third layer 78. The self-supported capacitor 70 is removed from the substrate 16 by applying water to the assembly 12, thereby dissolving the sacrificial layer 18 and separating the capacitor 70 from the substrate 16.

[0051] One variation of the capacitor 70 illustrated in Figs. 6 and 7 is a supercapacitor 82, one embodiment of which is illustrated in Figs. 8-10. The embodiment of the super capacitor 82 as disclosed herein is formed by rolling a 4 layer capacitor 71 with a first device layer 73 comprising a dielectric material, a second device layer 75 comprising a conductive material, a third device layer 77 comprising a dielectric material, and a fourth device layer 79 comprising a conductive material. To form the 4-layer capacitor 71, the sacrificial layer 18 is printed on a substrate 16, and then the first device layer 73 is printed using dielectric ink. The second device layer 75 is printed over the first device layer 73 using conductive ink after the first device layer 73 is cured. The second device layer 75 is then cured, and the third device layer 77 is printed over the second device layer 75 using dielectric ink and cured. To complete the 4-layer capacitor 71, the fourth device layer 79 is printed using conductive ink over the third device layer 77, and is cured. The flexibility of the capacitor 71 allows the capacitor 71 to be rolled to form the super capacitor 82,as shown in Fig. 10.

[0052] Another variation of the capacitor 70 illustrated in Figs. 6 and 7 is a capacitive pressure sensor 90, one embodiment of which is illustrated in Fig. 11 The capacitive pressure sensor 90 as shown in Fig. 11 is formed by coating a sacrificial layer 18 on a substrate 16, and then printing a first device layer 92 of bars using conductive ink. A second device layer 94 of dielectric ink is printed over the first layer 92 of conductive ink. A third device layer 96 of conductive ink is printed, having bars positioned generally perpendicularly from the bars of the first device layer 92. A fourth device layer 98 is printed over the remaining device layers 92, 94, 96, using a passivation material.

[0053] Yet another self-supported electronic device 10 is a cantilevered sensor 100, one embodiment of which is shown in Fig. 12. The embodiment of the cantilevered sensor 100 is formed by applying a shaping sacrificial layer 102 under the cantilevered sensor 100. The shaping sacrificial layer 102 is optionally applied over a full sacrificial layer 104.

In other embodiments, the shaping sacrificial layer 102 is applied directly to the substrate 106. A first device layer 108 of conductive ink is then printed or otherwise applied over the shaping sacrificial layer 102, resulting in a first device layer 108 with at least two portions, with a first or beam portion 110 having a first thickness x over the shaping sacrificial layer 102, and a second or base portion 112 having a second thickness y where the shaping sacrificial layer 102 is not present. After forming the cantilever sensor 100 on the substrate 106 over the shaping sacrificial layer 102, a solvent is applied to solubilize the shaping sacrificial layer 102, leaving a void beneath the first portion 110 of the cantilever sensor 100. In one preferred embodiment, the shaping sacrificial layer 102 is 1 micron thick, and is 1" wide. The conductive first device layer 108 printed over the shaping sacrificial layer 102 is 4" wide, with a first portion 110 that is 1 micron thick and a second portion 112 that is 2 microns thick.

[0054] Another aspect of the present invention is a stretchable printed strain sensor 120 (Fig. 13). Stretchable printed strain sensor 120 has a wavy form including a plurality of oppositely-oriented U-shaped portions 122 that are joined together to form a plurality of S-shaped bends. The S-shaped bends of sensor 120 may be sinusoidal in shape, or other suitable shape. Enlarged rectangular ends 130 of the sensor 120 form electrodes that may be utilized to electrically connect the sensor to other electronic devices. As discussed in more detail below, strain sensor 120 may be fabricated by screen printing Carbon nano-tubes (CNTs) ink onto a water-soluble sacrificial substrate. The printed sensor, along with the sacrificial layer, may be transferred onto the skin of a human (e.g. an arm). Water may then be used to dissolve the sacrificial layer, leaving the sensor 120 disposed/adhered to the skin. The capability of printed sensor 120 for tracking the movement of the human body was demonstrated by subjecting the sensor 120 to extension and flexion of an arm.

EXAMPLE

[0055] *A. Chemicals, and Sample Preparation*

Polyvinyl Alcohol (PVA) substrate (Watson QSA 2000) was used as a sacrificial layer for printing and transferring the sensor directly onto the skin of a human subject. CNT ink (VC101 from SWENT) was used for the fabrication of a resistive wavy form strain sensor 120 that may include a plurality of S-bends and enlarged end portions/electrodes 130 (Fig. 13). An silver ink (Electrodag 479SS) from Henkel was used for printing of

interconnects in the wavy form on the Thermoplastic polyurethane (TPU) from Bemis Associates, Inc. Conductive silver epoxy from CircuitWorks® (CW-2400) was used for attaching the interconnects to the sensor 120.

[0056] *B. Sensor Fabrication*

Sensor 120 (Fig. 13) has a wavy shape with a 800 μm line width and overall dimensions of 3.0 cm × 0.4 cm. Sensor 120 was screen printed using CNT ink (SWeNT CV100) on a sacrificial water-soluble polymer based PVA substrate (Watson QSA 2000). Printed sensor 120 on sacrificial substrate 124 is shown in Fig. 14. A semiautomatic screen printing press (AMI 485) was used for deposition of CNTS and Isopropyl alcohol was used for cleaning of the screen. The CNT ink was cured in a VWR oven at 100 °C for 10 minutes. In the next step, in order to transfer sensor 120 onto a human body, the skin 126 of a human forearm 128 (Fig. 15) was wetted and the printed sensor was then mounted on the left forearm 128. The sacrificial PVA layer was then washed away using water, thereby completing the transfer of sensor 120 onto the skin 126. The sensor 120 after placement on skin 126 of a human forearm 128 is shown in Fig. 15. Sensor 120 may also be positioned on skin 126 of other body parts (e.g. upper arm/bicep) as shown in Fig. 15A. A Bruker Contour GTL EN 61010 profilometer was used to study the thickness of the deposited CNTs. The average thickness of the printed CNT layer was measured as 5.6 μm.

[0057] *C. Experimental Procedure*

Interconnects (not shown) were attached to the electrodes 130 of sensor 120 prior to mounting on the skin 126 utilizing conductive silver epoxy. The interconnects were connected to an Agilent E4980A precision LCR meter (not shown) for measuring/recording the resistive response of the strain sensor 120 during flexion and extension of the forearm 128. The change in the resistance of the sensor 120 was recorded after each time movement of the elbow.

[0058] *RESULTS AND DISCUSSION*

The response of the printed wearable sensor 120, after placing on the arm, is shown in Fig. 16. The sensor 120 was subjected to both flexion and extension movement of the arm, thereby resulting in a change of resistance of the sensor 120. It was observed that the average resistance of the sensor 120 increased from 32.8 kΩ to 36 kΩ for multiple flexion and extension movements of the elbow, which corresponds to a 10 % change in the sensor response. In addition, a 2 % change in the base resistance of the

sensor 120 was observed, when the elbow was brought back to the original position after 10 cycles.

In order to reduce potential breakage of sensor 120, the thickness of the conductive layer of sensor 120 may be increased to 20 microns, 30 microns, 40 microns, or more. Multiple layers of conductive and/or non-conductive materials may also be utilized to provide increased strength and reduce breakage of sensor 120.

[0059] The sensor 120 may also be encapsulated using spin coated poly-imide or Silicone based materials such as Polydimethylsiloxane (PDMS) to strengthen sensor 120 and reduce breakage of the structure after mounting on a human body.

[0060] It is also important to note that the construction and arrangement of the elements of the device as shown in the exemplary embodiments is illustrative only. Although only a few embodiments of the present innovations have been described in detail in this disclosure, those skilled in the art who review this disclosure will readily appreciate that many modifications are possible (e.g., variations in sizes, dimensions, structures, shapes and proportions of the various elements, values of parameters, mounting arrangements, use of materials, colors, orientations, etc.) without materially departing from the novel teachings and advantages of the subject matter recited. For example, elements shown as integrally formed may be constructed of multiple parts or elements shown as multiple parts may be integrally formed, the operation of the interfaces may be reversed or otherwise varied, the length or width of the structures and/or members or connector or other elements of the system may be varied, the nature or number of adjustment positions provided between the elements may be varied. It should be noted that the elements and/or assemblies of the system may be constructed from any of a wide variety of materials that provide sufficient strength or durability, in any of a wide variety of colors, textures, and combinations. Accordingly, all such modifications are intended to be included within the scope of the present innovations. Other substitutions, modifications, changes, and omissions may be made in the design, operating conditions, and arrangement of the desired and other exemplary embodiments without departing from the spirit of the present innovations.

[0061] It will be understood that any described processes or steps within described processes may be combined with other disclosed processes or steps to form structures

within the scope of the present device. The exemplary structures and processes disclosed herein are for illustrative purposes and are not to be construed as limiting.

[0062] It is also to be understood that variations and modifications can be made on the aforementioned structures and methods without departing from the concepts of the present device, and further it is to be understood that such concepts are intended to be covered by the following claims unless these claims by their language expressly state otherwise.

[0063] The above description is considered that of the illustrated embodiments only. Modifications of the device will occur to those skilled in the art and to those who make or use the device. Therefore, it is understood that the embodiments shown in the drawings and described above is merely for illustrative purposes and not intended to limit the scope of the device, which is defined by the following claims as interpreted according to the principles of patent law, including the Doctrine of Equivalents.

CLAIMS

What is claimed is:

1. A method of forming a self-supported electronic device, comprising:

depositing a sacrificial layer on a first surface substrate, wherein the sacrificial layer is substantially soluble in a first solvent;

depositing at least one device layer in a desired pattern on the sacrificial layer, wherein the at least one device layer is not substantially soluble in the first solvent and wherein the sacrificial layer is substantially insoluble in the at least one device layer; and

at least partially dissolving the sacrificial layer in the first solvent to release at least a portion of the first device layer from the substrate.

2. The method of claim 1, wherein:

the first solvent comprises water.

3. The method of claim 2, wherein:

the sacrificial layer comprises a water-soluble polymer.

4. The method of claim 3, wherein:

the sacrificial layer comprises a polysaccharide film.

5. The method of claim 4, wherein:

the sacrificial layer comprises a plasticizer.

6. The method of claim 5, wherein:

the plasticizer comprises about 10% to about 60% by weight of the sacrificial layer.

7. The method of any one of claims 1-6, wherein:

the sacrificial layer is completely dissolved and removed from the substrate.

8. The method of any one of claims 1-7, wherein:

the device layer comprises an electrically conductive material.

9. The method of claim 8, wherein:

the device layer comprises a stretchable strain sensor having at least one S-shaped bend.

10. The method of claim 9, including:

positioning the device layer and sacrificial layer on a subject's skin prior to at least partially dissolving the sacrificial layer.

11. The method of claim 10, wherein:

the device layer comprises carbon nanotubes that are deposited on the sacrificial layer.

12. The method of any one of claims 1-11, wherein:

the at least one device layer comprises a conductive layer and a dielectric layer.

13. The method of claim 12, wherein:

the self-supported electronic device comprises a heavy metal ion sensor;

the dielectric layer is deposited on the sacrificial layer;

the conductive layer is printed on the dielectric layer to form a counter electrode and at least two working electrodes that are spaced apart from the counter electrode.

14. The method of any one of claims 1-13, including:

depositing an encapsulating layer over the at least one device layer.

15. The method of claim 14, wherein:

the encapsulating layer is deposited over the at least one device layer prior to at least partially dissolving the sacrificial layer.

16. The method of claim 14, wherein:

the encapsulating layer is deposited over the at least one device layer after at least partially dissolving the sacrificial layer, and wherein the encapsulating layer has a surface area equal to or larger than a surface area of the at least one device layer.

17. The method of any one of claims 1-16, wherein:

the at least one device layer comprises conductive material deposited in a continuous spiral that is removed from the first surface substrate to form an inductance coil.

18. The method of any one of claims 1-17, wherein:

the at least one device layer comprises conductive material defining first and second triangular regions, each triangular region defining a first corner, and wherein the first corners are disposed directly adjacent one another to define an RFID antenna.

19. The method of any one of claims 1-18, wherein:

the at least one device layer comprises a plurality of device layers including at least a first conductive layer that is deposited on the sacrificial layer, a dielectric layer that is deposited on the first conductive layer, and a second conductive layer that is deposited on the dielectric layer to form a capacitor.

20. The method of claim 19, including:

rolling the device layers to form a capacitor that is generally cylindrical in form.

21. The method of any one of claims 1-20, wherein:

the at least one device layer comprises a first layer including a plurality of spaced apart parallel bars of conductive material, a second layer of dielectric material covering at least a central portion of the bars, and a third layer comprising a plurality of spaced apart parallel bars of conductive material disposed on the layer of dielectric material, wherein the parallel bars of the third layer are generally perpendicular to the bars of the first layer.

22. The method of any one of claims 1-21, wherein:

the sacrificial layer comprises a shaping sacrificial layer that only covers a first portion of the first surface substrate whereby a second portion of the first surface substrate is not covered by the shaping sacrificial layer;

the at least one device layer includes a beam portion that is deposited over the shaping sacrificial layer and a base portion that is deposited over the second portion of the surface substrate;

the shaping sacrificial layer is dissolved such that the beam portion has a thickness that is significantly less than a thickness of the base portion whereby the device layer forms a cantilevered sensor.

23. An assembly for producing a self-supported electronic device, comprising:

a substrate;

a sacrificial layer disposed on a top surface of the substrate, the sacrificial layer being soluble in a first solvent;

at least one device layer disposed on a top surface of the sacrificial layer, having a thickness greater than about 10 nm, wherein the device layer is substantially insoluble in the first solvent, and wherein the sacrificial layer is substantially insoluble in the at least one device layer.

24. The assembly of claim 23, wherein:

the at least one device layer comprises an electrically conductive material.

25. The assembly of claims 23 and 24, wherein:

the at least one device layer comprises a conductive layer and a dielectric layer.

26. The assembly of any one of claims 23-25, including:

an encapsulating layer extending over at least a portion of the at least one device layer.

27. The assembly of any one of claims 23-26, wherein:

the sacrificial layer is water soluble.

28. The assembly of claim 27, wherein;
the sacrificial layer comprises a water soluble polymer.

29. The assembly of any one of claims 23-28, wherein:
The substrate comprises a rigid material.

30. A self-supported electronic device, comprising:
a thin film electronic device, wherein at least a portion of the electronic device is not supported by a material carrier.

31. The electronic device of claim 30, wherein:
the thin film electronic device comprises at least one dielectric layer and at least one conductive layer.

32. The electronic device of claim 31, wherein:
the thin film electronic device is formed into a roll.

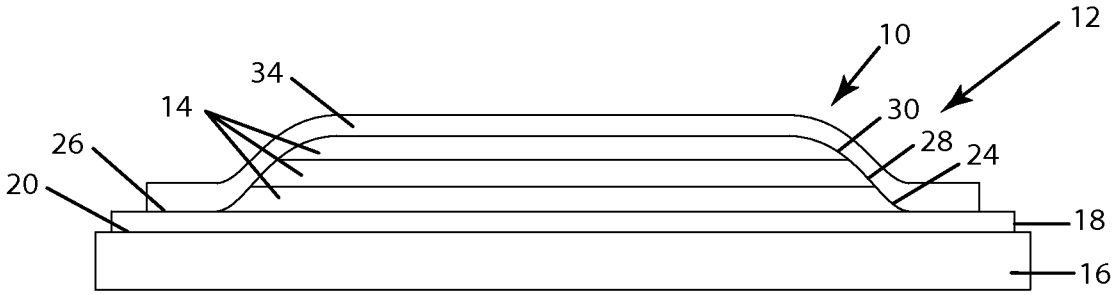

Fig. 1

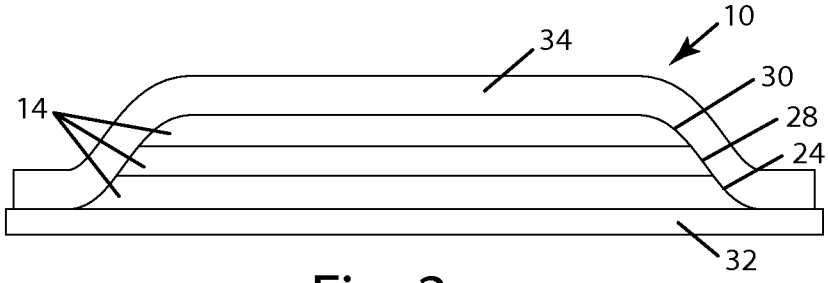

Fig. 2

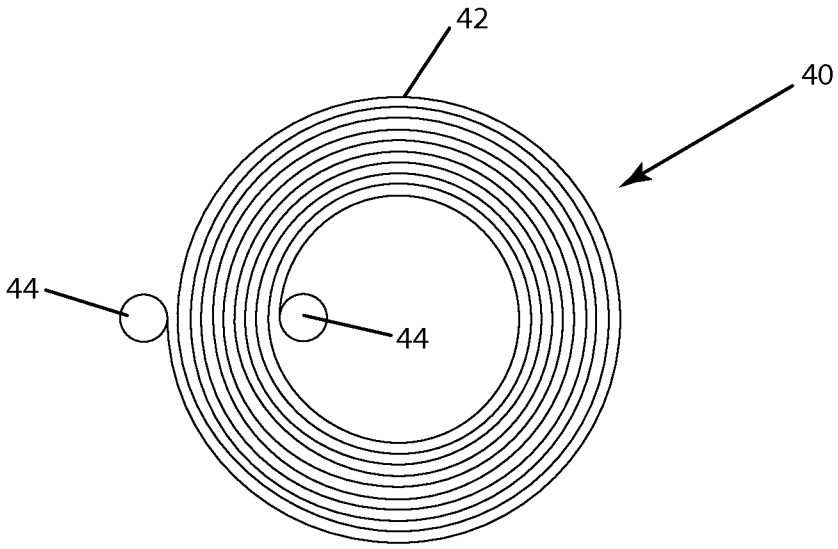

Fig. 3

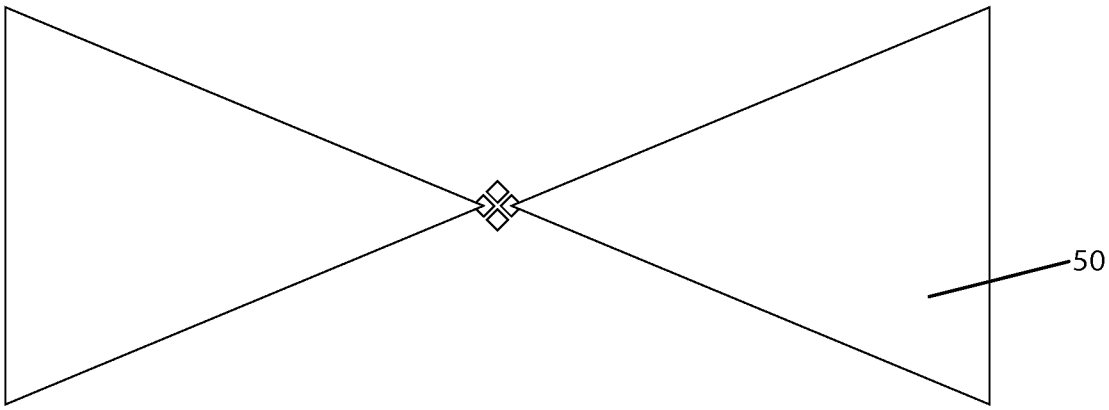

Fig. 4

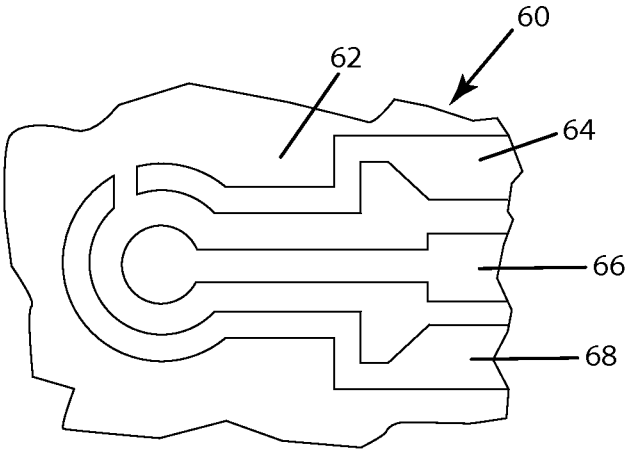

Fig. 5

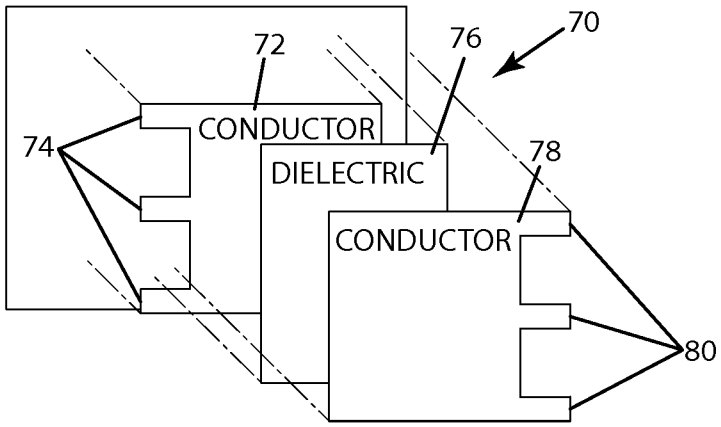
70
72
76
CONDUCTOR
74
78
DIELECTRIC
CONDUCTOR
80

Fig. 6

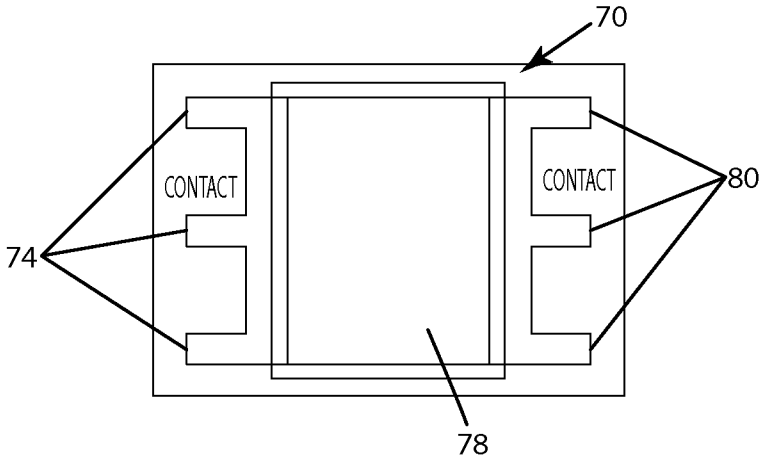
70
CONTACT
CONTACT
80
74
78

Fig. 7

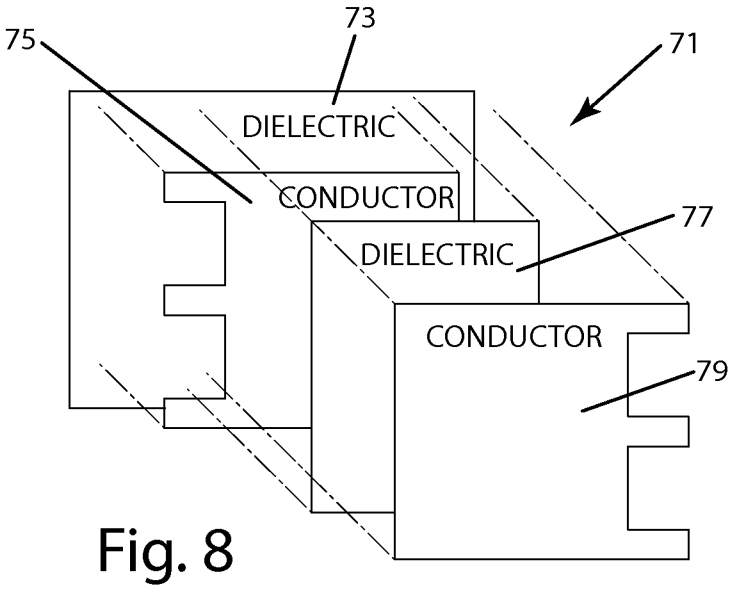

Fig. 8

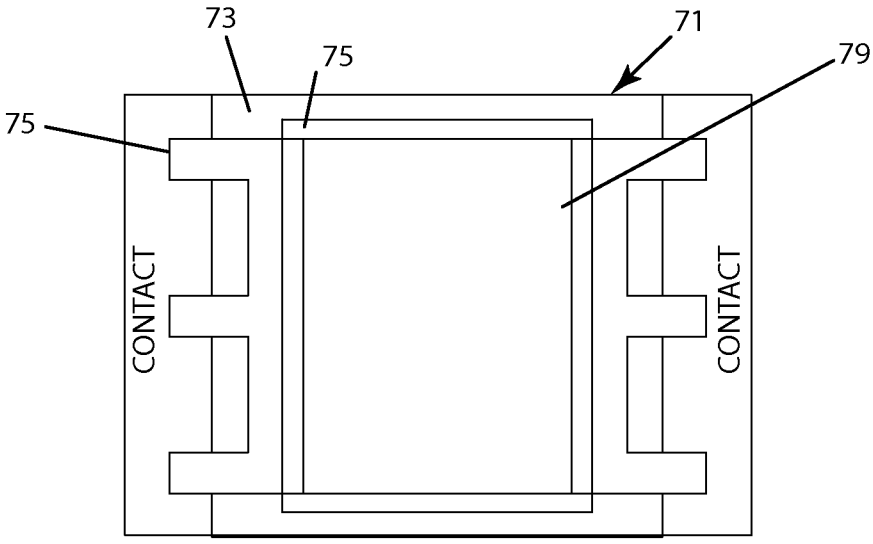

Fig. 9

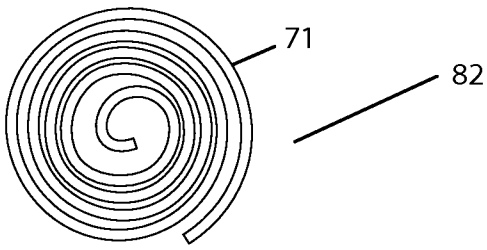

Fig. 10

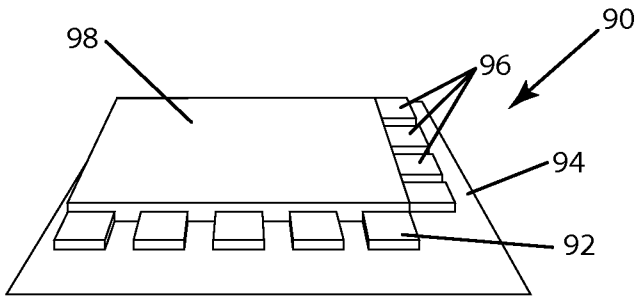

Fig. 11

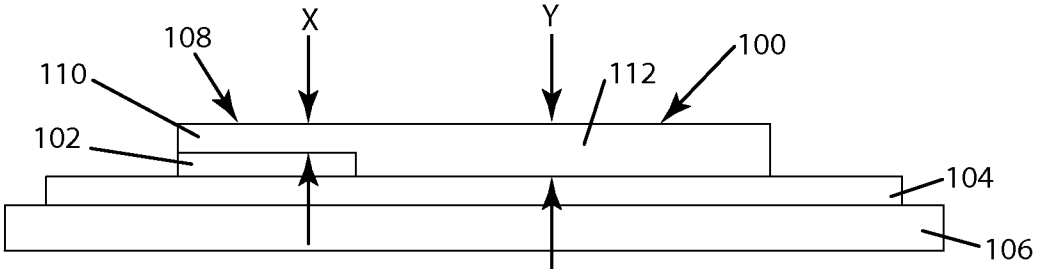

Fig. 12

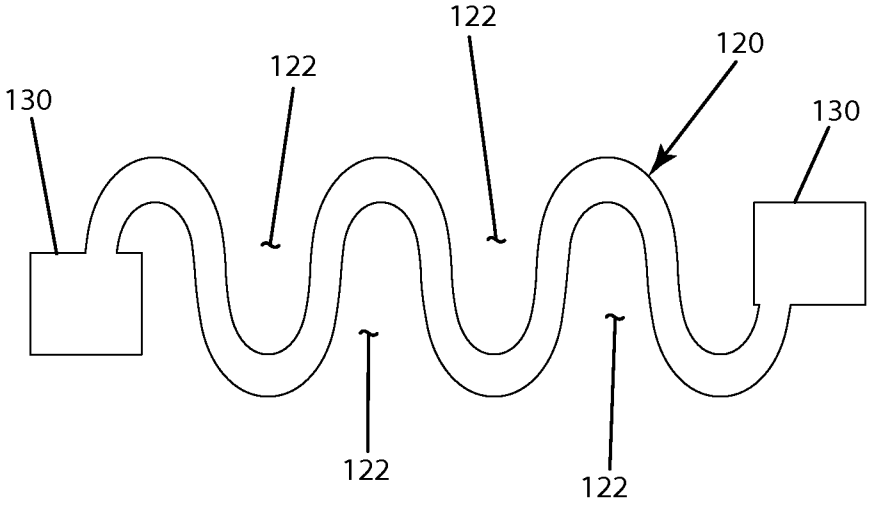

Fig. 13

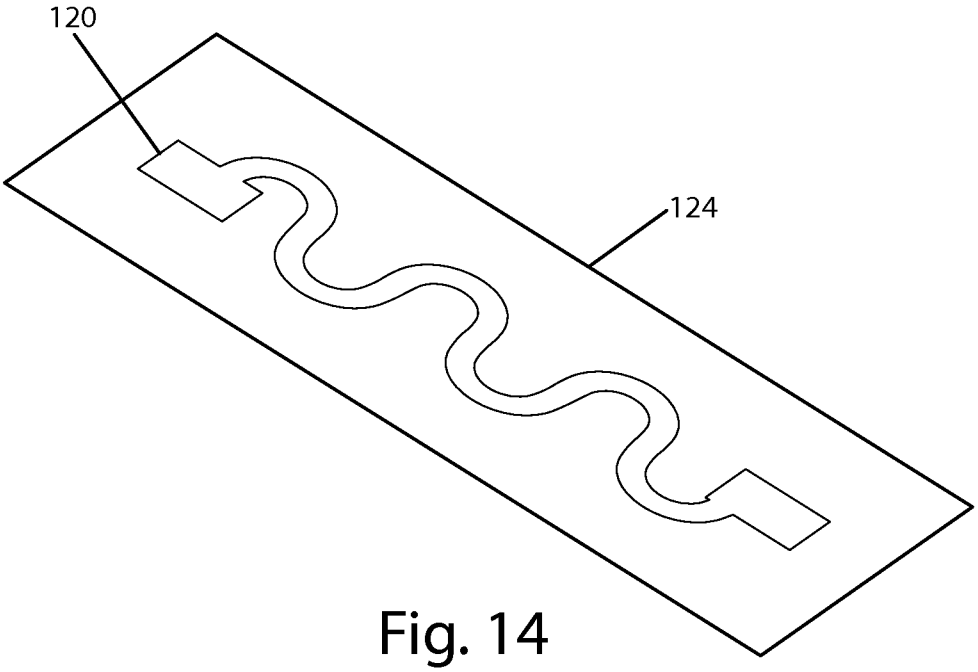

Fig. 14

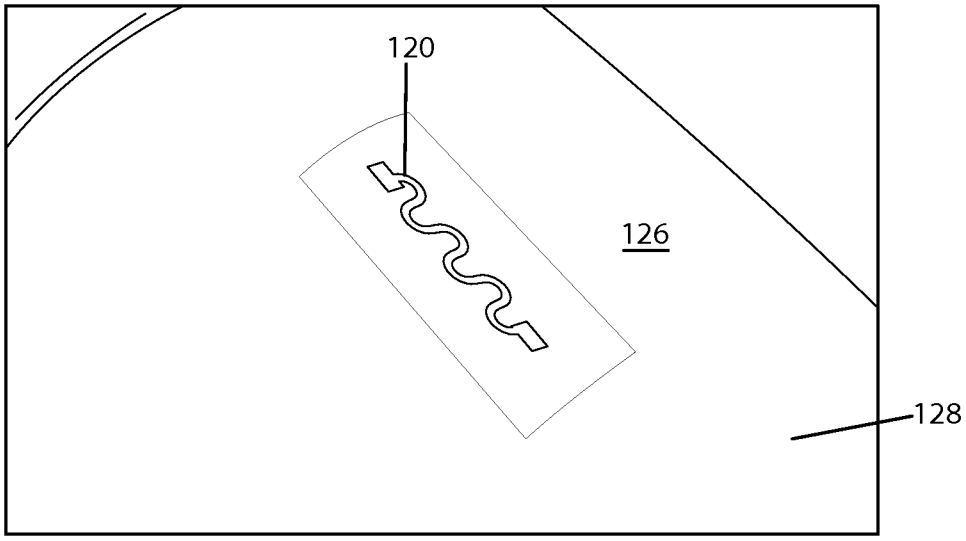

Fig. 15

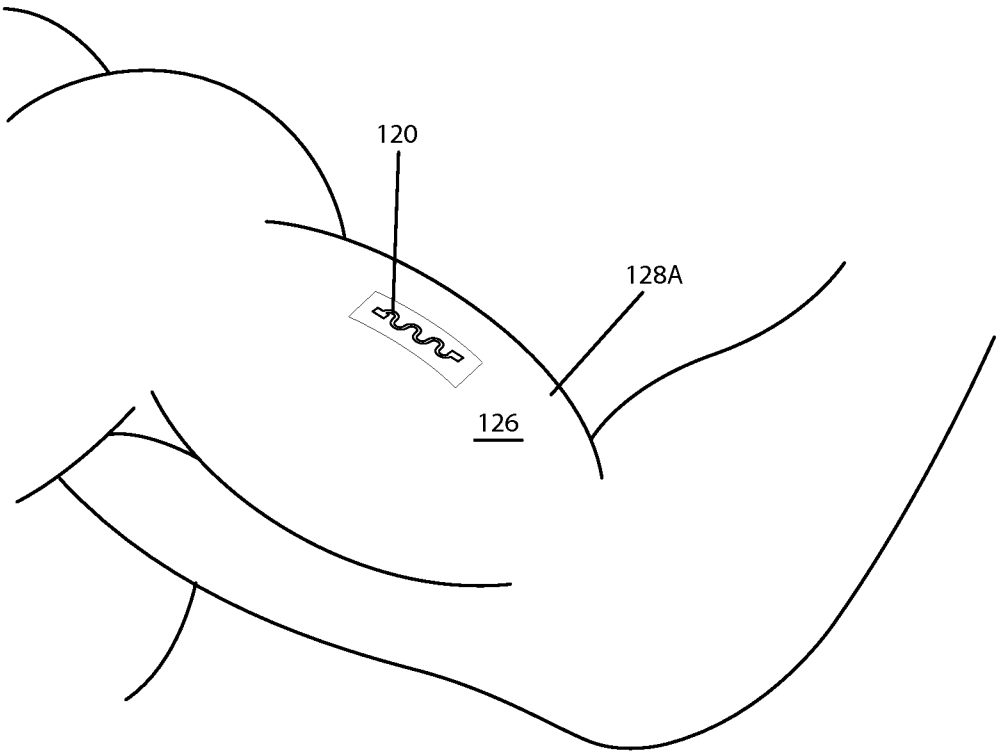

Fig. 15A

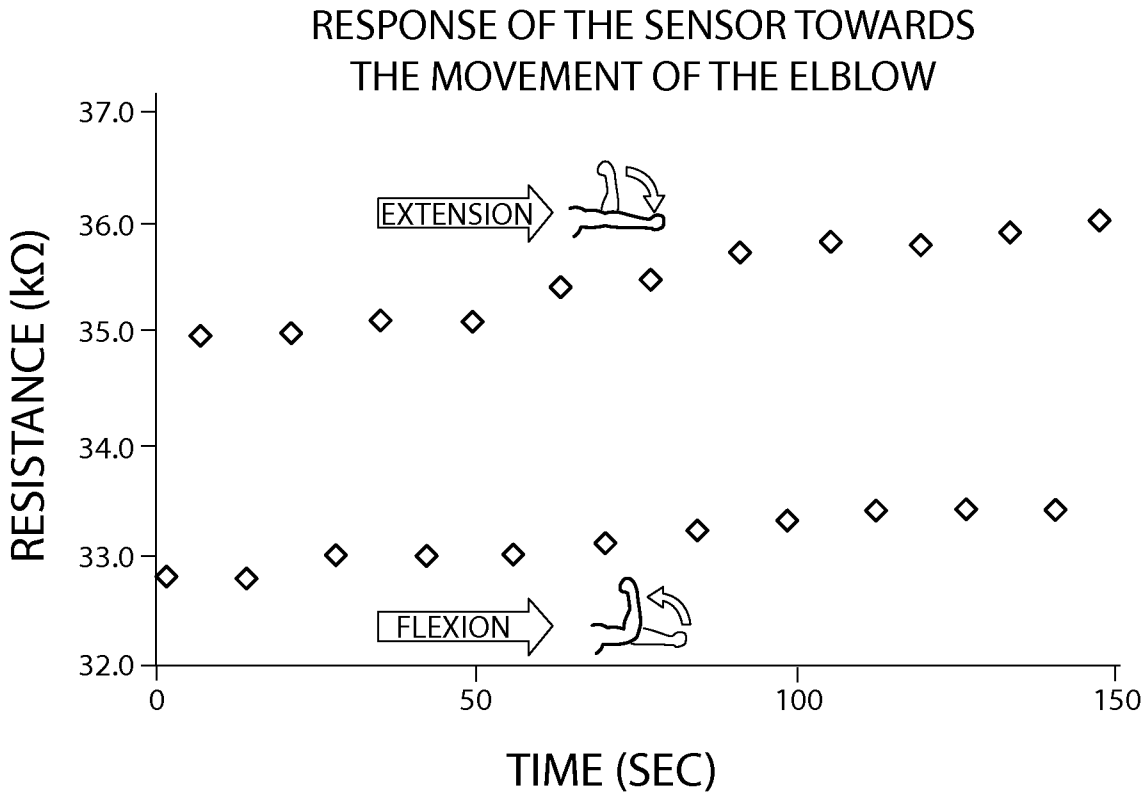

Fig. 16

INTERNATIONAL SEARCH REPORT

International application No.
PCT/US 2015/043076

A. CLASSIFICATION OF SUBJECT MATTER

H01G 4/33 *(2006.01)*
H01L 21/64 *(2006.01)*
H01F 5/00 *(2006.01)*
H01Q 9/00 *(2015.01)*

According to International Patent Classification (IPC) or to both national classification and IPC

B. FIELDS SEARCHED

Minimum documentation searched (classification system followed by classification symbols)

H01G 4/01, 4/33, 15/00, H01L 21/26, 21/64, 27/20, 41/193, H01F 5/00, H01Q 9/00, H01B 1/20, H01M 8/12, A61B 5/1473, B32B 15/08, 38/10, B44C 1/22, H01C 17/28

Documentation searched other than minimum documentation to the extent that such documents are included in the fields searched

Electronic data base consulted during the international search (name of data base and, where practicable, search terms used)

PatSearch (RUPTO internal), USPTO, PAJ, Esp@cenet, DWPI, EAPATIS, PATENTSCOPE

C. DOCUMENTS CONSIDERED TO BE RELEVANT

Category*	Citation of document, with indication, where appropriate, of the relevant passages	Relevant to claim No.
X	WO 2005/065433 A2 (MICROFABRICA INC. et al.) 21.07.2005, [19], drawing 21/34, [321]	1-2, 7, 23-25, 30-31
Y		3-6, 32
Y	WO 2011/115643 A1 (THE BOARD OF TRUSTEES OF THE UNIVERSITY OF ILLINOIS et al.) 22.09.2011, [0016]-[0018], [0041]	3-4
Y	US 2012/0256720 A1 (SAMSUNG ELECTRONICS CO., LTD.) 11.10.2012, abstract, fig. 14a-14b, [0031], claims	32
Y	US 2007/0259474 A1 (KOREAN INSTITUTE OF MACHINERY & MATERIALS) 08.11.2007, claims 1, 5, 13	5-6

☐ Further documents are listed in the continuation of Box C.

☐ See patent family annex.

* Special categories of cited documents:

"A" document defining the general state of the art which is not considered to be of particular relevance

"E" earlier document but published on or after the international filing date

"L" document which may throw doubts on priority claim(s) or which is cited to establish the publication date of another citation or other special reason (as specified)

"O" document referring to an oral disclosure, use, exhibition or other means

"P" document published prior to the international filing date but later than the priority date claimed

"T" later document published after the international filing date or priority date and not in conflict with the application but cited to understand the principle or theory underlying the invention

"X" document of particular relevance; the claimed invention cannot be considered novel or cannot be considered to involve an inventive step when the document is taken alone

"Y" document of particular relevance; the claimed invention cannot be considered to involve an inventive step when the document is combined with one or more other such documents, such combination being obvious to a person skilled in the art

"&" document member of the same patent family

Date of the actual completion of the international search	Date of mailing of the international search report
12 October 2015 (12.10.2015)	12 November 2015 (12.11.2015)

Name and mailing address of the ISA/RU:	Authorized officer
Federal Institute of Industrial Property, Berezhkovskaya nab., 30-1, Moscow, G-59, GSP-3, Russia, 125993 Facsimile No: (8-495) 531-63-18, (8-499) 243-33-37	E. Guseva Telephone No. 499-240-25-91

Form PCT/ISA/210 (second sheet) (January 2015)

INTERNATIONAL SEARCH REPORT

International application No.
PCT/US 2015/043076

Box No. II Observations where certain claims were found unsearchable (Continuation of item 2 of first sheet)

This international search report has not been established in respect of certain claims under Article 17(2)(a) for the following reasons:

1. ☐ Claims Nos.:
because they relate to subject matter not required to be searched by this Authority, namely:

2. ☐ Claims Nos.:
because they relate to parts of the international application that do not comply with the prescribed requirements to such an extent that no meaningful international search can be carried out, specifically:

3. ☒ Claims Nos.: 8-22, 26-29
because they are dependent claims and are not drafted in accordance with the second and third sentences of Rule 6.4(a).

Box No. III Observations where unity of invention is lacking (Continuation of item 3 of first sheet)

This International Searching Authority found multiple inventions in this international application, as follows:

1. ☐ As all required additional search fees were timely paid by the applicant, this international search report covers all searchable claims.

2. ☐ As all searchable claims could be searched without effort justifying additional fees, this Authority did not invite payment of additional fees.

3. ☐ As only some of the required additional search fees were timely paid by the applicant, this international search report covers only those claims for which fees were paid, specifically claims Nos.:

4. ☐ No required additional search fees were timely paid by the applicant. Consequently, this international search report is restricted to the invention first mentioned in the claims; it is covered by claims Nos.:

Remark on Protest

☐ The additional search fees were accompanied by the applicant's protest and, where applicable, the payment of a protest fee.

☐ The additional search fees were accompanied by the applicant's protest but the applicable protest fee was not paid within the time limit specified in the invitation.

☐ No protest accompanied the payment of additional search fees.